

NSL 65-16
FEBRUARY 1965

C

FACILITY FORM 602	N66-10628	
	(ACCESSION NUMBER)	(THRU)
	42	1
	(PAGES)	(CODE)
	CR 67695	33
	(NASA CR OR TMX OR AD NUMBER)	(CATEGORY)

GPO PRICE \$ _____

CFSTI PRICE(S) \$ _____

Hard copy (HC) 3.00

Microfiche (MF) 75

INTERIM REPORT

CONTRACT NO. NAS 8-11163

ff 653 July 65

GEORGE C. MARSHALL SPACE FLIGHT CENTER
NATIONAL AERONAUTICS AND SPACE ADMINISTRATION
HUNTSVILLE, ALABAMA

**RESEARCH AND DEVELOPMENT
STUDY ON THERMAL CONTROL
BY USE OF FUSIBLE MATERIALS**

BY
A. P. SHLOSINGER
E. W. BENTILLA

NORTHROP SPACE LABORATORIES
3401 WEST BROADWAY, HAWTHORNE, CALIFORNIA 90250

NORTHROP CORPORATION

SQT-30728

NSL 65-16
FEBRUARY 1965

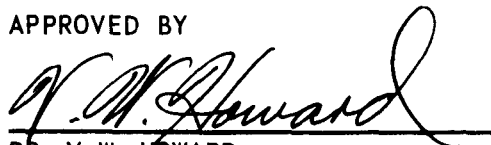
INTERIM REPORT

CONTRACT NO. NAS 8-11163

GEORGE C. MARSHALL SPACE FLIGHT CENTER
NATIONAL AERONAUTICS AND SPACE ADMINISTRATION
HUNTSVILLE, ALABAMA

**RESEARCH AND DEVELOPMENT
STUDY ON THERMAL CONTROL
BY USE OF FUSIBLE MATERIALS**

APPROVED BY



DR. V. W. HOWARD

VICE PRESIDENT
AND
MANAGER
SYSTEMS DEPARTMENT

NORTHROP SPACE LABORATORIES

3401 WEST BROADWAY, HAWTHORNE, CALIFORNIA 90250

NORTHROP CORPORATION

NORTHROP SPACE LABORATORIES

FOREWORD

This report covers an R & D program, conducted from March 1964 to January 1965, for the purpose of developing techniques and design data for the use of fusible materials in thermal control of spacecraft subsystems.

The study program is sponsored by the George C. Marshall Space Flight Center, National Aeronautics and Space Administration, Huntsville, Alabama, under Contract No. NAS 8-11163. The program was conducted under the direction of T. C. Bannister, MSFC Research Project Laboratory, Space Thermodynamics Branch. A. P. Shlosinger, Supervisor of the Temperature and Environmental Control Systems Branch, Systems Engineering Section, Northrop Space Laboratories, is the program manager and principal investigator.

The report was prepared by E. W. Bentilla, Senior Engineer, and A. P. Shlosinger, Supervisor, NSL Temperature and Environmental Control Systems Branch. Major contributions were made by Mr. L. Karre, Senior Research Analyst, NSL Space Materials Lab, and by Mr. W. Woo, Senior Engineer, NSL Temperature and Environmental Control Systems Branch.

SUMMARY

This report presents the results of the first phase of a research program on the application of the melting and solidification of materials to thermal control of space vehicle subsystems. The program objective is to provide specific design data for the application of this concept. This includes selection of suitable fusible materials, providing required thermophysical properties of these materials, defining the practical limits of heat absorption, determining material weight relative to performance, integration of this concept with other heat rejection systems and methods of design of fusible materials temperature control packages. Theoretical and experimental methods have been used to obtain these results.

During the phase of the program covered by this report, fusible materials were selected, the required thermophysical properties required for analysis and packaging design determined, the analysis of two temperature control techniques completed and work started on experimental verification of temperature control package design.

A literature search and preliminary screening resulted in a listing of potential candidate fusible materials. After more extensive evaluation of these materials, the normal (n-) paraffins, containing from fourteen to thirty carbon atoms were considered as the best candidate materials for this study. Four n-paraffins, with an even number of carbon atoms, i.e. tetradecane $C_{14}H_{30}$, hexadecane $C_{16}H_{34}$, octadecane $C_{18}H_{38}$, eicosane $C_{20}H_{42}$, were selected for further study. Two other materials (formic acid and camphene) were considered, but discarded when preliminary tests showed that they had undesirable characteristics.

The solid and liquid densities and other thermophysical properties of the selected materials required for the analytical evaluation and system design, but not available in the literature, were determined experimentally. Very little data is available in the literature for the solid phase properties of

any of the materials considered.

Two models of passive temperature control techniques (or systems) using fusible materials as a heat sink were selected for analytical evaluation and experimental verification.

The first model is adiabatic. All the waste heat rejected by the electronic structure is absorbed by melting of the fusible material and by the temperature rise of the melted material. This analysis predicts the completely passive, zero-gravity, heat absorbing capability of the four selected paraffins considering both the thermal insulating effect of the liquid layer buildup and its varying thermophysical properties. The results of this analysis are presented by charts and graphs suitable for system design.

The second model analyzed is a radiating fin with attached fusible material. The fusible material increases the thermal inertia of the radiator by melting and absorbing heat during peak load conditions and by solidifying and emitting heat during low (or zero) load conditions. This system was studied for several conditions using Octadecane as the fusible material and compared to the performance of the same radiating fin without any attached fusible material.

The results show that for short time limited heat pulses the fin root temperature rise can be greatly reduced by the attached fusible material. The analysis also indicates that the heat rejection temperature during the low load condition must be considerably below the fusible material melt point if short resolidification times are required.

TABLE OF CONTENTS

SUMMARY	<u>Page</u> ii
SECTION I: INTRODUCTION	I-1
SECTION II: LITERATURE SEARCH AND MATERIAL SELECTION	II-1
Properties of Selected Materials	II-7
SECTION III: EXPERIMENTAL DETERMINATION OF PROPERTIES	III-1
Experimental Verification of Material Selection	III-1
Melting and Solidification Points	III-3
Density Measurements	III-3
Measurement of Thermal Conductivity of Liquids	III-7
SECTION IV: THERMAL ANALYSIS	IV-1
Transient Thermal Analysis Techniques	IV-1
Analytical Models and Preliminary Analysis	IV-4
One-Dimensional Adiabatic System	IV-8
Radiating Fin With Attached Fusible Material	IV-8
SECTION V: PERFORMANCE OF TEMPERATURE CONTROL SYSTEMS	V-1
One-Dimensional Adiabatic System	V-1
Parametric Analysis	V-2
Radiating Fin With and Without Attached Fusible Material	V-2
SECTION VI: THERMAL CONTROL SYSTEM PACKAGE DESIGN AND VERIFICATION EXPERIMENTS	VI-1
SECTION VII: POTENTIAL IMPROVEMENTS OF THERMAL CONTROL PACKAGE DESIGN	VII-1
SECTION VIII: CONCLUSIONS	VII-1
SECTION IX: RECOMMENDATIONS	IX-1
REFERENCES	R-1

NORTHROP SPACE LABORATORIES

LIST OF ILLUSTRATIONS

<u>Figure No.</u>	<u>Title</u>	<u>Page</u>
1	Typical Applications of Fusible Materials for Thermal Control	I-3
2	Melt and Transition Temperature of Normal Paraffins ($C_n H_{2n+2}$) from C_{14} to C_{30}	II-5
3	Heat of Fusion and Transition of Normal Paraffins ($C_n H_{2n+2}$) from C_{14} to C_{30}	II-6
4	Density of Tetradecane ($C_{14}H_{30}$)	II-9
5	Density of Hexadecane ($C_{16}H_{34}$)	II-10
6	Density of Octadecane ($C_{18}H_{38}$)	II-11
7	Density of Eicosane ($C_{20}H_{42}$)	II-12
8	Specific Heat of Tetradecane ($C_{14}H_{30}$)	II-13
9	Specific Heat of Hexadecane ($C_{16}H_{34}$)	II-14
10	Specific Heat of Octadecane ($C_{18}H_{38}$)	II-15
11	Specific Heat of Eicosane ($C_{20}H_{42}$)	II-16
12	Thermal Conductivity of Tetradecane ($C_{14}H_{30}$)	II-17
13	Thermal Conductivity of Hexadecane ($C_{16}H_{34}$)	II-18
14	Thermal Conductivity of Octadecane ($C_{18}H_{38}$)	II-19
15	Thermal Conductivity of Eicosane ($C_{20}H_{42}$)	II-20

<u>Figure No.</u>	<u>Title</u>	<u>Page</u>
16.	Correlation of Thermal Conductivity Data for Normal Paraffins ($C_n H_{2n+2}$)	II-21
17.	Vapor Pressure of the Four Selected Fusible Materials	II-22
18.	Cell for Measuring Thermal Conductivity of Liquids	III-8
19.	Analytical Model (1-D) Adiabatic System	IV-5
20.	Analytical Model (2-D) System of Radiating Fin With Attached Fusible Material	IV-5
21.	Thermal Conductance of Selected Materials for a Slab One Square Foot by One Inch Thick	IV-6
22.	Thermal Capacity of Selected Materials for a Slab One Square Foot by One Inch Thick	IV-7
23.	Radiating Fin Thickness Selection and Comparison	IV-9
24.	Radiating Fin Performance	IV-11
25.	Radiating Fin Temperature Distribution	IV-11
26.	Fusible Material Performance - Tetradecane (0-15 Min) For the One Dimensional Adiabatic Model	V-5
27.	Fusible Material Performance - Hexadecane (0-15 Min) For the One Dimensional Adiabatic Model	V-6
28.	Fusible Material Performance - Octadecane (0-15 Min) For the One Dimensional Adiabatic Model	V-7
29.	Fusible Material Performance - Eicosane (0-15 Min) For the One Dimensional Adiabatic Model	V-8
30.	Fusible Material Performance - Tetradecane (1 Hour) For the One Dimensional Adiabatic Model	V-9
31.	Fusible Material Performance - Hexadecane (1 Hour) For the One Dimensional Adiabatic Model	V-10

<u>Figure No.</u>	<u>Title</u>	<u>Page</u>
32.	Fusible Material Performance - Octadecane (1 Hour) For the One Dimensional Adiabatic Model	V-11
33.	Fusible Material Performance - Eicosane (1 Hour) For the One Dimensional Adiabatic Model	V-12
34.	Melt Layer Depth and Weight, Tetradecane For the One Dimensional Adiabatic Model	V-13
35.	Melt Layer Depth and Weight, Hexadecane For the One Dimensional Adiabatic Model	V-14
36.	Melt Layer Depth and Weight, Octadecane For the One Dimensional Adiabatic Model	V-15
37.	Melt Layer Depth and Weight, Eicosane For the One Dimensional Adiabatic Model	V-16
38.	Temperature Parameter Versus Time Parameter for Melting of Semi-Infinite Slabs	V-17
39.	Melt Thickness Parameter Versus Time Parameter for Melting of Semi-Infinite Slabs	V-18
40.	Root Temperature History of a Radiating Fin With and Without Attached Fusible Material	V-19
41.	Steady-State Root Temperature of a Fin Radiating to Space From One Side Only	V-20
42.	Fusible Material Melt and Solidification Rate When Attached to Radiating Fin	V-21
43.	Root Temperature History of a Radiating Fin With and Without Attached Fusible Material at 50 Watts/Ft.	V-22
44.	Melt Layer History of Fusible Material Attached to a Radiating Fin at 50 Watts/Ft.	V-23

<u>Figure No.</u>	<u>Title</u>	<u>Page</u>
45.	Heat Flux History of a Radiating Fin With Attached Fusible Material at 50 Watts/Ft.	V-24
46.	Root Temperature History of a Radiating Fin With and Without Attached Fusible Material With the Maximum Heat Rate for Maintaining Solid Fusible Material Before and After a 15 Minute 50 Watt/Ft Heat Pulse	V-25
47.	Test Apparatus for the One-Dimensional Adiabatic Model, Thermal Control by Use of a Fusible Material	VI-4
48.	Fusible Material - Constant Temperature Heat Sink Apparatus	VII-4

NORTHROP SPACE LABORATORIES

LIST OF TABLES

<u>Table No.</u>	<u>Title</u>	<u>Page</u>
1	Fusible Materials With a Heat of Fusion Greater Than 80 BTU/Lb Listed in Order of Increasing Melt Temperature, From 40 to 150°F	II-2
2	Commercially Available Normal Paraffins With Melt Temperature From 40 to 150°F	II-7
3	Comparison of Fusion Properties of Selected Materials	III-2
4	Results of Density Measurements of Liquid Fusible Materials	III-4
5	Results of Density Measurements of Solid Fusible Materials	III-5

NORTHROP SPACE LABORATORIES

SECTION I

INTRODUCTION

Where missions of limited length and/or small power dissipations result in total mission heat dissipations in the order of a few thousand watt-minutes, storage of heat by enthalpy change in materials provided for absorption of heat can be the most advantageous method of thermal control of temperature sensitive and heat dissipating equipment. The enthalpy change of melting and solidification of materials that have a melt point close to the design environments of electronic equipment (40 to 150°F) provide a promising approach.

Such material on melting or solidifying have enthalpy changes in the range of 100 BTU per pound. They can be applied in close contact with the devices requiring temperature control, and will absorb heat when melting or supply heat when solidifying. They can be used in combination with a radiator as a means for increasing thermal mass and thereby permit radiators to be sized for average rather than peak system heat dissipation.

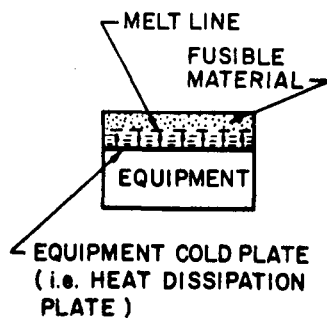
When compared to heat absorption or emission capabilities of solids, resulting from the product of allowable temperature changes and specific heat, they provide approximately an order of magnitude higher capacity for equal weight. When compared with liquid to vapor phase changes, like boiling of water to the vacuum of space, solid to liquid phase changes provide about an order of magnitude smaller heat capacities for equal material weight. But the simplicity of the solid-liquid phase change system which is entirely passive, compared with the controls, tank expulsion systems, heat exchangers and miscellaneous plumbing of the water boiler system show a definite advantage of the solid-liquid system where total time integrated mission loads are small.

Where it is the purpose to increase the thermal mass of a system, liquid to vapor phase change is not applicable. The large volume increase on vaporization makes expelling of the vapor mandatory. The much smaller volume increase of melting can be accommodated by flexible packaging. Repeated melting and solidification of a fusible material with an appropriate melting point appears

to be a very practical way to increase the thermal mass or inertia of a system. Three techniques using the heat of fusion for temperature control of electronic equipment are presented on Figure 1. These systems are all completely passive. The first system (a), Figure 1, is assumed to be essentially adiabatic. All the waste heat given off by an electronic package is absorbed by melting of the solid fusible material plus some sensible heat absorption by the melted liquid material. Systems (b) and (c), Figure 1, use the heat of fusion and thermal radiation for temperature control. The fusible material melts and supplements the radiator only during high equipment heat dissipation periods and solidifies during low heat dissipation periods. System (b) has fusible material attached to the radiator fin allowing good conductive heat transfer to the surfaces radiating to space. This arrangement allows the maximum heat rejection by radiating directly from the equipment, but decreases the temperature potential at the fin-fusible material interface because of the temperature decay along the fin. System (c) has fusible material between the equipment heat source and the radiator. The heat rejection by radiation is limited by this technique. The radiator will be at or below the fusible material melt temperature until all the material is melted and the fusible material acts as an insulator between the heat source and the radiator. The adiabatic system (a) and the radiating fin with attached fusible material (b), Figure 1, were selected for further study.

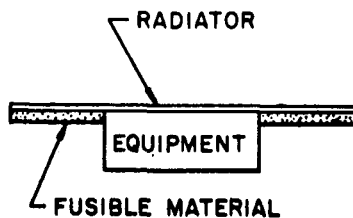
In order to predict the performance of these two systems by analysis and proceed to the design, development and experimental performance verification of thermal control packages, data are required on suitable materials and their pertinent thermophysical properties. The effects of the formation of the layer of molten material, which forms during heat addition, on heat transfer can be predicted by transient heat transfer analysis. The adiabatic system can be represented by a one-dimensional adiabatic analytical model with heat applied at one end representing the electronics equipment. The radiating fin with attached fusible material system is represented by a two dimension analytical model with heat applied at the fin root.

(a)



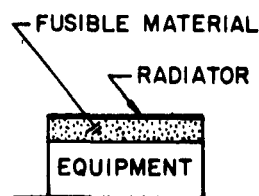
All of equipment waste heat absorbed by melting fusible material (at constant temperature of fusion and zero heat exchange with environment). Fusible material selected so that its melting point is below the equipment temperature limit.

(b)



Radiator acts as a thermally conductive fin. Addition of fusible material (increased thermal mass), controls the temperature of the equipment by melting during high equipment heat loads and solidifying during low equipment heat loads.

(c)



Same as above configuration except that radiator size equals equipment cold plate. Heat must pass through fusible material. The useful amount of fusible material is limited by the trade-off between the amount of heat absorbed by the fusible material and the radiator effectiveness which is reduced due to the temperature drop across the fusible material.

FIGURE 1 TYPICAL APPLICATIONS OF FUSIBLE MATERIALS FOR THERMAL CONTROL

NORTHROP SPACE LABORATORIES

SECTION II

LITERATURE SEARCH AND MATERIAL SELECTION

A literature search was conducted to identify materials with melting points in the operational temperature range of electronic equipment (Table 1) and to review previous efforts in this area (Reference 5 and 7).

The selected melting temperature range of this study was 40°F to 150°F which covers the range of heat rejection temperatures required for most of the electronic and electrical equipment used in satellites and space vehicles.

Materials with a heat of fusion less than 80 BTU/lb were not considered to be of interest for this study. This limit of heat absorbing capability limited the materials to be screened to a reasonable number. Also deleted were materials that were obviously not practical for an engineering application because they were explosive, extremely corrosive, or melted only at extreme pressure, etc. Table 1 is the list of materials that resulted from the literature search and preliminary material screening.

The materials finally selected from this list as most applicable for this temperature control technique were the normal paraffins containing from fourteen (14) to thirty (30) carbon atoms. Two (2) other materials (formic acid and camphene) were investigated, but discarded when tests showed that they had undesirable characteristics. Formic acid supercooled and is toxic and corrosive. Camphene cannot be readily purified. Therefore it has a wide range of melting temperature and shows erratic behavior in the solid phase.

The melt and crystalline phase transition points, and the heat of fusion (including the heat of crystalline phase transition where applicable and indicated by a transition temperature point) for the selected paraffins with even and odd number of carbon atoms are presented in Figures 2 and 3, (References 2, 4 & 6) The even paraffins show the better potential for this application. In the temperature range of interest, the paraffins with an

TABLE 1

FUSIBLE MATERIALS WITH A HEAT OF FUSION GREATER THAN 80 BTU/LB LISTED IN ORDER OF INCREASING MELT TEMPERATURE, FROM 40 TO 150°F

NO.	MATERIAL-FORMULA	MELT PT. °F	HEAT OF FUSION BTU/LB	REF.
1.	Tetradecane $C_{14}H_{30}$	42	98	2
2.	Formic Acid $HCOOH$	46	106	3
3.	Pentadecane $C_{15}H_{32}$	50	89	4
4.	Myristic Acid Ethyl Ester $CH_3(CH_2)_{12}COOC_2H_5$	51	80	5
5.	Acetic Acid CH_3CO_2H	62	80	3
6.	Hexadecane $C_{16}H_{34}$	64	102	2
7.	Lithium Chloride Ethanolate $LiCl \cdot 4C_2H_6O$	69	80	5
8.	n-Heptadecane $C_{17}H_{36}$	71	92	4
9.	d-Lactic Acid $CH_3CHOHCOOH$	79	80	5
10.	Octadecane $C_{18}H_{38}$	82	105	6
11.	13-Methyl Pentacosane $C_{26}H_{54}$	84	84	5
12.	Methyl Palmitate $C_{17}H_{34}O_2$	84	88	5
13.	Nonodecane $C_{19}H_{40}$	90	95	4
14.	2-Dimethyl-n-docosane $C_{24}H_{50}$	95	85	6
15.	Eicosane $C_{20}H_{42}$	98	106	2
16.	1-Tetradecanol $CH_3(CH_2)_{12}CH_2OH$	100	99	5
17.	Camphenilone $C_9H_{14}O$	102	88	5
18.	Caprylone $(CH_3(CH_2)_6)_2CO$	104	111	5
19.	Docosyl Bromide $C_{22}H_{45}BR$	104	87	5

TABLE 1 (Continued)

FUSIBLE MATERIALS WITH A HEAT OF FUSION GREATER THAN 80 BTU/LB LISTED IN ORDER OF INCREASING MELT TEMPERATURE, FROM 40 to 150°F

NO.	MATERIAL-FORMULA	MELT PT. °F	HEAT OF FUSION BTU/LB	REF.
20.	Heneicosane $C_{21}H_{44}$	105	92	4
21.	7-Heptadecanone $C_{17}H_{34}O$	105	86	5
22.	1-Cyclohexyloctadecane $C_{24}H_{48}$	106	94	5
23.	4-Heptadecanone $C_{17}H_{34}O$	106	85	5
24.	8-Heptadecanone $C_{17}H_{34}O$	107	87	3
25.	Cyanamide CH_2N_2	111	90	1
26.	Docosane $C_{22}H_{46}$	112	107	4
27.	Methyl Eicosanate $C_{21}H_{42}O_2$	113	98	5
28.	Tricosane $C_{23}H_{48}$	117	100	4
29.	3-Heptadecanone $C_{17}H_{34}O$	118	93	5
30.	2-Eptadecanone $C_{17}H_{34}O$	119	93	5
31.	Camphene $C_{10}H_{16}$	122	103	1
32.	9-Heptadecanone $C_{17}H_{34}O$	123	91	5
33.	Tetracosane $C_{24}H_{50}$	124	109	4
34.	Elaidic Acid $C_{18}H_{34}O_2$	124	94	1
35.	Methyl Behenate $C_{24}H_{46}O_2$	126	100	5
36.	Pentacosane $C_{25}H_{52}$	129	102	4
37.	Ethyl Lignocerate $C_{26}H_{52}O_2$	129	93	5

TABLE 1 (Continued)

FUSIBLE MATERIALS WITH A HEAT OF FUSION GREATER THAN 80 BTU/LB LISTED IN
ORDER OF INCREASING MELT TEMPERATURE, FROM 40 TO 150°F

NO.	MATERIAL -FORMULA	MELT PT. °F	HEAT OF FUSION BTU/LB	REF.
38.	Hypo Phosphoric Acid $H_4P_2O_6$	131	92	5
39.	n-Hexacosane $C_{26}H_{54}$	133	110	4
40.	Trimyristin $(C_{13}H_{27}COO)_3C_3H_3$	91 135	87 91	5
41.	Myristic Acid $C_{13}H_{27}COOH$	135	86	5
42.	Heptacosane $C_{27}H_{56}$	138	101	4
43.	Ethyl Cerotate $C_{28}H_{56}O_2$	140	96	5
44.	Octacosane $C_{28}H_{58}$	142	109	4
45.	Nonacosane $C_{29}H_{60}$	147	103	4
46.	Stearic Acid $C_{17}H_{35}CO_2H$	148	86	3
47.	Triacontane $C_{30}H_{62}$	150	108	4

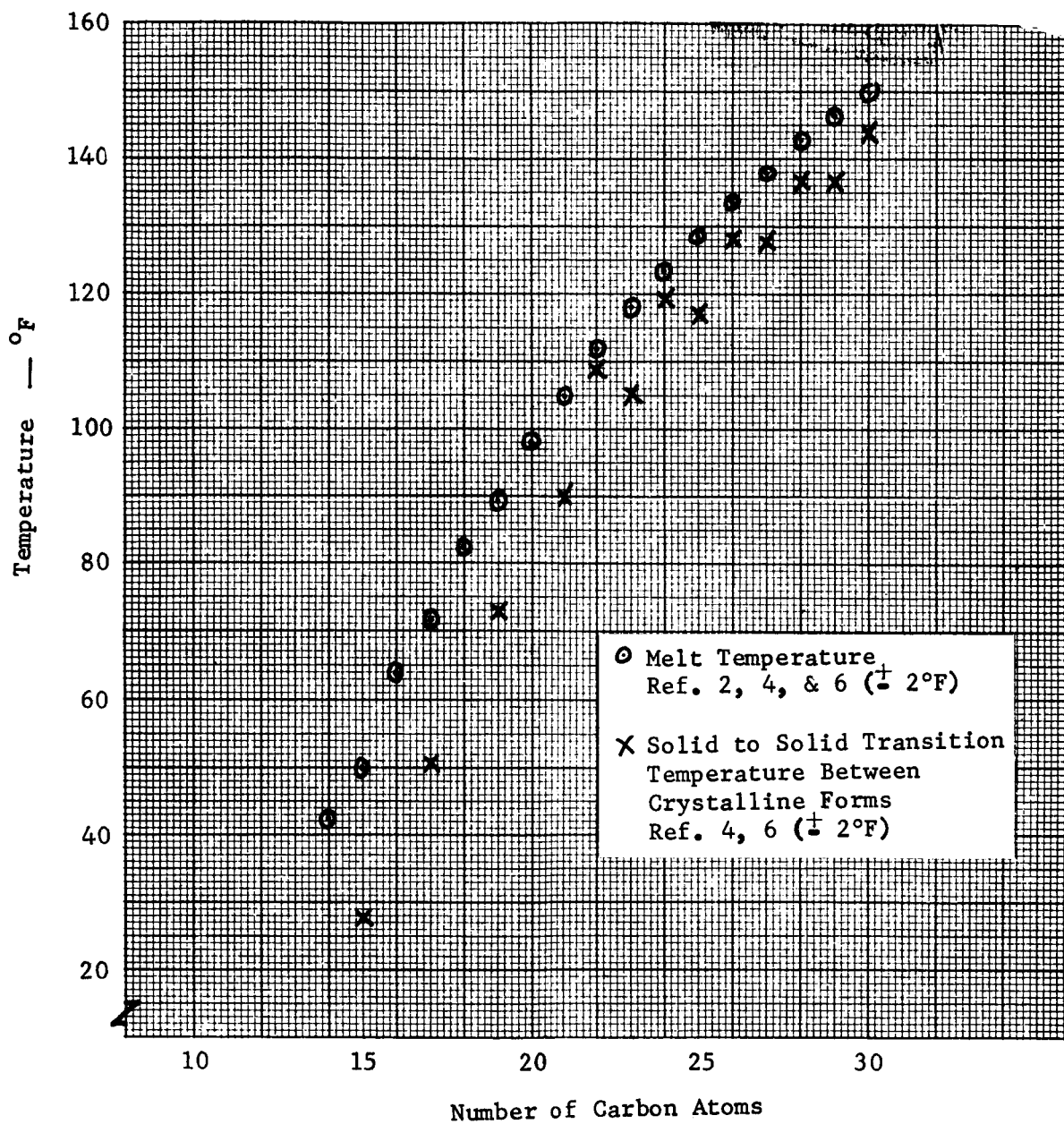


FIGURE 2 - MELT AND TRANSITION TEMPERATURE OF NORMAL PARAFFINS ($\text{C}_n\text{H}_{2n+2}$) FROM C_{14} TO C_{30} IN AIR AT 1 ATMOSPHERE

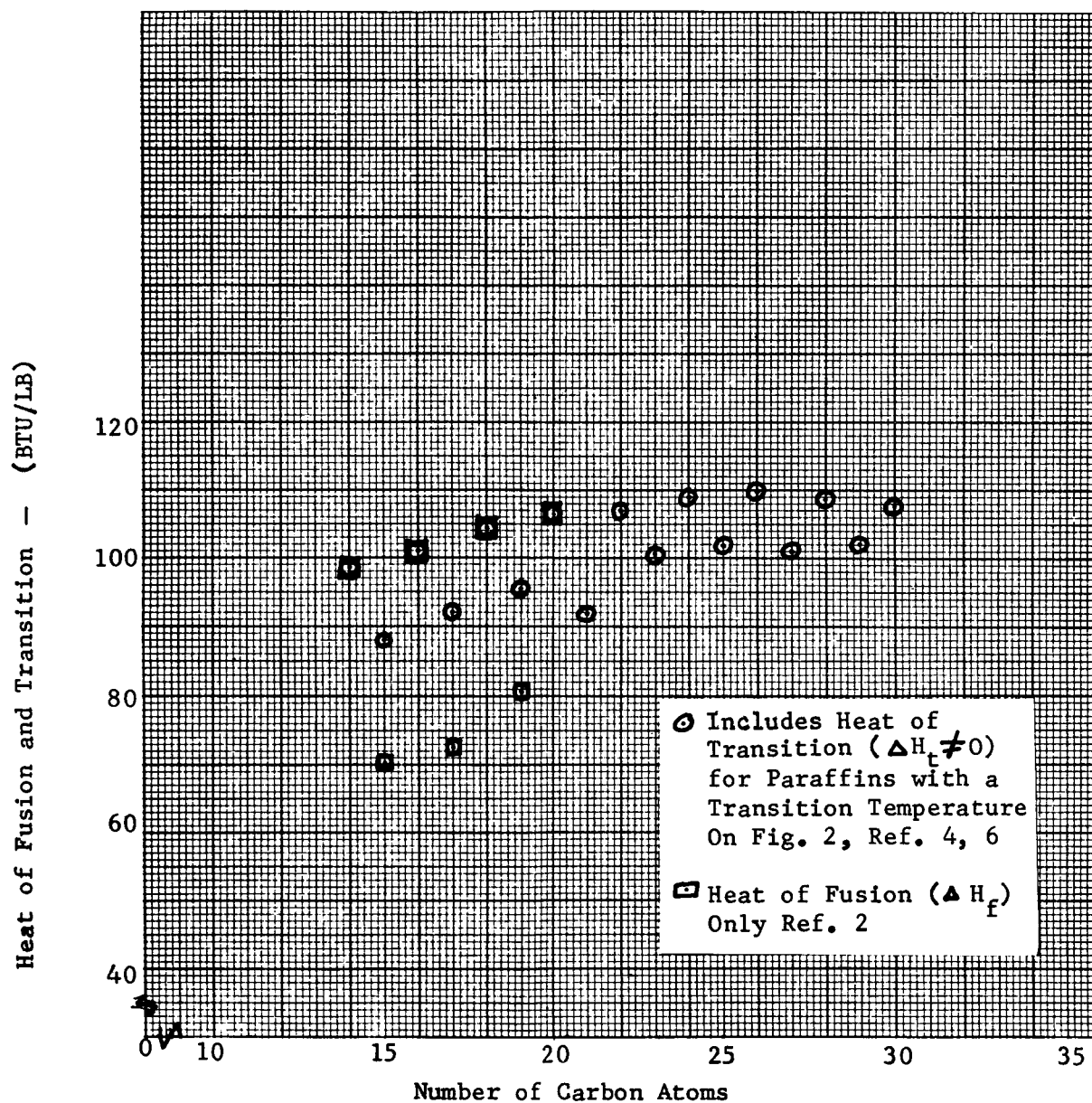


FIGURE 3 - HEAT OF FUSION AND TRANSITION OF NORMAL PARAFFINS ($C_n H_{2n+2}$)
FROM C_{14} TO C_{30}

even number of carbon atoms have higher heats of fusion and their transition temperature is closer to their melt point.

Five (5) of the even paraffins shown in Table 2 are commercially available from laboratory chemical suppliers.

TABLE 2
COMMERCIALY AVAILABLE NORMAL PARAFFINS
WITH MELT TEMPERATURE FROM 40 TO 150°F

n-Paraffin	Formula	Melt Point °F (An indication of purity)	Approximate Price for Small Lots \$/Lb
Tetradecane	C ₁₄ H ₃₀	35 - 39	13
Hexadecane	C ₁₆ H ₃₄	62 - 64	13
Octadecane	C ₁₈ H ₃₈	81 - 84	13
Eicosane	C ₂₀ H ₄₂	97 - 100	80
Octacosane	C ₂₈ H ₅₈	140 - 142	200

Four of these materials, C₁₄, C₁₆, C₁₈, and C₂₀ were selected for analytical evaluation and experiment verification of their effectiveness as fusible materials for temperature control.

Properties of Selected Materials

The selected normal paraffins have many desirable properties when compared with other materials in the specified melting temperature range. Compared to other materials, a relatively large amount of experimentally determined data of their liquid phase thermophysical properties has been published. The solid phase thermophysical properties of most of the materials in Table 1, including the paraffins could not be found in the literature. The paraffins are essentially chemically inert.

A definite advantage of the normal paraffins is the predictability of their chemical and thermophysical behavior. The number of carbon atoms (or molecular weight) and the critical temperature are common parameters used in the literature

to empirically define the thermodynamic properties of hydrocarbons. The consistency of the properties of the liquid normal paraffins appears very good, apparently due to their similar molecular structure.

The thermophysical properties of the selected materials required for the analytical evaluation (liquid thermal conductivity, specific heat and density) are presented in Figures 4 through 15. The solid densities included on Figures 4 through 7 and the vapor pressure, Figure 17, are data required for thermal control package design. The thermal conductivity of liquid eicosane or any normal paraffin of higher molecular weight could not be found in the literature. A correlation of thermal conductivity data for $C_{14}H_{30}$ to $C_{18}H_{38}$ is presented in Figure 16 as a function of the number of carbon atoms and extrapolated to $C_{20}H_{42}$, eicosane. A method presented in Reference 8 was also used to predict the thermal conductivity of eicosane. The authors stated that their method was good for hydrocarbons up to 18 carbon atoms. The reason for this statement could be that the longest chain material tested was octadecane $C_{18}H_{38}$.

Eicosane's critical temperature is required for this second method (Reference 8) and was estimated at 925°F from a correlation presented in Reference 17.

The thermal conductivity of eicosane obtained by the two methods are presented on Figure 15. The results are in good agreement with an approximate variation of 3%. Experimental verification of the thermal conductivity of eicosane is planned, but has not been completed.

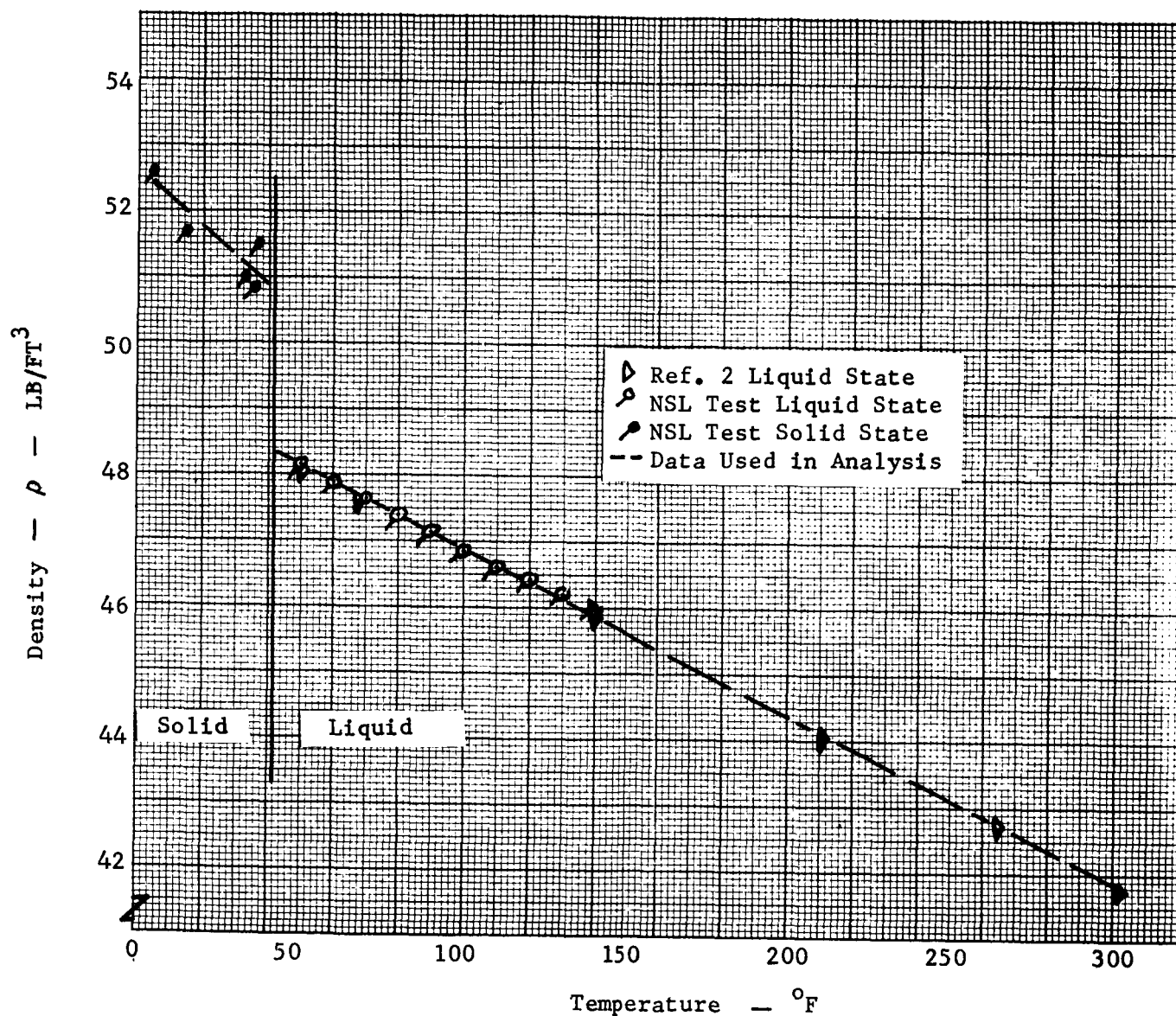


FIGURE 4 - DENSITY OF TETRADECANE ($C_{14}H_{30}$)

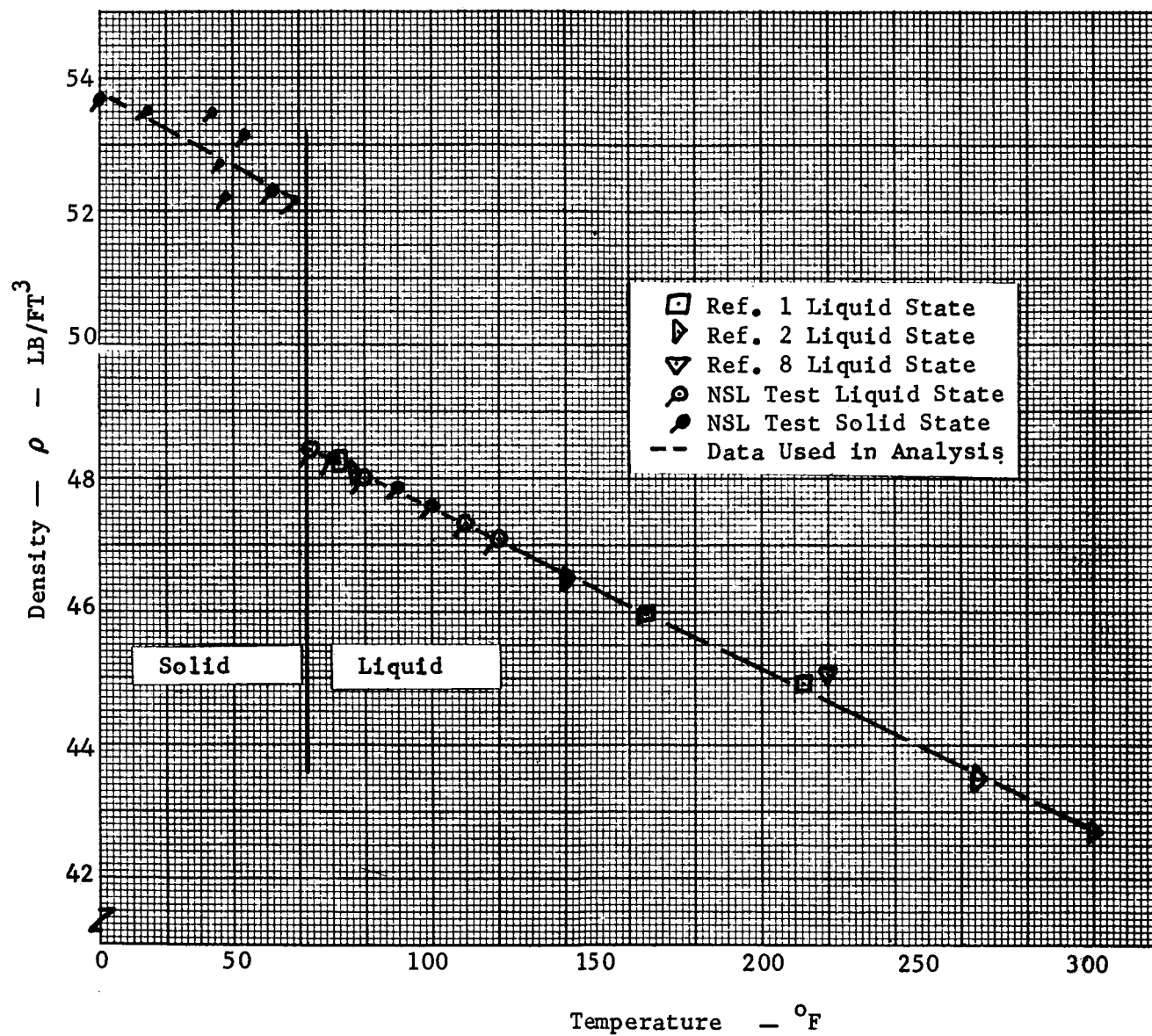


FIGURE 5 - DENSITY OF HEXADECANE ($\text{C}_{16}\text{H}_{34}$)

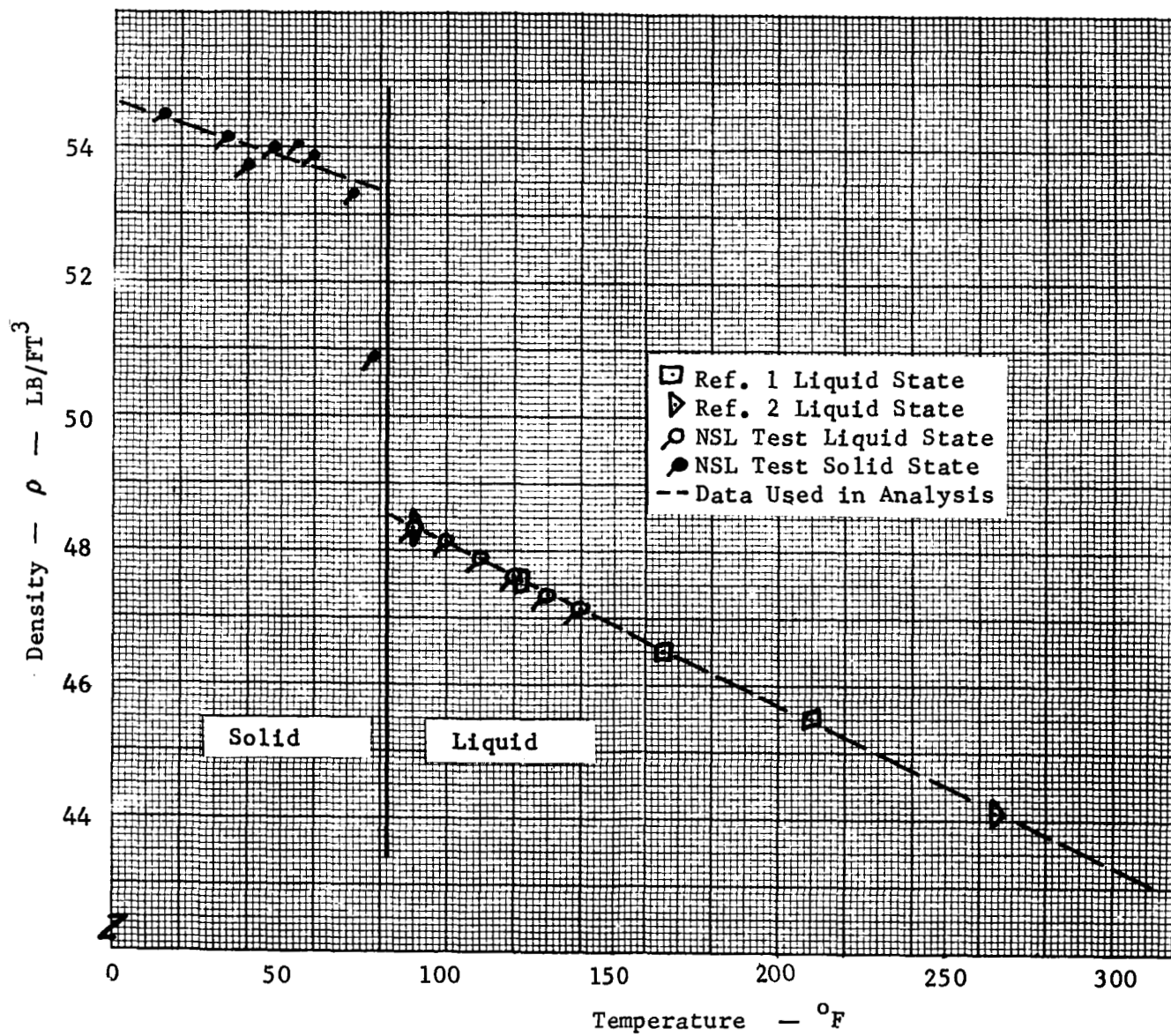


FIGURE 6 - DENSITY OF OCTADECANE ($C_{18}H_{38}$)

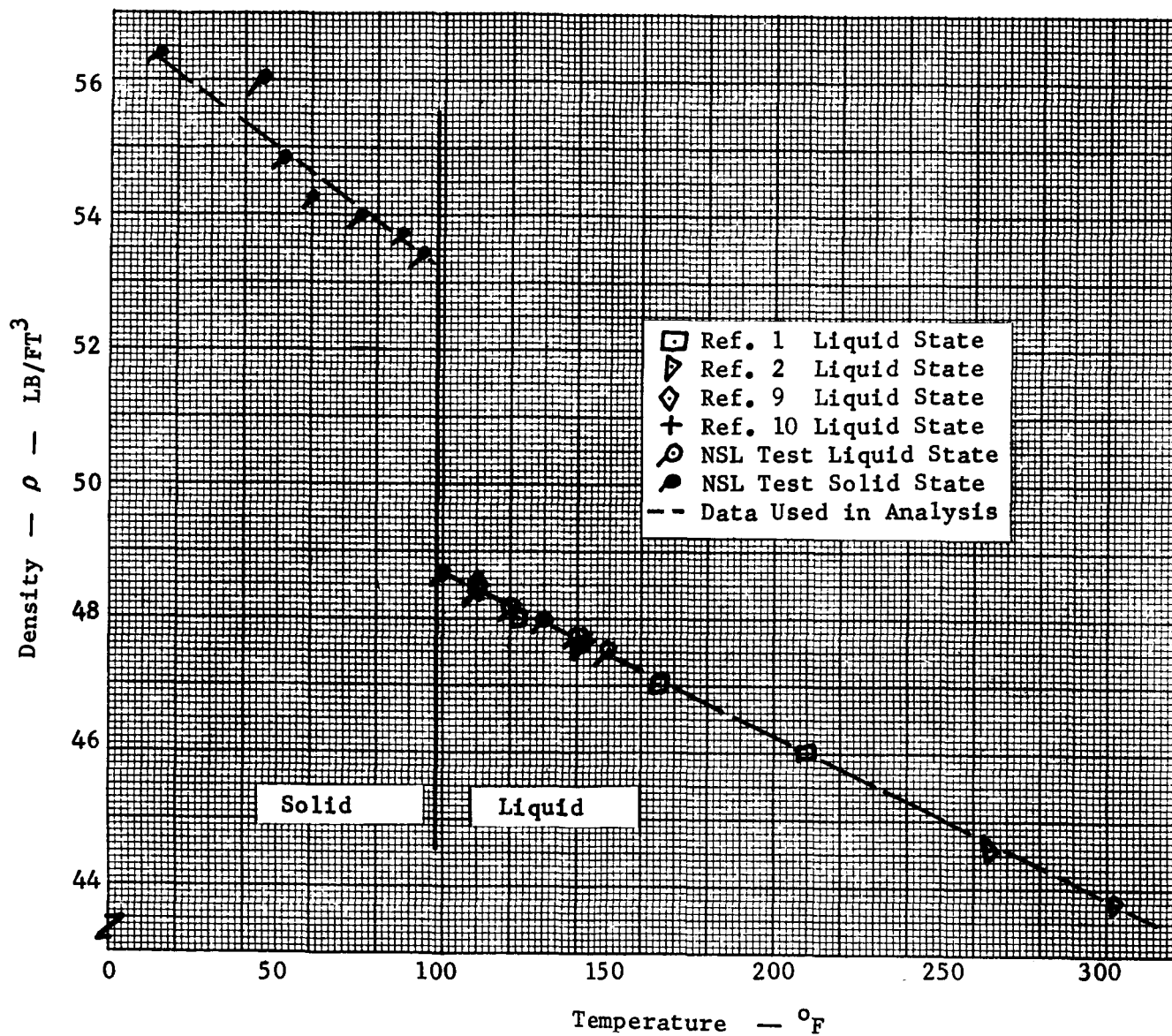


FIGURE 7 - DENSITY OF EICOSANE (C₂₀H₄₂)

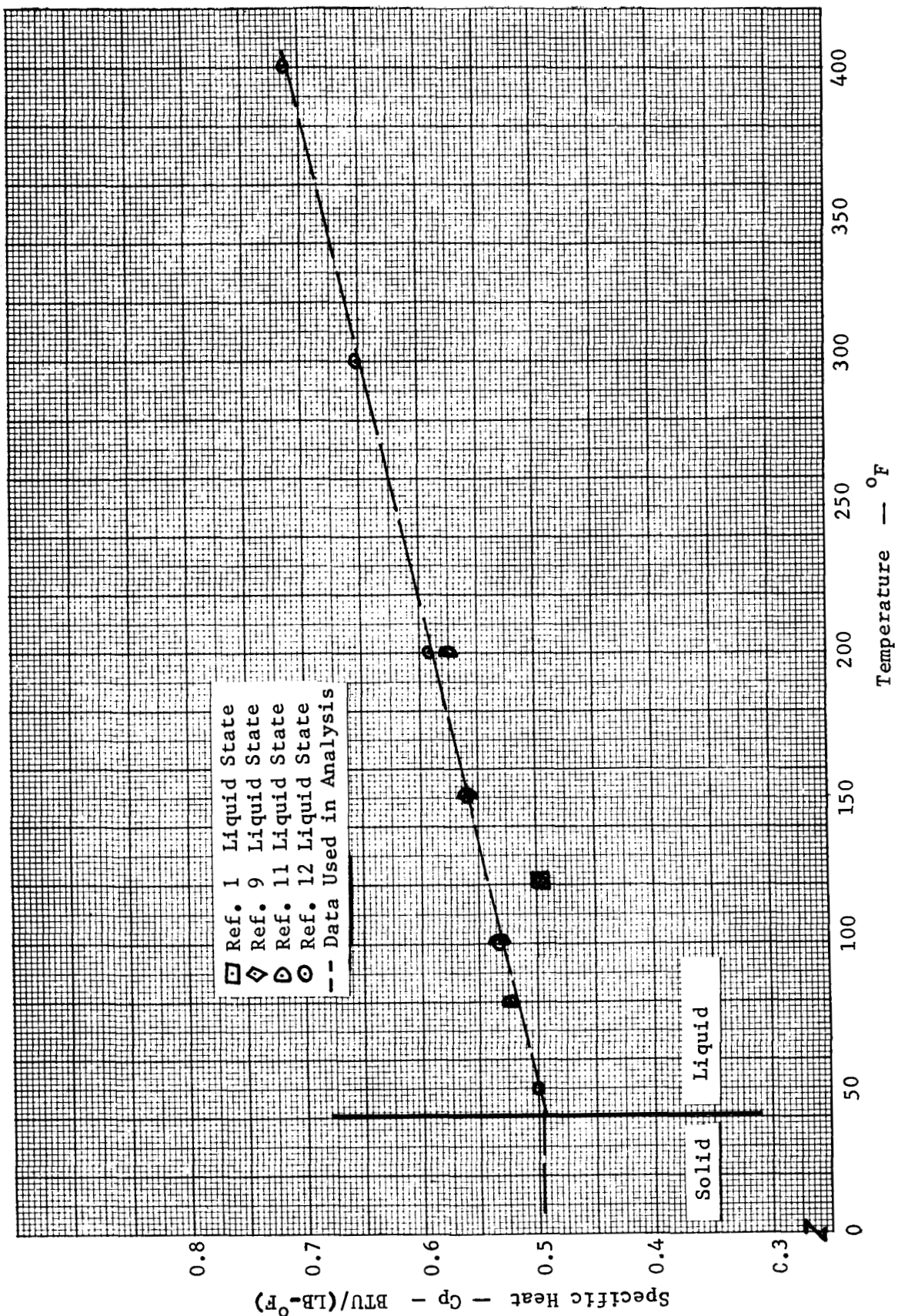


FIGURE 8 - SPECIFIC HEAT OF TETRADECANE ($C_{14}H_{30}$)

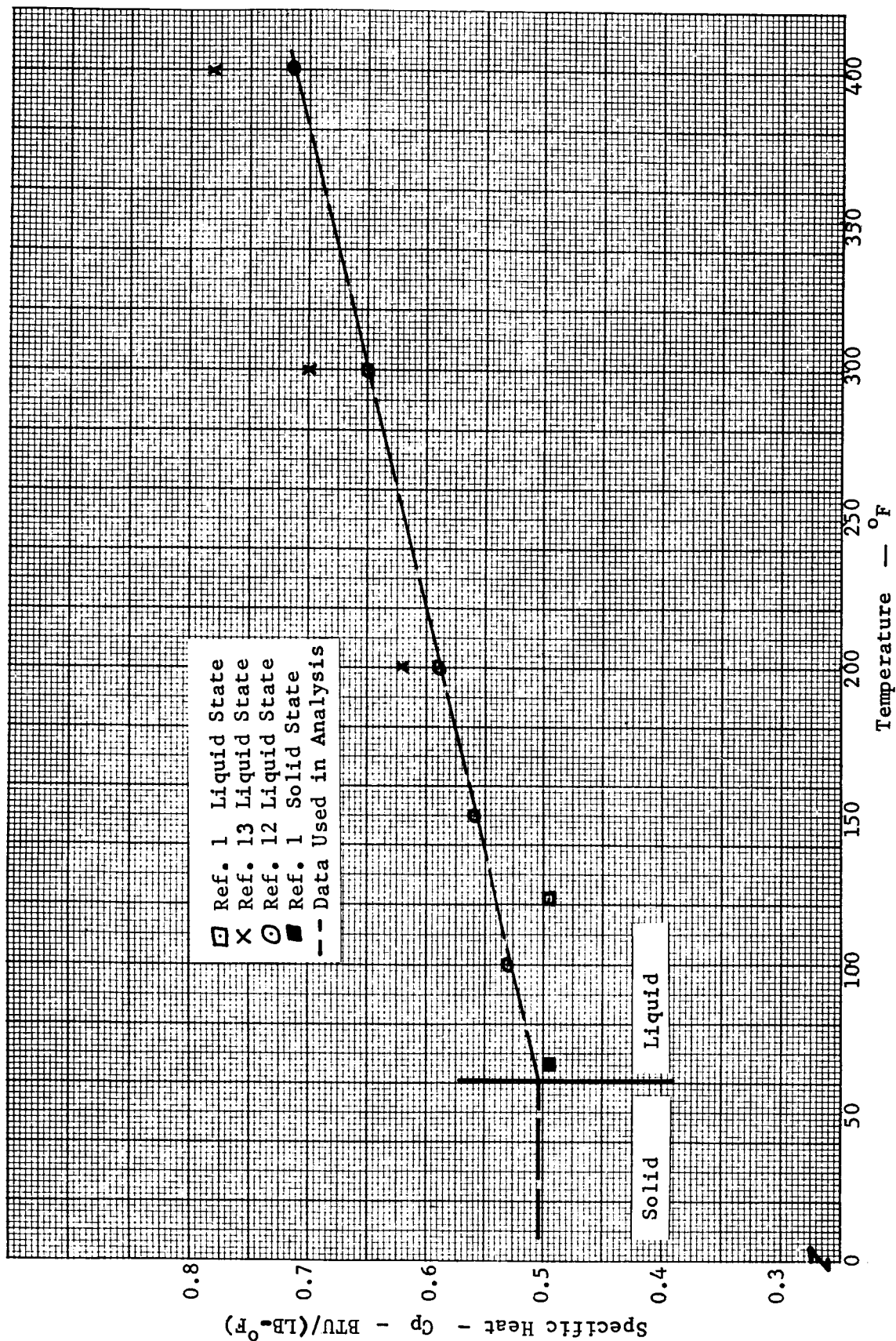


FIGURE 9 • SPECIFIC HEAT OF HEXADECANE ($C_{16}H_{34}$)

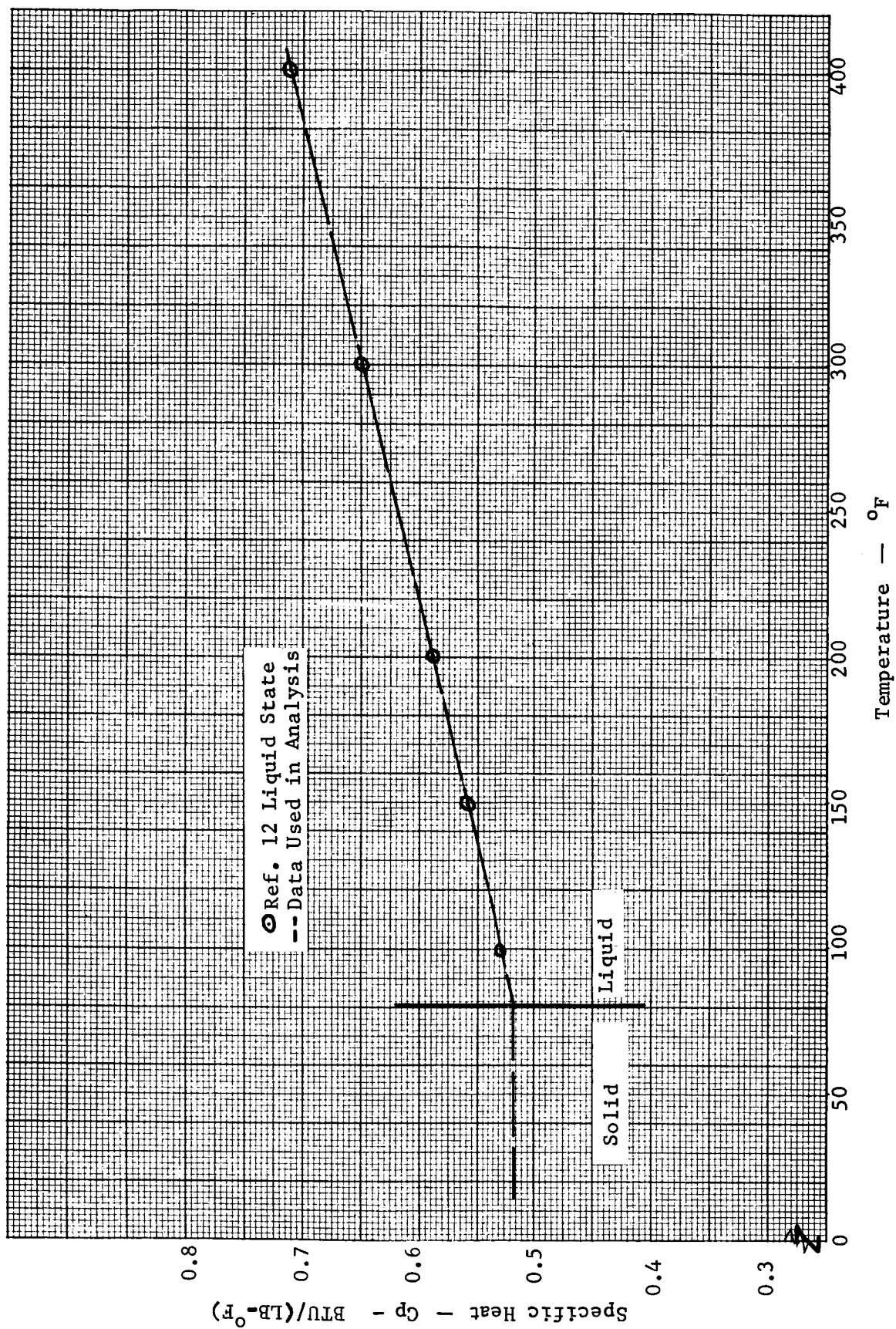


FIGURE 10 - SPECIFIC HEAT OF OCTADECANE ($C_{18}H_{38}$)

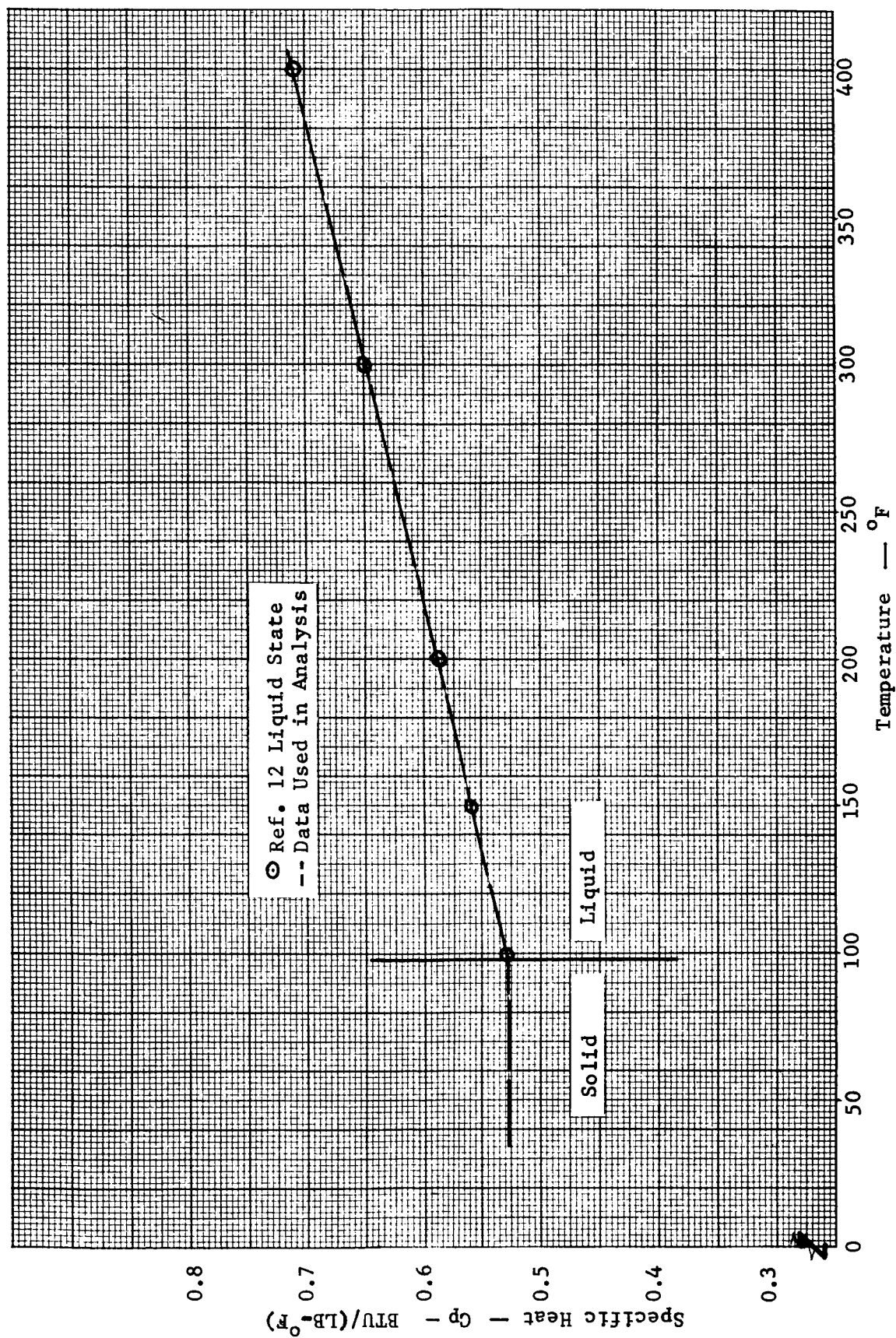


FIGURE 11 - SPECIFIC HEAT OF EICOSANE ($C_{20}H_{42}$)

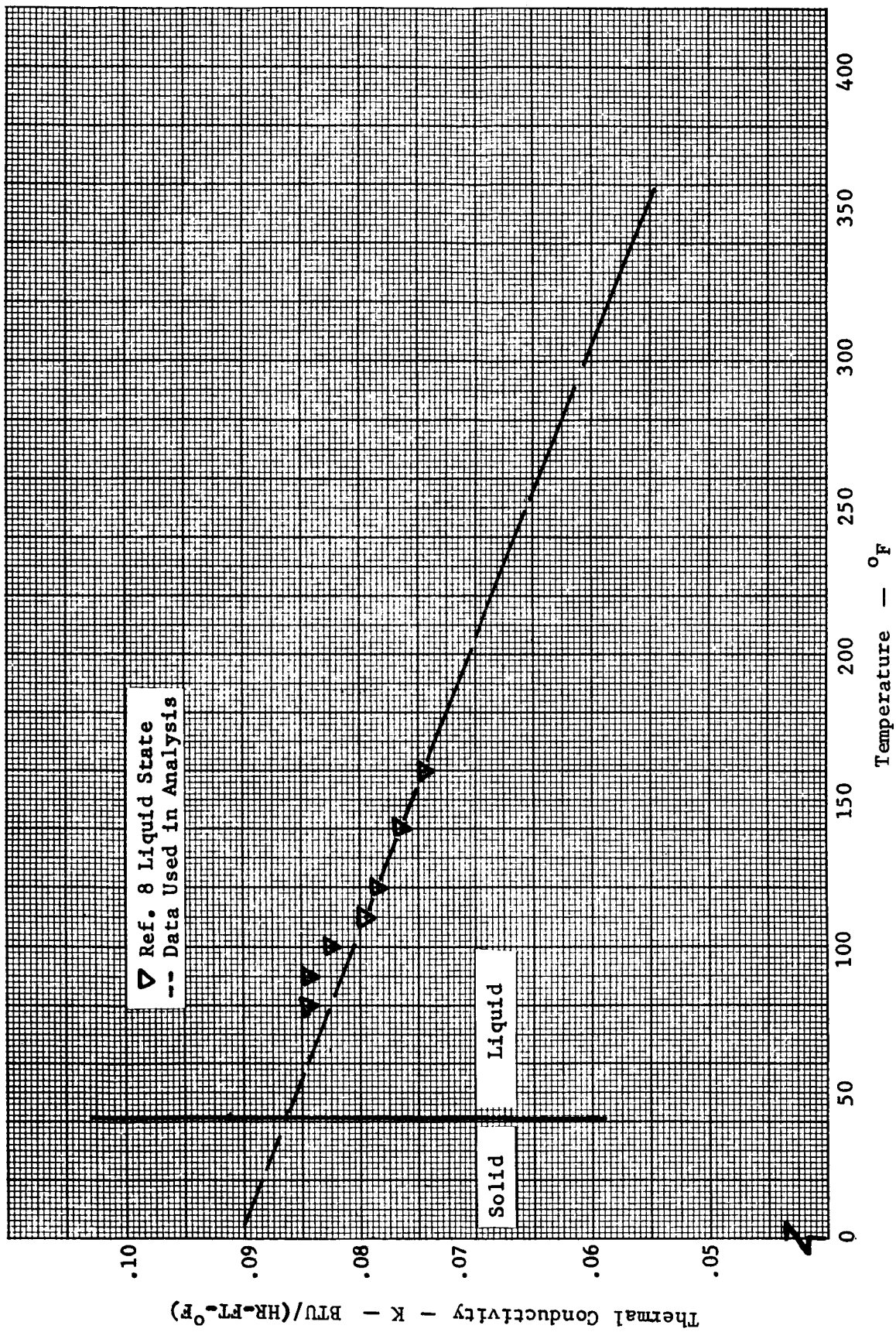


FIGURE 12 - THERMAL CONDUCTIVITY OF TETRADECANE ($C_{14}H_{30}$)

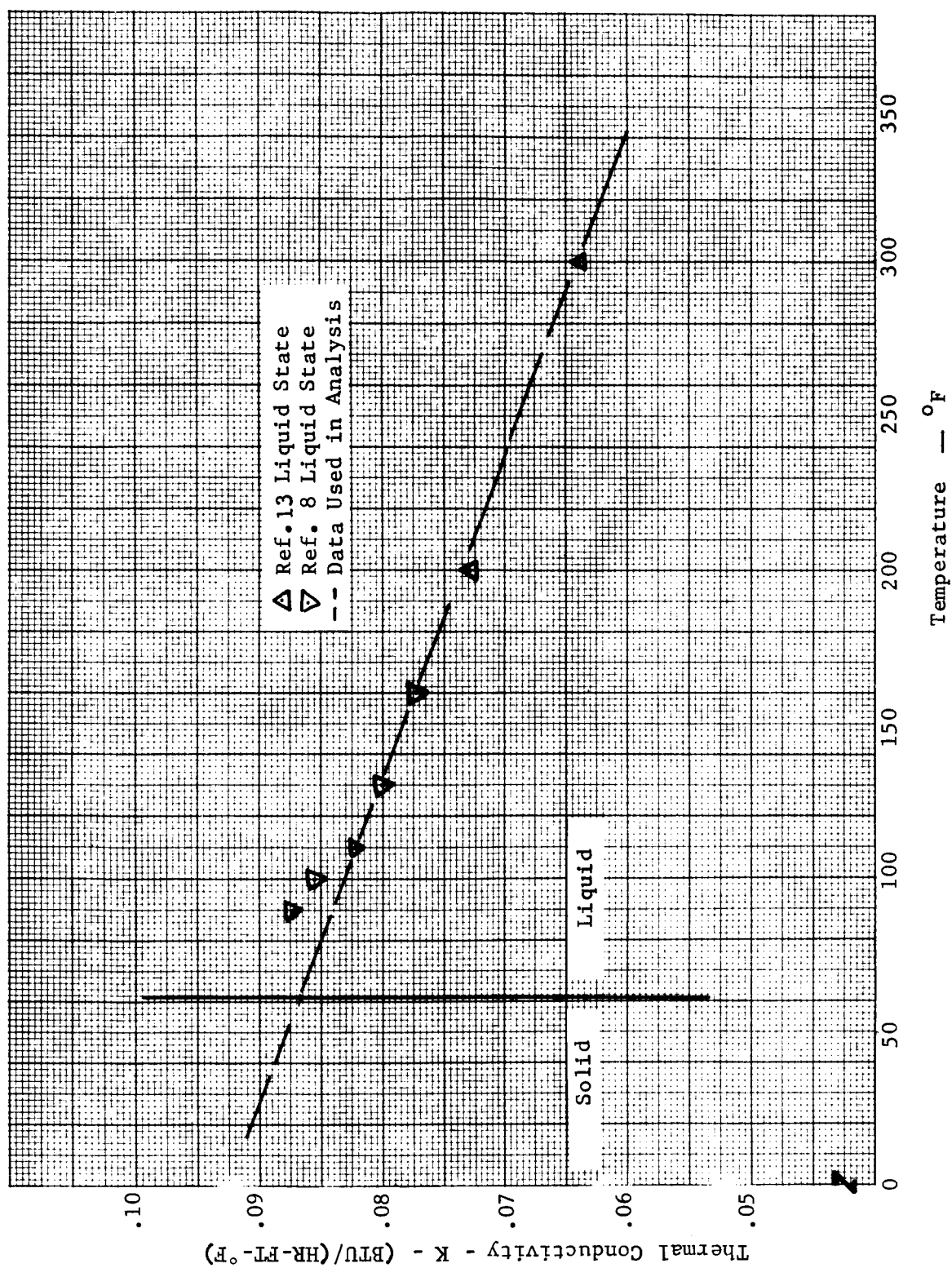


FIGURE 13 - THERMAL CONDUCTIVITY OF HEXADECANE ($C_{16}H_{34}$)

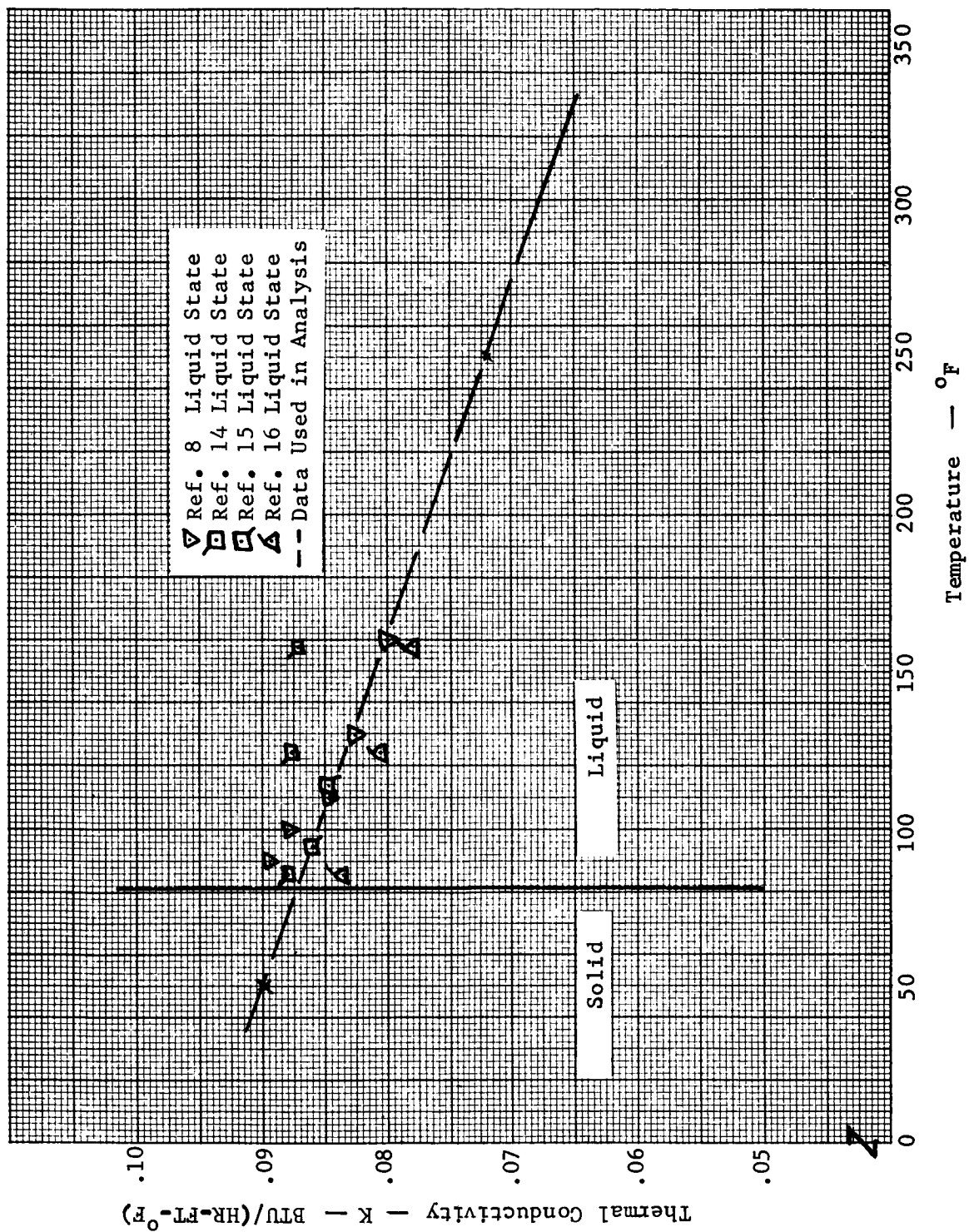


FIGURE 14 - THERMAL CONDUCTIVITY OF OCTADECANE ($\text{C}_{18}\text{H}_{38}$)

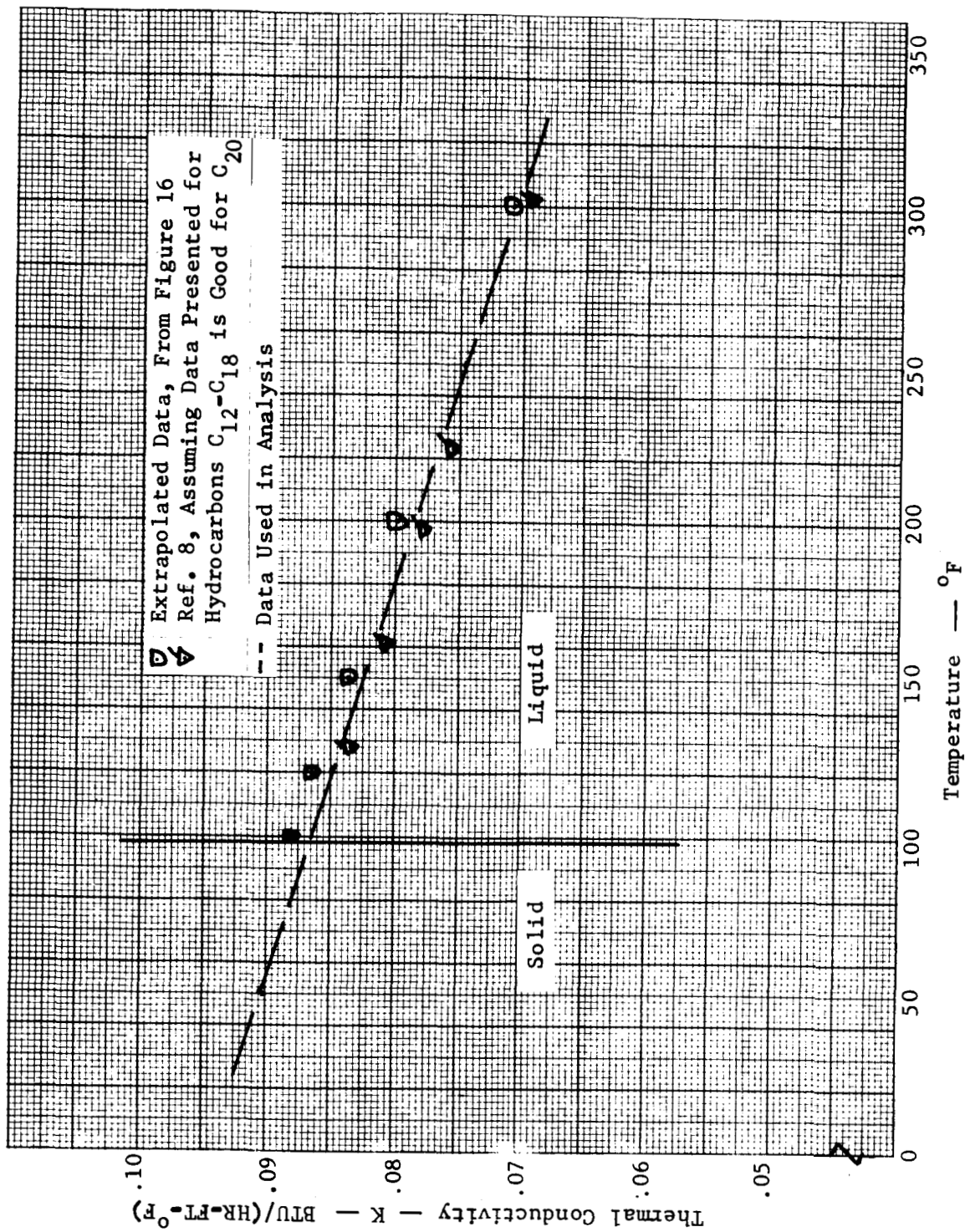


FIGURE 15 - THERMAL CONDUCTIVITY OF EICOSANE ($C_{20}H_{42}$)

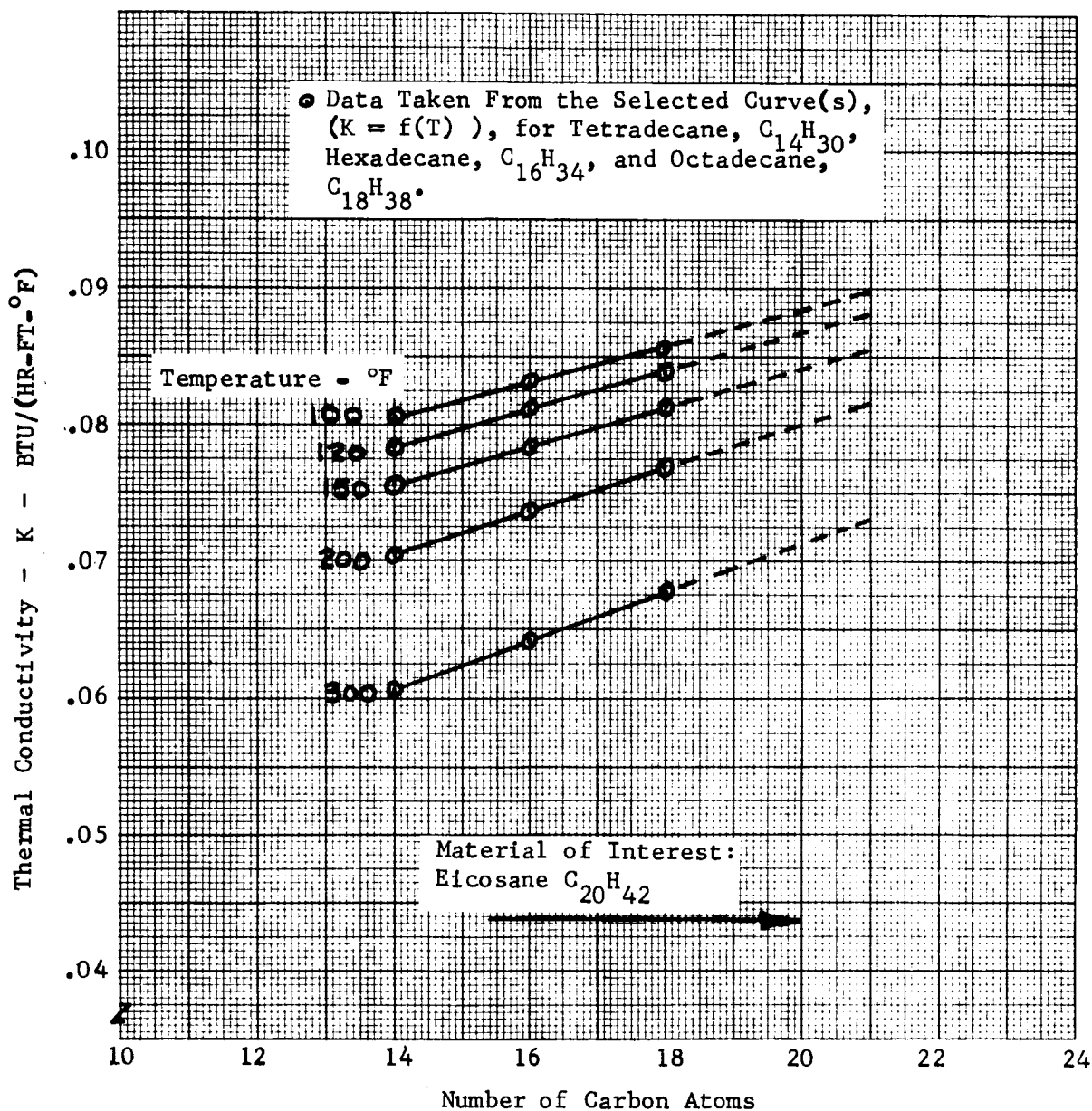


FIGURE 16 - CORRELATION OF THERMAL CONDUCTIVITY DATA FOR NORMAL
PARAFFINS ($C_n H_{2n+2}$)

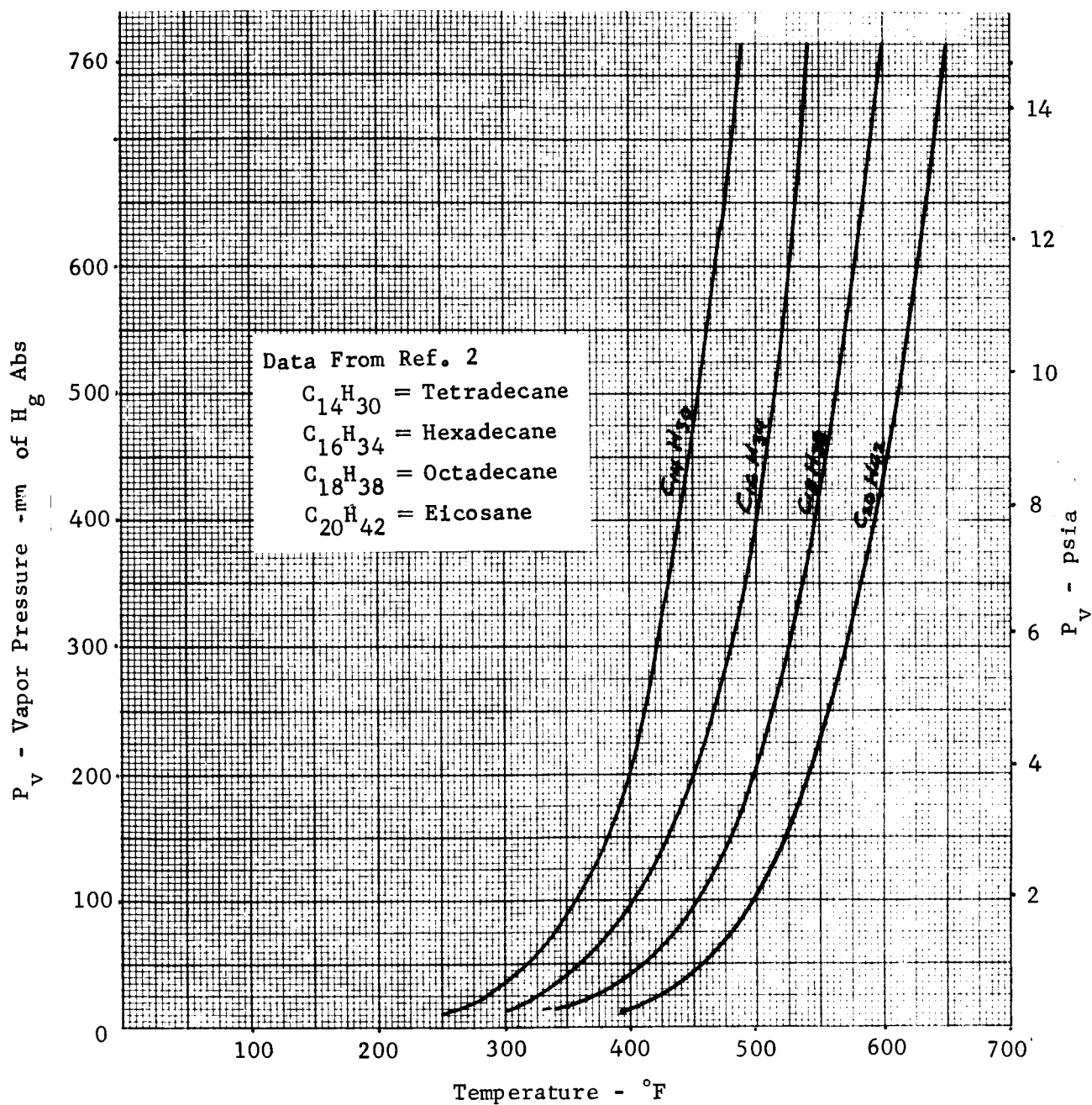


FIGURE 17 - VAPOR PRESSURE OF THE FOUR SELECTED FUSIBLE MATERIALS

NORTHROP SPACE LABORATORIES

SECTION III

EXPERIMENTAL DETERMINATION OF PROPERTIES

This experimental program had two major objectives:

1. To determine if a tentatively selected fusible material was suitable for use in the application of temperature control of space vehicle subsystems.
2. To measure the thermophysical properties of selected materials required for the thermal analysis or system design but not available in the literature or not predictable by analytical methods.

The solid and liquid densities of the selected materials were measured and the melting and solidification temperature data given in the literature verified.

Experimental Verification of Material Selection

Two of the initially selected fusible materials, camphene and formic acid, were discarded after experiments showed some undesirable properties. They were replaced by two normal paraffins, tetradecane and eicosane, which showed more desirable properties. The reasons for the discontinuation of these materials was a drastic super-cooling effect with formic acid and the erratic behavior of camphene in the solid phase.

During the series of tests on camphene the measured melting temperature varied from 105-115°F for samples from the same batch of material. When solidifying, camphene appeared to segregate into more than one crystalline form. It also out-gassed upon melting even after being heated to near boiling for two hours, and held under a vacuum to remove dissolved air. It was concluded that the commercially available compound is probably the racemic mixture dl-camphene plus other impurities, with thermo physical properties depending on the composition. This was also indicated by the wide melt point range, (Table 3) given by the suppliers.

Table 3

Comparison of Fusion Properties of Selected Materials

	Formic Acid	Tetradecane	Camphene	Eicosane	Hexadecane	Octadecane
<u>Heat of Fusion</u>						
From: Literature, BTU/lb	106	98	103	106	102	105
<u>Melt Temperature</u> (°F)						
From:						
Literature	46	42	122	98	64	82
Supplier	--	35-39	95-113	97-100	62-64	81-84
NSL Test	47	41	105-115	98	61	81
Supercooling to (°F)	33-35	None Observed	No sharp com- plete crystal- lization point	None Observed	None Observed	None Observed

The experiments on formic acid showed that it super cooled below the melt temperature. This phenomenon was investigated by cooling the acid in a graduated cylinder slowly below its melting point, while continuously monitoring its temperature. It would supercool to a temperature range of 33°F-35°F before the material solidified. After solidification, the solid material would cool in a linear fashion. No further work on how this super cooling effect can be avoided was performed. The formic acid melted at 47°F.

The tests performed on paraffinic hydrocarbons (hexadecane and octadecane) showed that they behave dependably. Additional members of this family appeared to be desirable choices.

Two normal paraffins that have desirable thermophysical properties close to those of formic acid HCOOH and camphene $\text{C}_{10}\text{H}_{16}$ are tetradecane $\text{C}_{14}\text{H}_{30}$ and eicosane $\text{C}_{20}\text{H}_{42}$ as shown in Table 3. The only data required to perform the thermal analysis for these materials and not available in the literature is the thermal conductivity of liquid eicosane. This was equally true of camphene. However, due to the family behavior of the normal paraffins, analytical prediction of the thermal conductivity of eicosane should be reliable. Another advantage of these paraffins when compared with formic acid and camphene are their low vapor pressures, Figure 17. This minimizes the container design problem.

Melting and Solidification Point

The melting points of the four paraffin materials were checked using melting point capillary tubes immersed in a constant temperature bath. The observed variation of the melt point of the four normal paraffins during testing was less than 1 degree F. Observed differences between solidification point and melt point were also less than 1 degree F for the paraffins, indicating absence of any significant supercooling effects. The data for camphene and formic acid were discussed in the preceding sections. Table 3 presents the melt points observed, those presented in the literature and the values indicated by the supplier for the selected paraffins, camphene and formic acid.

Density Measurements

The density of tetradecane, hexadecane, octadecane and eicosane were measured in both the liquid and solid state. The test results are presented on Table 4 and 5 respectively and on Figures 4 through 7. Also included on Tables 4 and 5 are some density results for camphene and formic acid.

The liquid density measurements were made using standard density determination methods with a Reischauer pycnometer. The estimated precision of these measurements was ± 0.002 g/ml. The liquid density measured varies linearly as a function of temperature from just above the melting points, to the 150 degree F range. The results are in good agreement with the data available in the literature.

TABLE 4
RESULTS OF DENSITY MEASUREMENT
OF LIQUID FUSIBLE MATERIAL
(gm/ml)

Temp. (°F)	Formic Acid HCOOH	Camphene C ₁₀ H ₁₆	Tetradecane C ₁₄ H ₃₀	Hexadecane C ₁₆ H ₃₄	Octadecane C ₁₈ H ₃₈	Eicosane C ₂₀ H ₄₂
40	1.237*					
50			.771			
60	1.220		.767			
62				.776		
70			.763	.773		
80	1.208		.759	.769		
90	1.202		.755	.766	.774	
100	1.194		.751	.762	.771	.780
110	1.187		.747	.758	.767	.776
120	1.181	.849	.744	.754	.763	.772
130		.844	.740		.759	.768
140		.840	.736		.755	.765
150						.761

*supercooled liquid

NSL 65-16

TABLE 5
RESULTS OF DENSITY MEASUREMENT
OF SOLID FUSIBLE MATERIAL
(gm/ml)

Temp. (°F)	Formic Acid HCOOH	Camphene C ₁₀ H ₁₆	Tetradecane C ₁₄ H ₃₀	Hexadecane C ₁₆ H ₃₄	Octadecane C ₁₈ H ₃₈	Eicosane C ₂₀ H ₄₂
0				.860		
5			.842			
15			.828	.857	.872	.903
34			.817	.857	.868	
36			.814	.844		
38			.825	.837		
40		.849		.820	.860	
44				.852		
46						.899
48					.865	
52				.838		.878
55					.866	
59				.835		
60					.863	.869
76					.854	.865
80		.877			.814	
88						.861
94						.856
100		.887				
110		.878				

The solid density measurements were obtained with a modified Reischauer pycnometer method after more standard test methods proved unsatisfactory. Several attempts at the flotation method and at the technique of weighing pressed pellets proved unreliable. The apparent major difficulties encountered in the solid density measurements of the normal paraffins were the tendency for the materials to either trap or dissolve air or to "funnel" during solidification, leaving voids in the solid mass. These difficulties were circumvented by adding the liquid material slowly to the pycnometer while slowly lowering the pycnometer into a constant temperature bath kept at the desired temperature of the solid density measurement. This method assured solidification of the liquid layer on the surface of a solid phase already at the desired temperature for the density measurement. Prior to use in the experiment, the liquid material had been placed in a bell jar and a vacuum applied to "degas" any dissolved air. This combination of techniques ensured a compact solid mass in the pycnometer which was free of voids and dissolved air. Despite the painstaking care used in laying down a compact mass of material in the pycnometer, the density values obtained showed a wide variation. This effect seemed to be most pronounced in the temperature range just below the melting points of the respective paraffins. After many repeated trials in a very narrow temperature range, it became apparent that these results were due to the properties of the materials themselves rather than to faulty experimental technique.

A subsequent referral to chemical literature pertaining to the thermophysical properties of the n-paraffinic hydrocarbons indicated that the long chain paraffins possess a solid to solid transition point close to the melt temperature. This transition point is the temperature at which the hydrocarbon passes between two different crystal structures in the solid phase. However, for even number of carbon atom paraffins, the transition point appears to approach the melt temperature with decreasing carbon atoms.

At $C_{20}H_{42}$ the transition point practically coincides with the melting point, Reference 4. This would indicate that the selected materials $C_{14}H_{30}$ to $C_{20}H_{42}$

do not have a high temperature solid transition, and that the measured density variations are due to impurities.

Since the solid density values were needed primarily for temperature control package design information, the values obtained were considered of adequate accuracy and further detailed investigation did not appear justified. The estimated precision of the solid density measurements is ± 0.02 g/ml. No information on the solid densities of these hydrocarbons could be found in the literature for comparison, as was the case with some of the liquid density measurement results.

Measurements of Thermal Conductivity of Liquids

An apparatus for measuring the thermal conductivity of liquids was selected from Reference 18 and is shown in Figure 18. Reported agreement between known and measured values of thermal conductivity of some common liquids indicate that this method of determining thermal conductivities is reliable. Tests for verification of the thermal conductivity (k) of liquid eicosane have not been performed at this time.

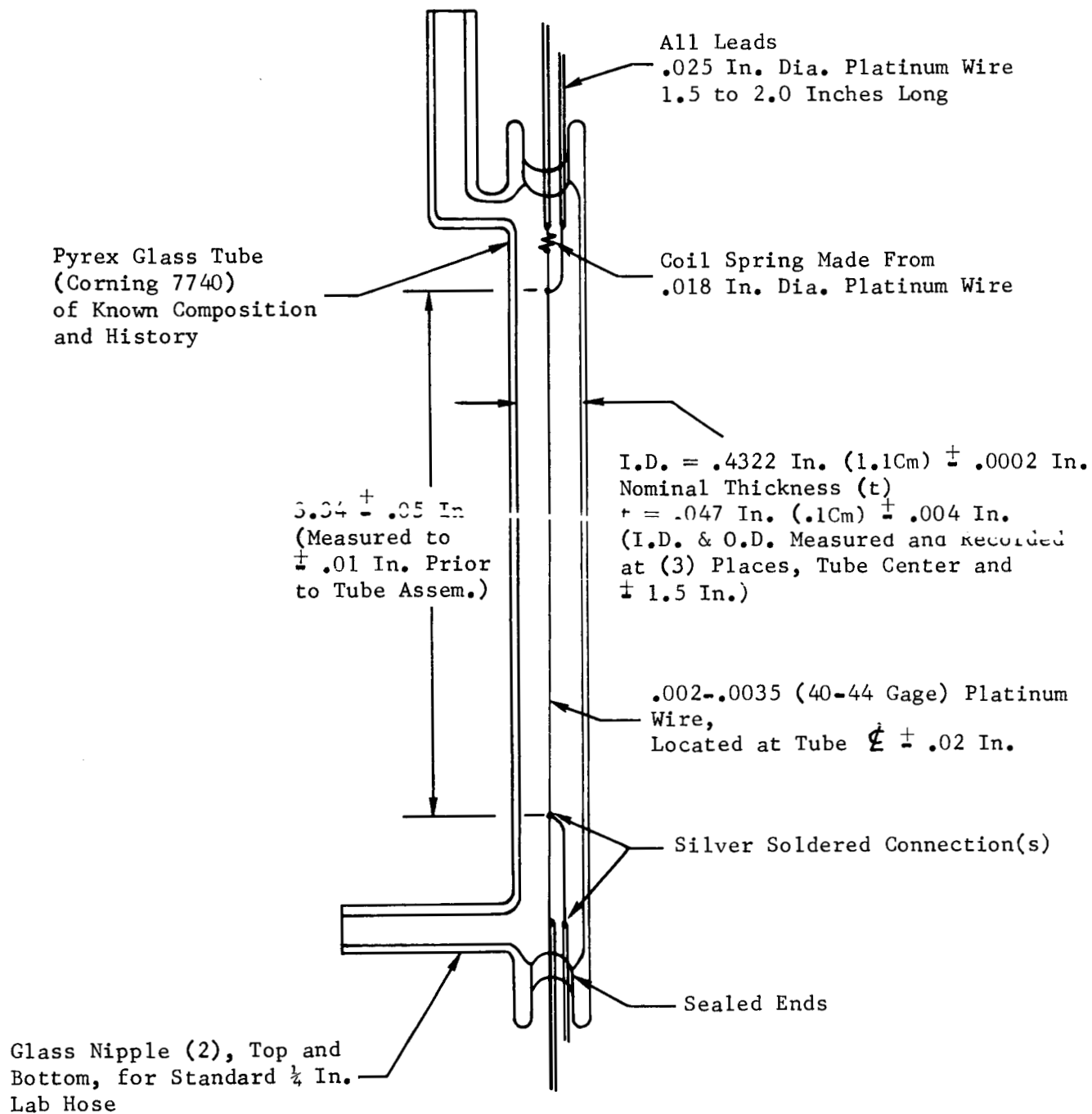


FIGURE 18 - CELL FOR MEASURING THERMAL CONDUCTIVITY OF LIQUIDS

NORTHROP SPACE LABORATORIES

SECTION IV

THERMAL ANALYSIS

The performance analysis of the two methods of temperature control using fusible material was conducted on a high speed digital computer. The basic computer program and analytical method used in the analysis are discussed under the heading "Transient Thermal Analysis Technique". The analytical models, preliminary analysis, boundary conditions and assumptions are described under the heading "Analytical Models and Preliminary Analysis". The results of the analysis are presented graphically and discussed under the heading "Performance of Temperature Control Systems".

Transient Thermal Analysis Techniques

The transient thermal analysis for the two temperature control systems studies were performed on the IBM 7090 digital computer with a modified SHARE Thermal Network Analyzer Program, Reference 19. This program produces a temperature history for a physical system which has, through the concept of lumped parameters, been expressed as a finite difference electrical analog of the heat transfer problem. The physical parameters are represented by a thermal resistance-thermal capacitance network with the capability of heat input at any of the discrete "nodes" in the network. A solution for the temperature at all nodes is calculated at the end of each of a series of finite time steps $\Delta\theta$. The heat balance which is solved for the temperature at each node at time $\theta + \Delta\theta$ is:

$$T_{\theta+\Delta\theta,i} = \frac{\Delta\theta}{C_i} \left(\sum_j \frac{T_{\theta,j}}{R_{ij}} + Q_i - T_{\theta,i} \sum_j \frac{1}{R_{ij}} \right) + T_{\theta,i} \quad (1)$$

where:

- $T_{\theta+\Delta\theta,i}$ = the temperature of node i at time $\theta + \Delta\theta$
- $T_{\theta,i}$ = the temperature of node i at time θ
- $\Delta\theta$ = time increment
- C_i = the capacitance of node i
- \sum_j = summation over all nodes connected by a resistor to node i

R_{ij} = the resistance between node i and any connected node j
 Q_i = the heat rate into node i from sources other than conduction, convection or radiation from neighboring nodes

If the capacitance value C_i is zero, the expression solved is:

$$T_{\theta} + \Delta\theta, i = \frac{\sum_j \frac{T_{\theta, i}}{R_{ij}} + Q_i}{\sum_j \frac{1}{R_{ij}}} \quad (2)$$

When any node "i" has phase transition capability, program control is transferred to the Latent Heat Subroutine after the temperature of all the nodes in the network have been calculated at time $\theta + \Delta\theta$.

The Latent Heat Subroutine computes the phase transition heat balance in the following manner. All the required parameters from the previous calculation interval (θ) are saved by the main program or the Latent Heat Subroutine. The temperatures at time (θ) and ($\theta + \Delta\theta$) are compared with the nodes phase transition temperatures (melting T_1 and boiling T_2). When the previous temperature (T_{θ}) is not equal to the phase transition point (T_1 or T_2) and the temperature change calculated in the main program ($T_{\theta} - T_{\theta + \Delta\theta}$) has not passed through a phase transition point, the node temperature remains $T_{\theta + \Delta\theta}$ as calculated in the main program. When the node was at a phase transition temperature (T_1 or T_2) or starts phase transition:

$$T_{\theta + \Delta\theta} \geq T_1 \text{ or } T_2 \text{ for } T_{\theta} \leq T_1 \text{ or } T_2$$

or:

$$T_{\theta + \Delta\theta} \leq T_1 \text{ or } T_2 \text{ for } T_{\theta} \geq T_1 \text{ or } T_2$$

The total heat flux (\bar{q}_i) to the node during transition is calculated:

$$\bar{q}_i = \Delta\theta \left(\sum_j \frac{T_{\theta j}}{R_{ij}} + Q_i - T_{\theta, i} \sum_j \frac{1}{R_{ij}} \right) + \Delta q_i \quad (3)$$

where:

Δq_i = the heat flux to node i during transition prior to time $(\theta + \Delta\theta)$;
equal to zero if the node was not in phase change at time (θ) .

The heat flux \bar{q}_i is then compared to the node's latent heat H_L of the respective transition mode (melting or boiling). When the heat flux \bar{q}_i is not sufficient for phase change, the node temperature at time $\theta + \Delta\theta$ is set equal to the transition temperature and Δq_i is set equal to \bar{q}_i . When the heat flux $|\bar{q}_i|$ is greater than the latent heat required for transition, a new temperature for time $(\theta + \Delta\theta)$ is calculated:

$$T_{\theta + \Delta\theta} = T_T + \frac{|\bar{q}_i| - H_L}{C_i} \quad (4)$$

where:

$$T_T = T_1 \text{ or } T_2$$

The node temperature is increased or decreased depending on the sign of the total heat flux \bar{q}_i .

This subroutine was modified from the SHARE Program, Reference 19, which did not allow for sensible temperature rise at the calculation time interval when a node passed through the transition phase (Equation 4). The SHARE routine was also modified so that the partial heat of transition \bar{q}_i was accounted for with a change of direction in phase transition.

For thermal radiation, a pseudo resistance is calculated by Equation (5) and used in the same way as a simple conductive resistance in the temperature solution, Equation (1).

$$R_{ij} = \frac{1}{K_{ij} \left\{ (T_i + 459.6)^2 + (T_j + 459.6)^2 \right\} \times \left\{ T_i + 459.6 + T_j + 459.6 \right\}} \quad (5)$$

where K_{ij} is input data for computing the radiation resistance between nodes i and j. T_i and T_j are in degrees Fahrenheit.

The time interval used to advance the time in the transient solution is related to the physical parameters of the network. In particular, $\Delta \theta$ must not exceed the minimum RC product for the network as this will result in an instability in the solution of Equation (1), causing an undamped oscillation of the temperatures for those nodes whose RC product is smaller than $\Delta \theta$. The RC product of any node is in the foregoing nomenclature:

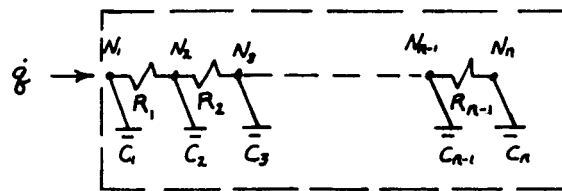
$$(RC)_i = \frac{C_i}{\sum_j 1/R_{ij}} \quad (6)$$

The SHARE Program was further modified to facilitate usage as applied to the analytical model of each of the temperature control systems and to conserve computer time. The modifications were extensive for the fin and fusible material two dimensional system which required a larger array of nodes and resistances.

Analytical Models and Preliminary Analysis

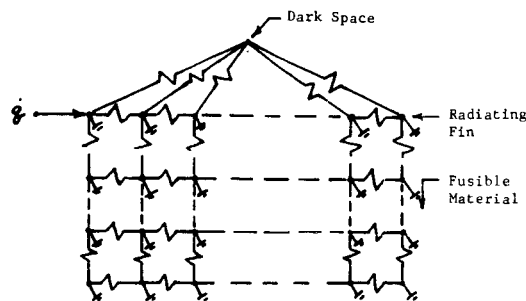
The mathematical representation of the two models of temperature control systems using fusible material was performed with an electrical analog and finite difference technique. This method of analysis uses finite nodes of constant temperature for each calculation time interval. The nodes are defined by lumped parameters and connected by a resistance network. The electrical analog network for the one dimensional adiabatic system and the radiating fin with attached fusible material are presented on Figures 19 and 20. The node size and spacing were kept continuous where possible to facilitate computer program usage. The nodes at material boundary and heating points were reduced in size by one-half to define a " π " network, Reference 19. This approach more closely predicts the boundary temperature by better representing the actual differential equations than a continuous network.

The thermal properties required for the analysis: Conductance, Capacitance, Latent Heat and Melt Temperature, are presented for the four fusible materials studied (even n-paraffin $C_{14}H_{30}$ to $C_{20}H_{42}$) on Figures 21 and 22, in a form

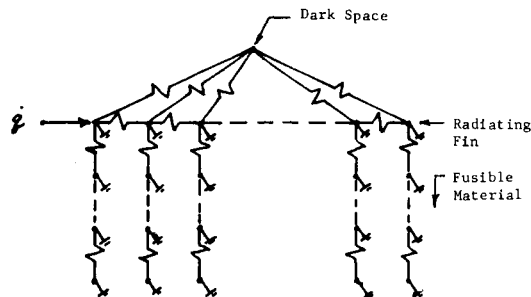


Electrical Analog
 \dot{q} = Heat Input To Node 1
 N = Nodes of Constant Temperature at Any Time Increment
 C = Node Thermal Capacity
 $C_2 = C_3 = C_n$, $C_1 = C_n / 2.0$
 R = Thermal Resistance
 $R_1 = R_2 = R_n$

FIGURE 19 - ANALYTICAL MODEL (1-D) ADIABATIC SYSTEM



Correct Electrical Analog



\dot{q} = Heat Input To Node 1
 N = Nodes of Constant Temperature at Any Time Increment
 C = Node Thermal Capacity
 R = Thermal Resistance

Simplified Electrical Analog
 Used in Final Analysis

FIGURE 20 - ANALYTICAL MODEL (2-D) SYSTEM OF RADIATING FIN WITH ATTACHED FUSIBLE MATERIAL

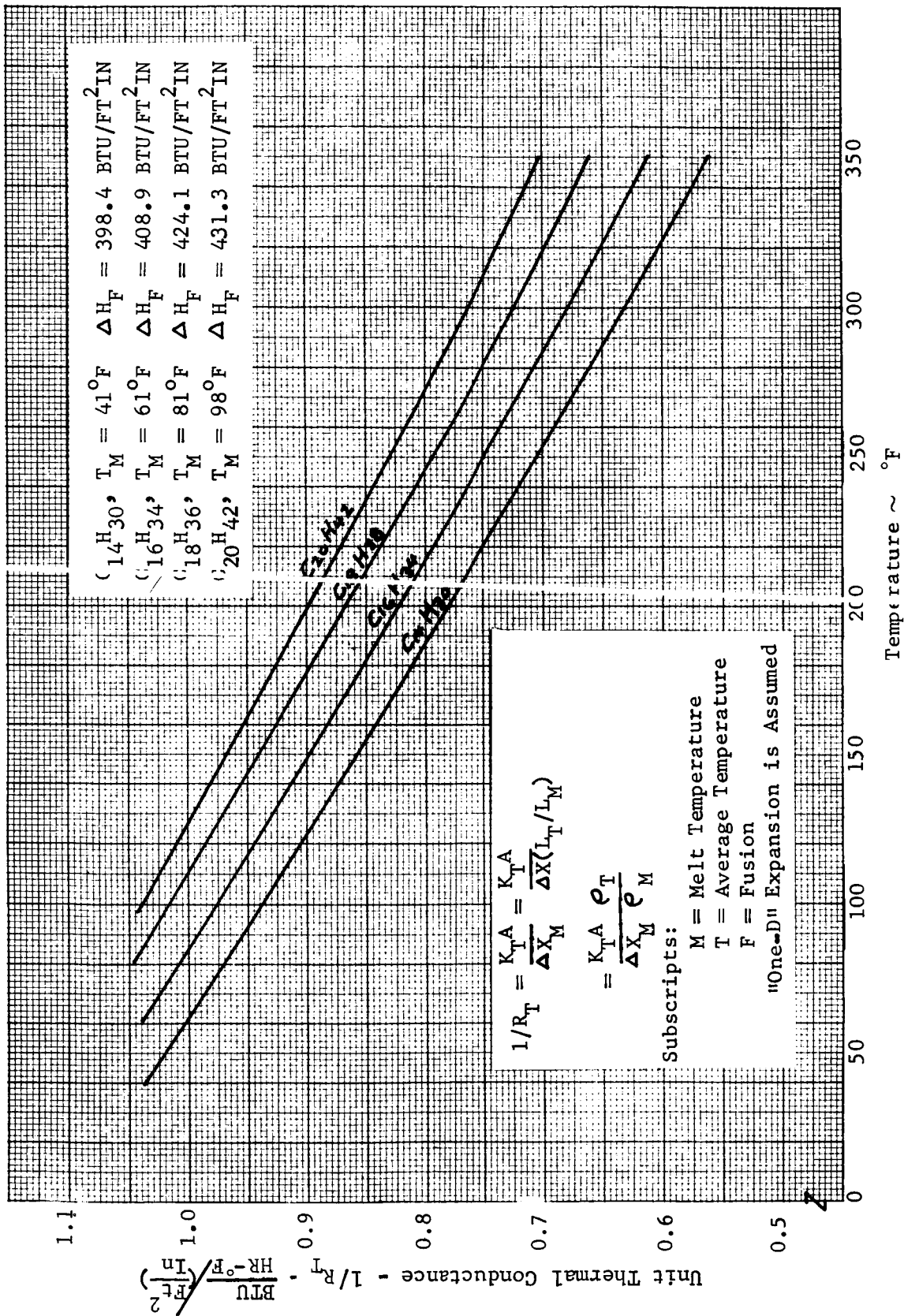


FIGURE 21 THERMAL CONDUCTANCE OF SELECTED MATERIALS
FOR A SLAB ONE SQUARE FOOT BY ONE INCH THICK

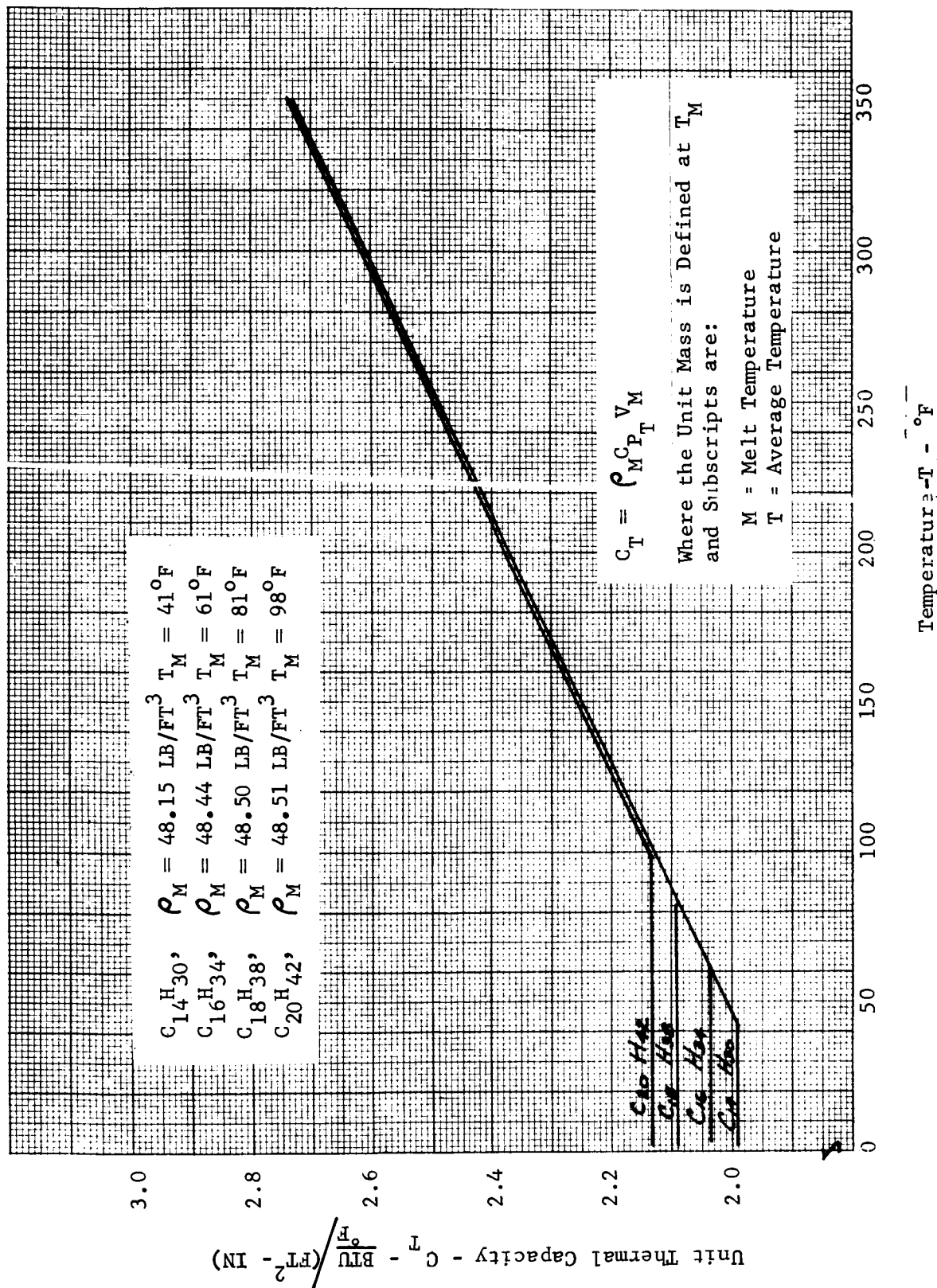


FIGURE 22 - THERMAL CAPACITY OF SELECTED MATERIALS
FOR A SLAB ONE SQUARE FOOT BY ONE INCH THICK

required for the computer program. The actual resistance, capacitance and latent heat for any size node and network arrangement is obtained by the ratio of the actual dimensions to the unit-dimensions presented on the figures.

One Dimensional Adiabatic System. This analysis was performed for a one square foot cross section of fusible material semi-infinite slab with five constant heat input rates at node 1, Figure 19, with no heat exchange at the other boundaries. The selected node thickness was .016667 inches for node 1, and .03333 inches for the remaining nodes. This node size was selected for the final analysis after a sensitivity analysis was performed to obtain good temperature stability (a smooth increase in the temperature of the melted material) and a steady progression of melt thickness.

There is a trade-off between program stability versus computer time. The analysis became unstable when the ratio of latent heat to heat rate $\frac{n_L/\dot{q}}{(\frac{\text{BTU/node}}{\text{BTU/hour}})}$ increased above .1. This ratio varied from approximately .015 to .075 for the heating rates and materials used in this analysis. For program stability, the computation was started with the first node one degree below melt point and the following node temperatures decreasing by .1°F per node.

Radiating Fin With Attached Fusible Material. The first step of this analysis was to select a typical fin size for the transient analysis. The fin analysis could not be generalized because of the temperature decay along the fin length which is a function of fin material, length and thickness. An optimum fin thickness study was performed for a fin of 4, 8 and 12 inches in length using the procedure presented in Reference 20. The results are presented on Figure 23. The theoretical minimum weight thickness is marginal in structural requirements for a spacecraft's exterior skin with electronic gear directly mounted to it, and therefore, .05 inches (Figure 23) was selected as the minimum fin thickness for this study. The assumed fin material is aluminum with a thermal conductivity of 120 BTU/Hr-Ft-°F and a surface coating having an infrared emissivity of .90. The radiative fin's steady state temperature distribution was calculated by an analytical method by J. W. Tatom in Reference 21 and checked by the transient

Flat Plate Radiating From One Side Only
Optimum Weight Configuration (Ref. 20)

Environmental Parameter

$$\frac{q_{in}}{q_{out}} = \frac{\text{External Radiation to Fin}}{\text{Radiation From Fin}}$$

Fin Effectiveness

$$\Omega = \frac{\text{Radiation From Fin}}{\text{Radiation From Fin at Constant Temperature, (Equal to Root Temperature)}}$$

— $q_{in} = 0.$, $\Omega = .57$, For Minimum Weight Fin

— — $q_{in} = .5q_{out}$, $\Omega = .31$ For Minimum Weight Fin

— — — Selected Fin Thickness for Study of Radiator Mounted Heat Sources (Electronic Equipment) = .05 Inches

$$\epsilon_{IR} = .9$$

$$K = 120 \text{ BTU/HR-FT-}^\circ\text{F}$$

Fin Thickness - δ - Inches

0.10

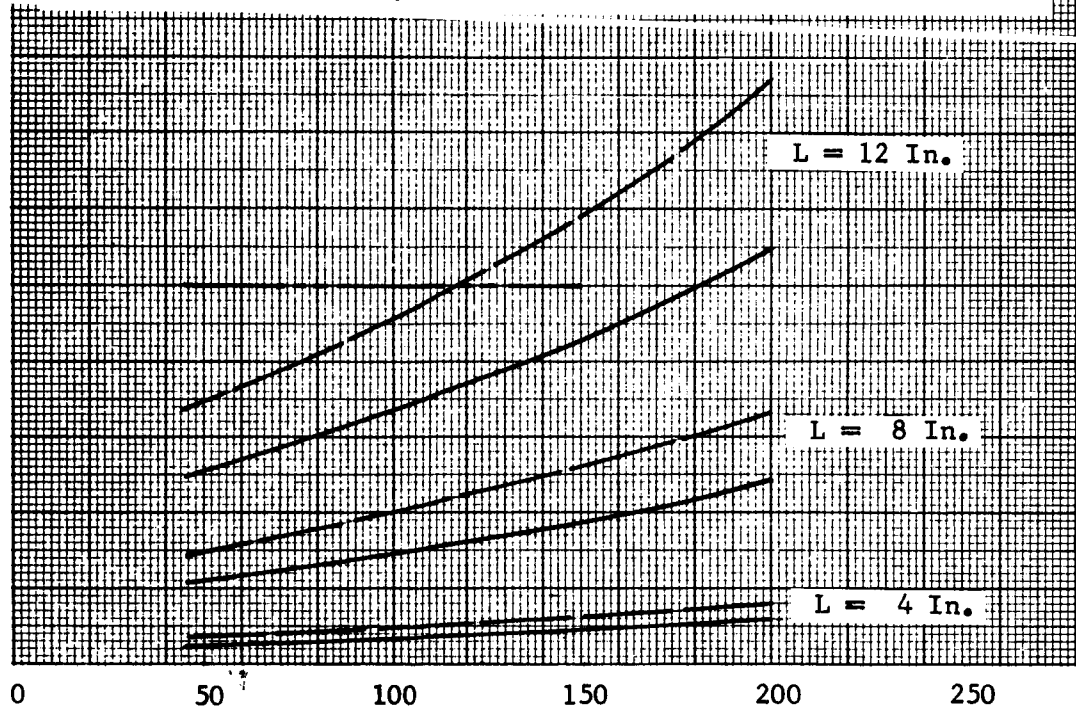
0.08

0.06

0.04

0.02

0



Root Temperature - T_R - $^\circ\text{F}$

FIGURE 23 - RADIATING FIN THICKNESS SELECTION AND COMPARISON

computer program of Reference 19, which was allowed to reach steady state. The sink was deep space with an assumed temperature of zero degree Rankine. The results were in good agreement and the procedure of J. W. Tatom was used to calculate fin temperature distribution for the three fin lengths with root temperature equal to the melt point of octadecane.

The transient analysis was performed for a fin with octadecane as the attached fusible material. Therefore, the results for a fin root temperature of 82°F, the melt-point of octadecane, are presented. The radiating fin tip temperature and total heat dissipation as a function of fin length are presented on Figure 24. The steady state fin temperature distribution for a 4, 8 and 12 inch fin are shown on Figure 25.

Including a solid fusible material at the non-radiating (rear) of a radiator fin will not significantly affect the longitudinal steady-state temperature distribution. This is because the ratio of thermal conductivity of aluminum to the fusible material is:

$$\frac{K_{\text{alum.}}}{K_{\text{fus. mat.}}} \simeq \frac{100}{1} = 10^3$$

and the thickness ratio will be less than:

$$\frac{\Delta X_{\text{alum.}}}{\Delta X_{\text{fus. mat.}}} < \frac{.05}{.5} = 10^{-1}$$

or the overall thermal resistance ratio:

$$\frac{R_{\text{alum.}}}{R_{\text{fus. mat.}}} \simeq \frac{1}{100}$$

Figures 24 and 25 show the decay of fin temperature as a function of fin length, for the assumed fin thickness of .05 inches. The addition of fusible material to the thermally radiating fin is useful only for a fin length where fin temperature is above the melt point of the fusible material. As Figure 24 shows,

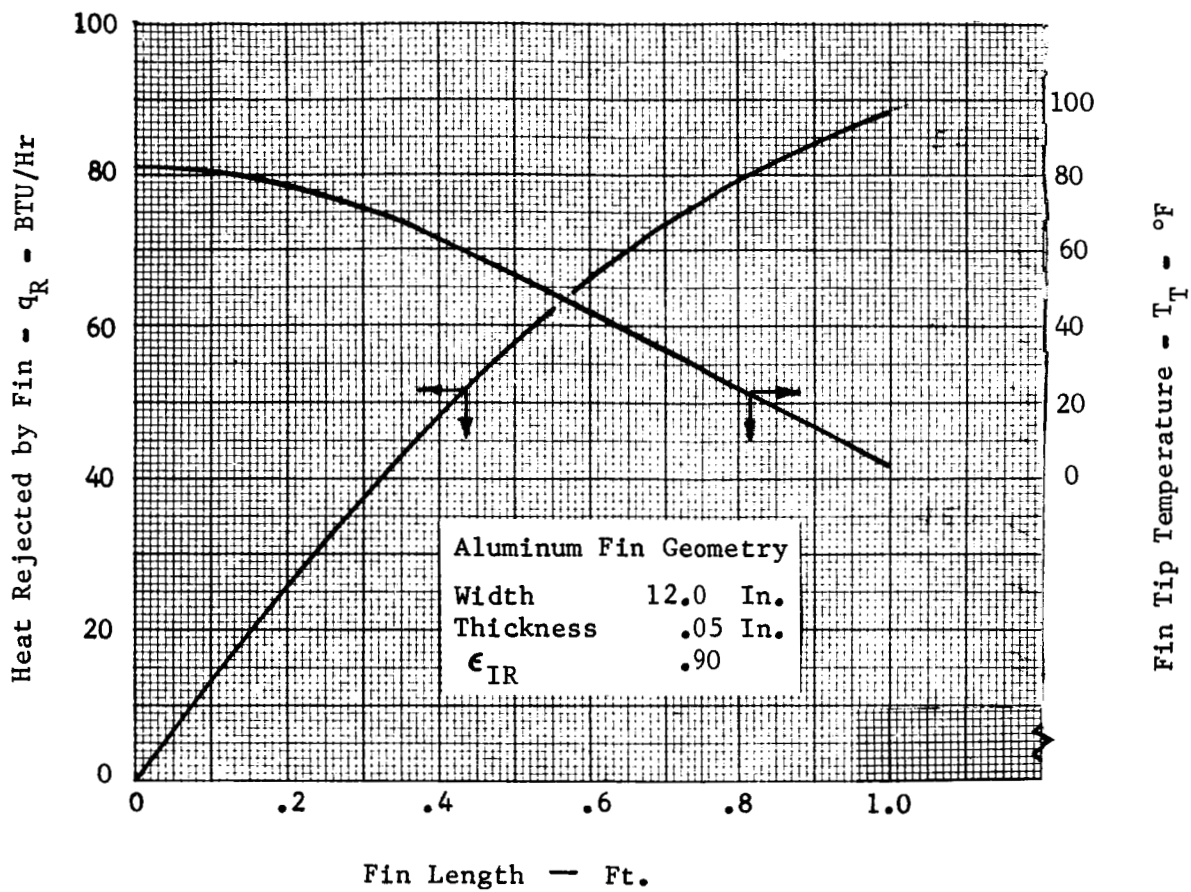


FIGURE 24 - RADIATING FIN PERFORMANCE

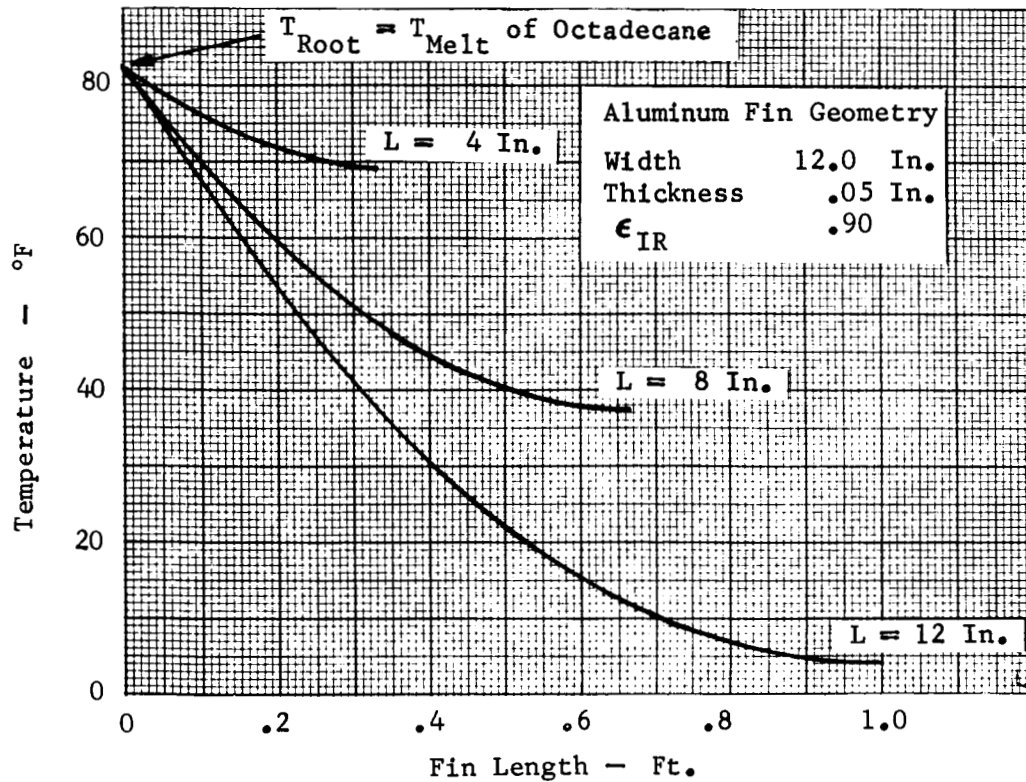


FIGURE 25 - RADIATING FIN TEMPERATURE DISTRIBUTION

the rate of temperature decay increases with fin length up to about .4 feet where it becomes essentially linear. It is reasonable to assume that for practical applications the length of the fin and thereby the temperature decay should be limited. A fin length of 4 inches (.333 ft.) was selected for the performance analysis of a radiating fin with attached fusible material (octadecane).

The final transient analysis of the radiating fin with and without attached fusible material was performed with the simplified electrical analog network, Figure 20. The selected size of an aluminum fin node was .4 inches along the fin, .05 in. thickness and 1 ft. width. The fusible material node size was the same in length and width, but only .025 in. thick. The conductances between fusible material nodes along the fin were neglected to conserve computer time. This had little effect on the analytical results due to the ratio of thermal resistances of aluminum and fusible material, as discussed earlier.

NORTHROP SPACE LABORATORIES

SECTION V

PERFORMANCE OF TEMPERATURE CONTROL SYSTEMS

One-Dimensional Adiabatic System

The results for the one-dimensional adiabatic system analysis (Figures 1a and 19) are presented on Figures 26 through 37. The heat absorption capability of the four selected fusible materials was predicted at five heating rates (50, 100, 150, 200 and 250 watts/ft²). The cold plate temperature and the thickness of the melt layer are presented as a function of time and heat flux on Figures 26 through 33. Figures 26 through 29 are for heat addition periods from 0 to 15 minutes. The same results are presented for periods up to an hour on Figures 30 through 33. The thickness and weight of the melted material for the same conditions are shown on Figures 34 through 37. These results are presented as a function of a constant heat rate. They can also be used to estimate the performance of systems with variable heat flux.

For example, a system shall be considered which uses Tetradecane and dissipates 100 watts/ft² to the cold plate for .062 hours. At this time an instantaneous increase of heat dissipation to 150 watts/ft² occurs and continues for an additional period of .043 hours. Assuming the starting temperature is at the melt point (41°F), the cold plate temperature after the first heating period (.062 hours) is 58°F and .05 inches of Tetradecane have melted, (Figure 26). To estimate the cold plate temperature after the second heating period transfer along a constant cold plate temperature line (Figure 26) from the 100 watt/ft² curve to the 150 watt/ft² curve (the coordinates of this point are $\theta = .028$ hrs. and $T_{CP} = 58^\circ\text{F}$). Then continue along the 150 watt/ft² curve for an additional .043 hours and read the resultant cold plate temperature $T_{CP} = 80^\circ\text{F}$ for the combined heating rates.

To obtain an estimate of the melt thickness after the second heating period transfer to the 150 watts/ft² curve from the 100 watt/ft² curve on the .05 melt thickness curve (Figure 26) and note the melt thickness after an additional .043 hours. The resulting melt thickness is .10 inches.

This procedure of estimating performance of the one-dimensional adiabatic system for varying heat rates neglects the variation in the melted (liquid) fusible material layer between the cold plate and the solid-liquid interface resulting from the change in heating rate. When estimating the melt thickness in the sample problem an incorrect cold plate temperature was assumed when starting the second heat pulse at $\Delta X = .05$ inches and $\dot{q} = 150$ watts/ft². This assumption increased the heat absorbed by the liquid layer above the correct value. In estimating the cold plate temperature, the melt layer was reduced below the actual condition before and after the second heat pulse. This assumption reduced the heat absorbed by the liquid layer below the actual condition and decreased the thermal resistance in the liquid layer. However, these estimated values of melt thickness and cold plate temperature are reasonably accurate as long as the major portion of the heat absorbed is by melting of the solid material and the thickness of the liquid layer is small.

Parametric Analysis

The computation techniques used in the analysis of the one-dimensional adiabatic model result in computation instabilities at rates of heat flow slightly below those presented in Figures 26 through 37. A parametric analysis, assuming constant thermo-physical properties for the molten fusible material was performed. For the heat rates below 50 watt/ft² the melt layer temperature does not increase significantly above the melt point for a considerable period of heat addition. Therefore, the assumption of constant fluid properties for the melt will not result in a significant error.

The parametric results are presented on Figures 38 and 39. These data are applicable for the four selected n-paraffin materials. Figure 38 can be used to calculate the temperature change across the liquid melt layer and Figure 39 provides the thickness of the liquid layer as a function of time.

Radiating Fin With and Without Attached Fusible Material

The predicted performance for the heat rejection system using fusible material in combination with a radiating fin is presented on Figures 40 through 46. The fusible material used is Octadecane attached along the total fin length of 4

inches. The fin root temperature history for three heating rates (25, 50 and 75 watts/foot of fin root) for a fin with and without attached fusible material is shown on Figure 40. The fusible material greatly retards the fin temperature rise. The steady state root temperature is presented on Figure 41 as a function of heat rate. The rate of fusible material melting for the conditions of Figure 40 are presented on Figure 42. Also shown on Figure 42 are solidification rates with zero heat input at the fin root for the 25, 50 and 75 watt/ft heat rates after 15, 10 and 5 minutes heating periods, respectively.

The fin root temperature rise and decay for the 50 watt/ft heating rate with a zero heat input during cooling is shown on Figure 43 for three heating periods (5, 10 and 15 minutes). Once the fin root heat input is stopped, the fin root temperature drops very sharply. With no heat pulse the temperature decay along the fin disappears and the temperature along the fin becomes a constant (independent of length) dropping very rapidly to the fusible material melt temperature (81°F). The period between the time when the root temperature T_R becomes 81°F until it intersects the line of solidification loci (Figure 43) is the time required to solidify all the fusible material melted during the heat pulse.

The melt profiles for the conditions of Figure 43 are presented on Figure 44. For weight effectiveness the melt profile is the most efficient fusible material package outline. Note that the melt profile is also a function of fin geometry due to the temperature decay along the fin as shown in Figure 25.

Figure 45 shows an example of a thermo-histogram of a radiating fin with attached fusible material. In this figure direction of heat flux is relative to the aluminum fin, i.e., positive fluxes indicate heat flow into, negative fluxes indicate heat flow out of the fin. The fusible material absorbs the majority of the heat introduced by the heat pulse restricting the fin temperature rise and thereby maintaining the heat rejected by radiation relatively constant. After the heat pulse the radiation to space solidifies the melted fusible material maintaining the fin temperature close to the fusible material's melt point.

The selected radiating fin with attached fusible material has a heat rejection

of 12.2 watts/ft with the fin root at the melt point of Octadecane. This is the maximum steady state heat rejection rate that can maintain solid fusible material at the fin root ready for a higher energy heat pulse. Figure 46 presents the fin root temperature history of the fin with and without attached fusible material for a 15 minute heat pulse of 50 watts/ft preceded and followed by a 12.2 watt/ft heating rate. Theoretically it would take an infinite time period for the system to return to the original condition.

The rate of temperature decay shown on Figure 46 is the upper limit for regeneration of solid fusible material for the stated condition and fin configuration. The maximum rate of regeneration (minimum regeneration time) is presented on Figure 43 with zero heat input to the fin.

Fusible Material Performance

Material: Tetradecane $C_{14}H_{30}$

Melt Pt: $41^{\circ}F$

Heat of Fusion: 98.4 BTU/LB

\dot{q} = Constant Heat Input Rate

$$\frac{\text{Watts}}{\text{Ft}^2}$$

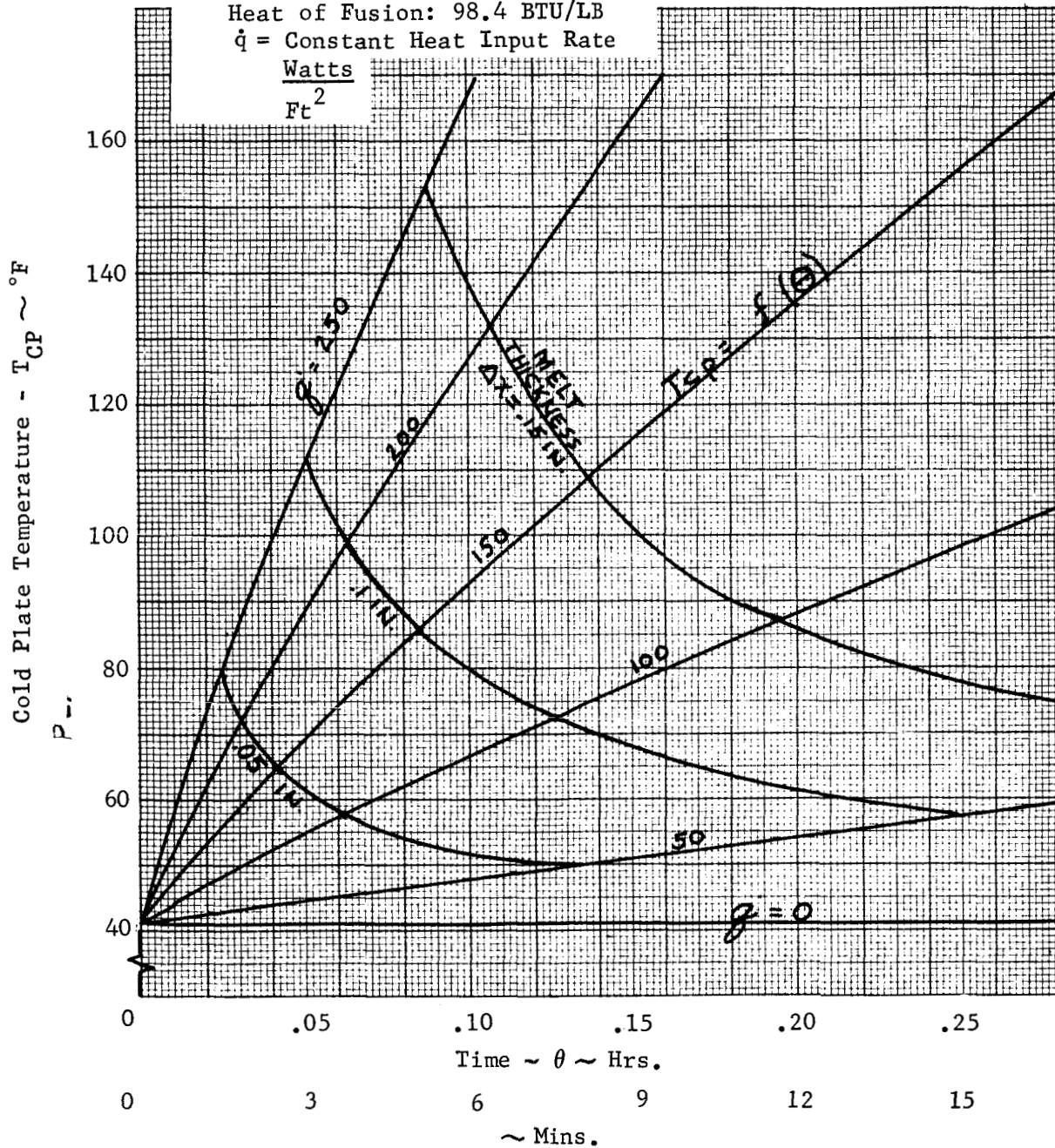


FIGURE 26 - FUSIBLE MATERIAL PERFORMANCE-TETRADECANE (0-15 Min)
FOR THE ONE DIMENSIONAL ADIABATIC MODEL

Material: Hexadecane, $C_{16}H_{34}$
 Melt Pt: $61^{\circ}F$
 Heat of Fusion: 108.8 BTU/LB
 \dot{q} = Constant Heat Input Rate

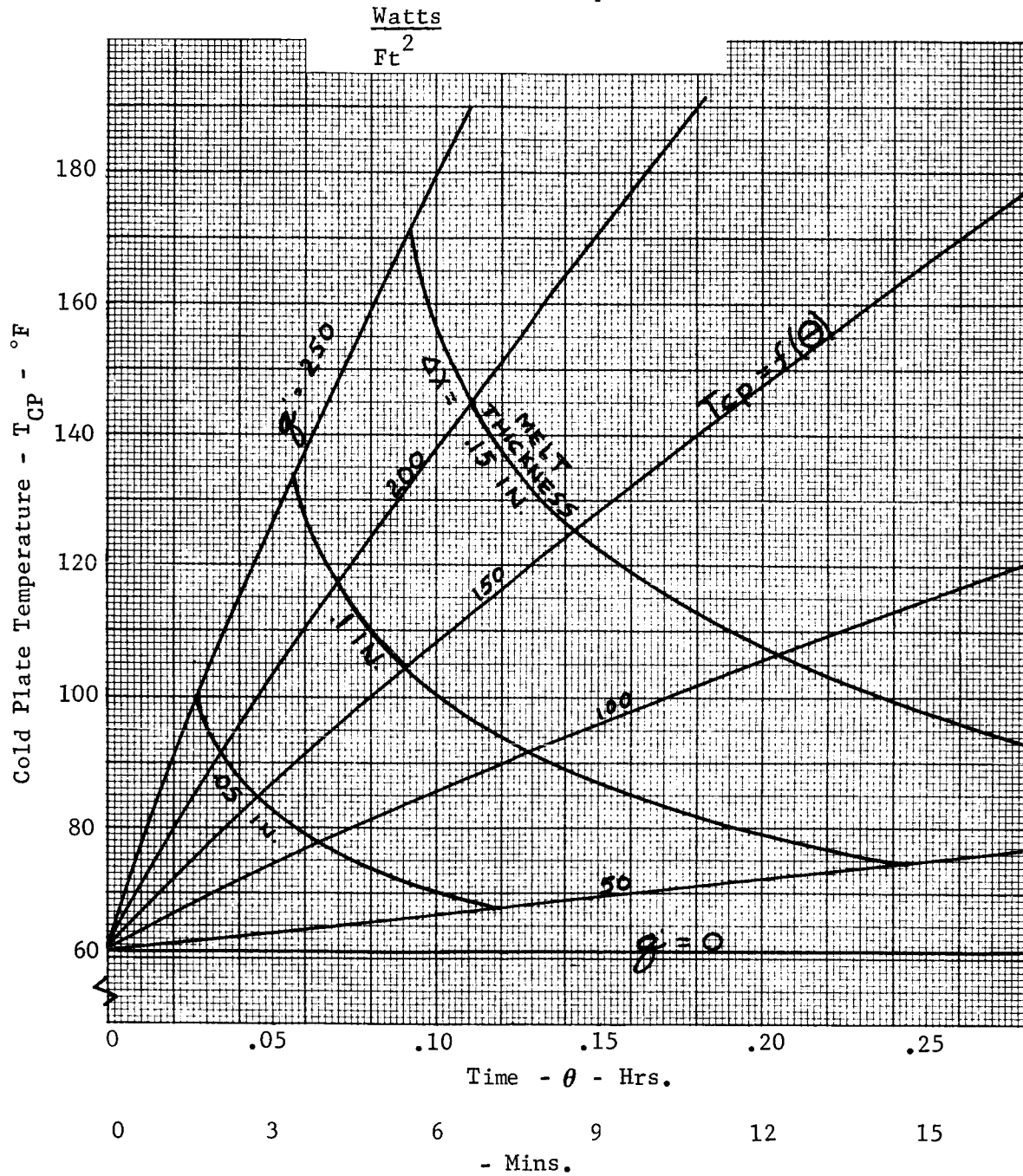


FIGURE 27 - FUSIBLE MATERIAL PERFORMANCE-HEXADECANE (0-15 Min)
 FOR THE ONE DIMENSIONAL ADIABATIC MODEL

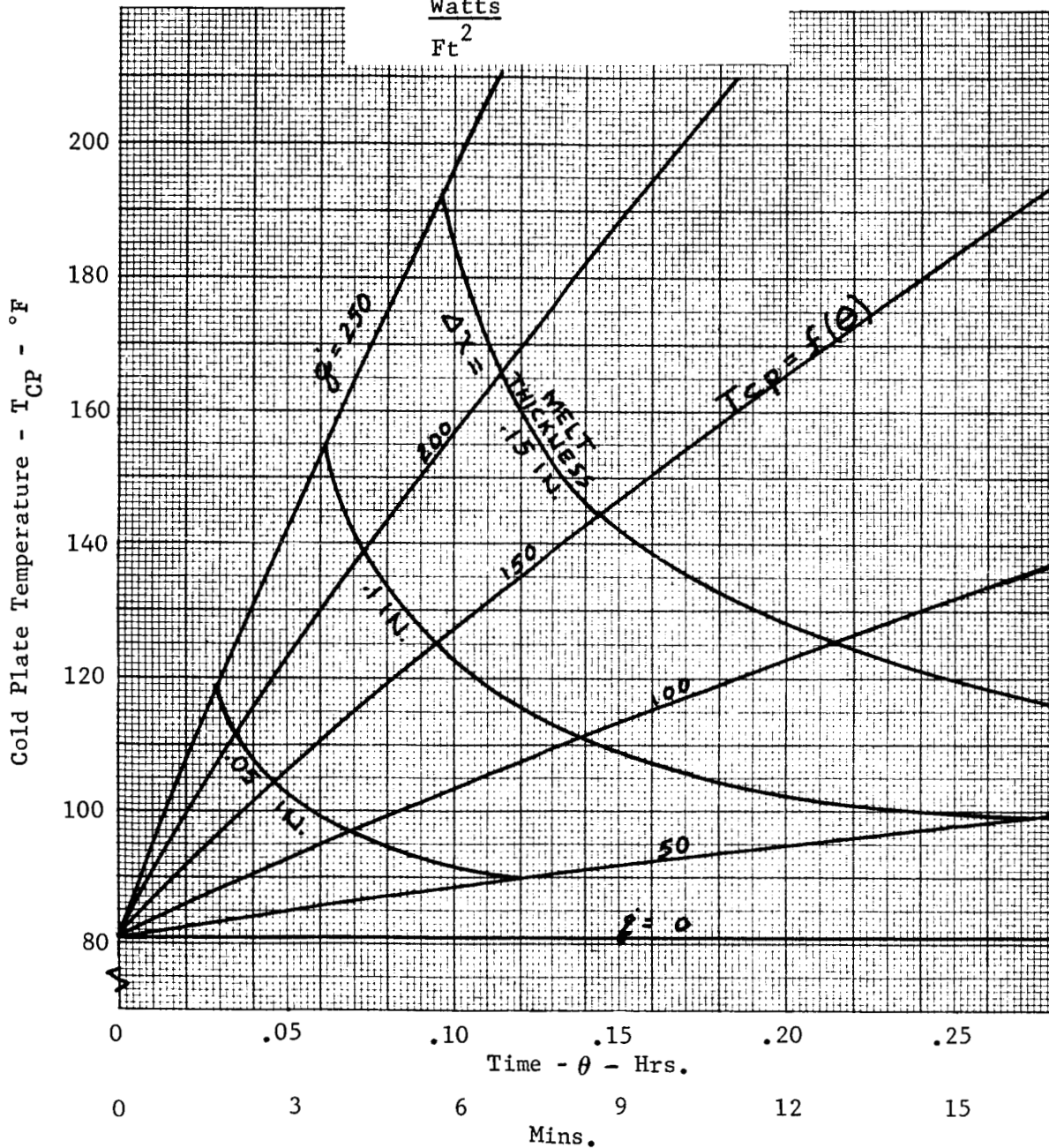
\dot{q} = Constant Heat Input Rate
$$\frac{\text{Watts}}{\text{Ft}^2}$$


FIGURE 28 - FUSIBLE MATERIAL PERFORMANCE-OCTADECANE (0-15 Min)
FOR THE ONE DIMENSIONAL ADIABATIC MODEL

Material: Eicosane $C_{20}H_{42}$
Melt Pt: $98^{\circ}F$
Heat of Fusion: 106.7 BTU/LB
 \dot{q} = Constant Heat Input Rate
 $\frac{\text{Watts}}{\text{Ft}^2}$

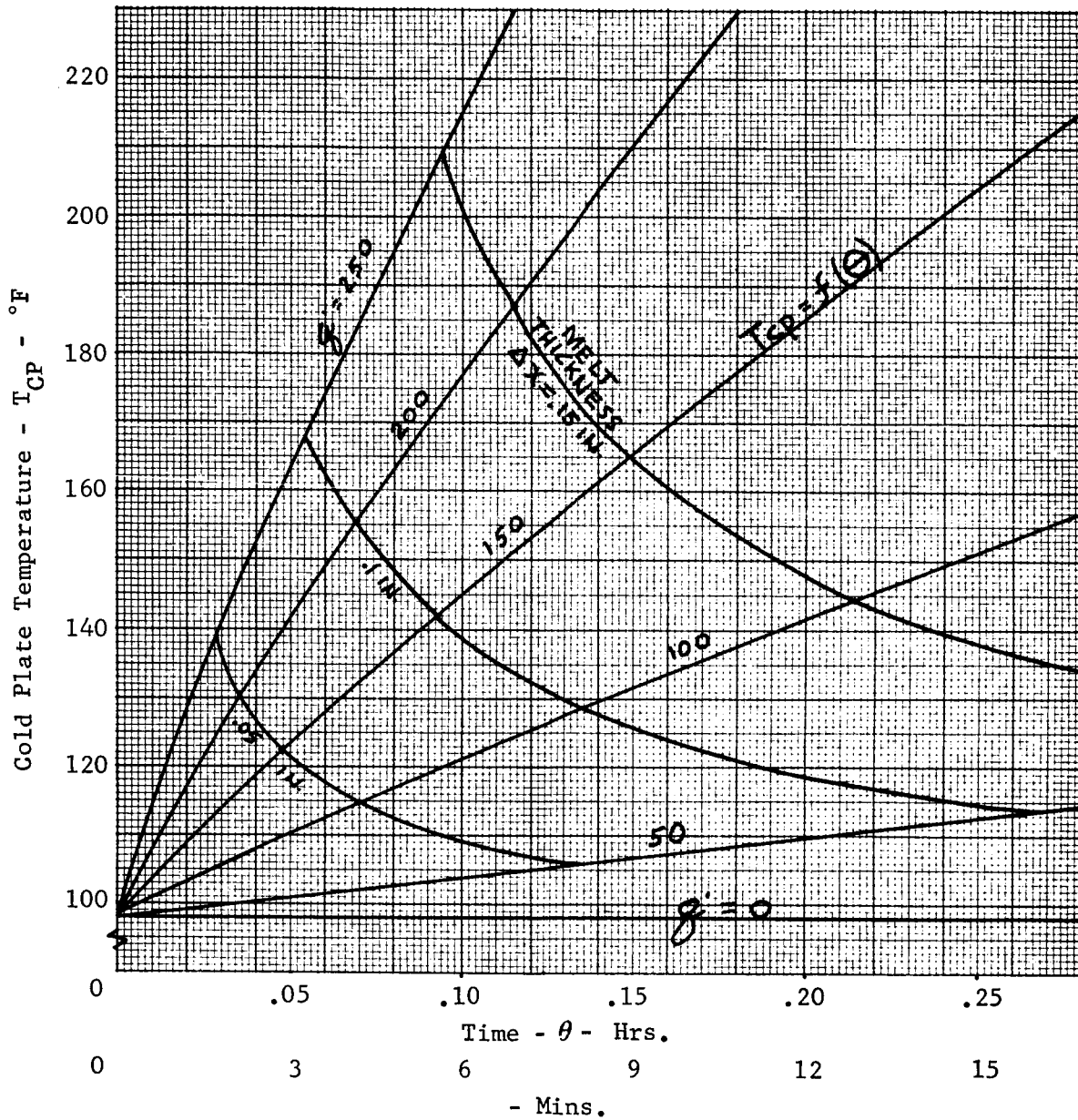
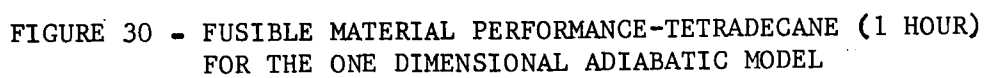


FIGURE 29 - FUSIBLE MATERIAL PERFORMANCE-EICOSANE (0-15 Min)
FOR THE ONE DIMENSIONAL ADIABATIC MODEL



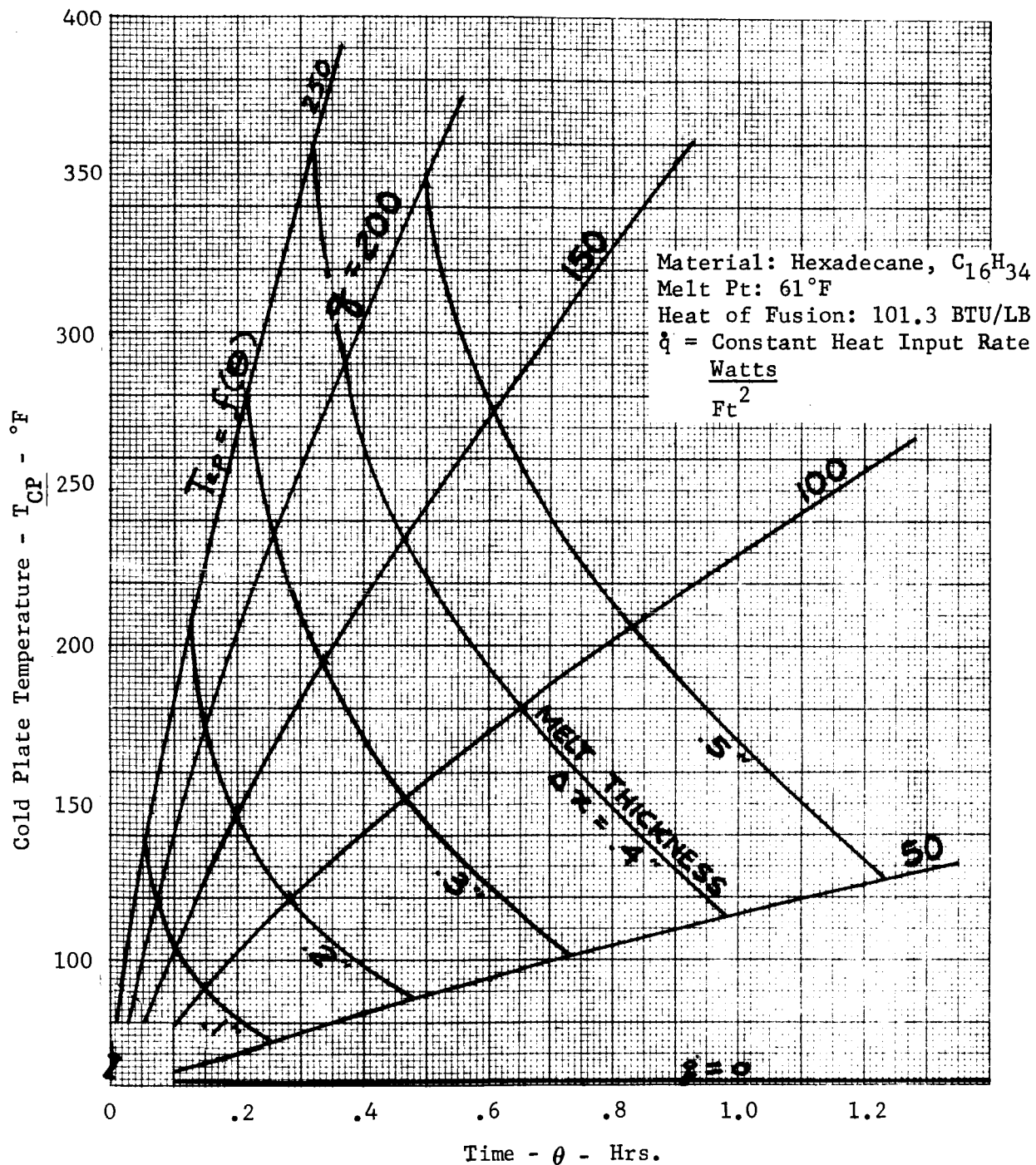


FIGURE 31 - FUSIBLE MATERIAL PERFORMANCE-HEXADECANE (1 HOUR)
 FOR THE ONE DIMENSIONAL ADIABATIC MODEL

Material: Octadecane, $C_{18}H_{38}$
 Melt Pt: $81^{\circ}F$
 Heat of Fusion: 104.9 BTU/LB
 \dot{q} = Constant Heat Input Rate

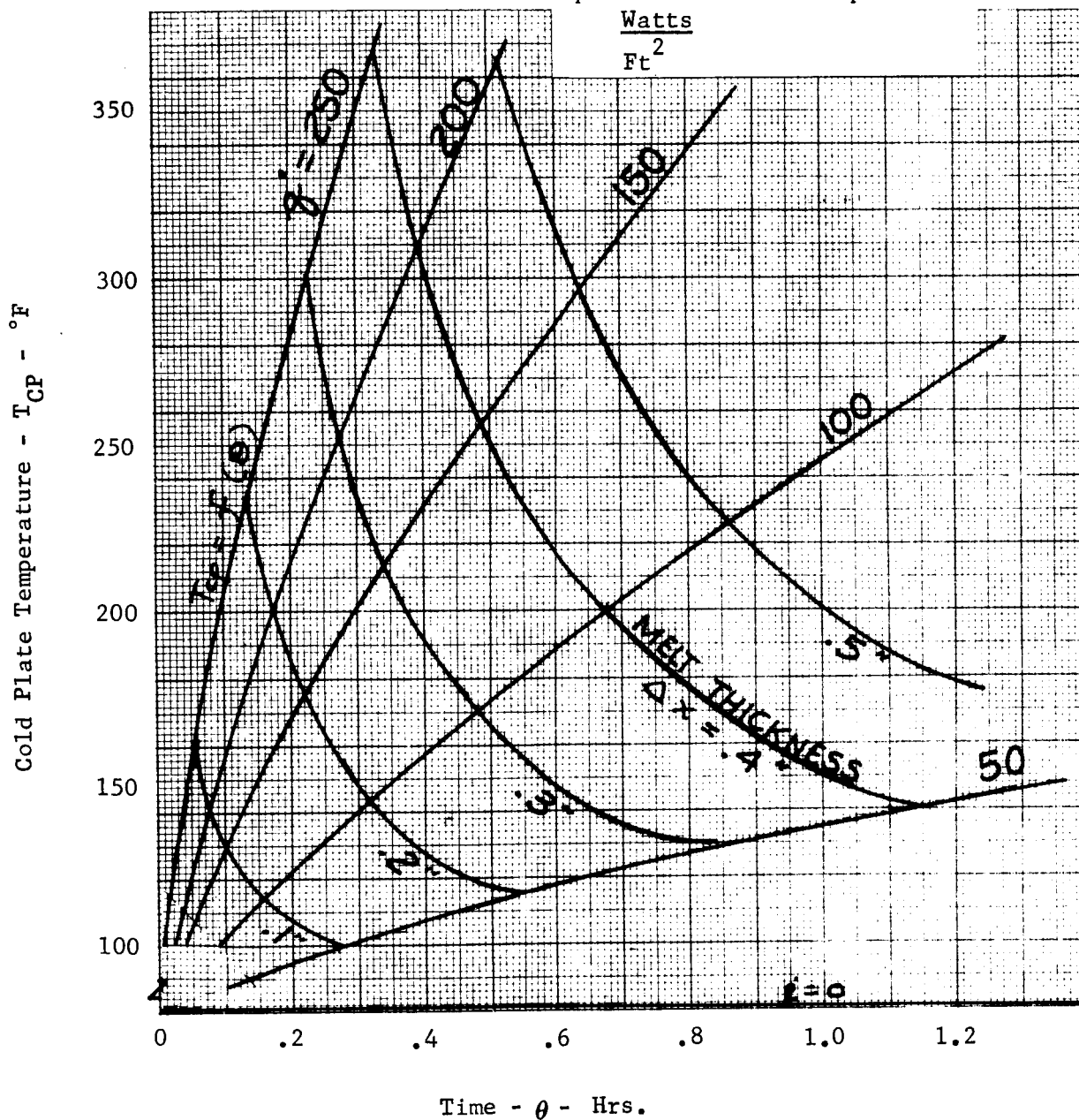


FIGURE 32 - FUSIBLE MATERIAL PERFORMANCE-OCTADECANE (1 HOUR)
 FOR THE ONE DIMENSIONAL ADIABATIC MODEL

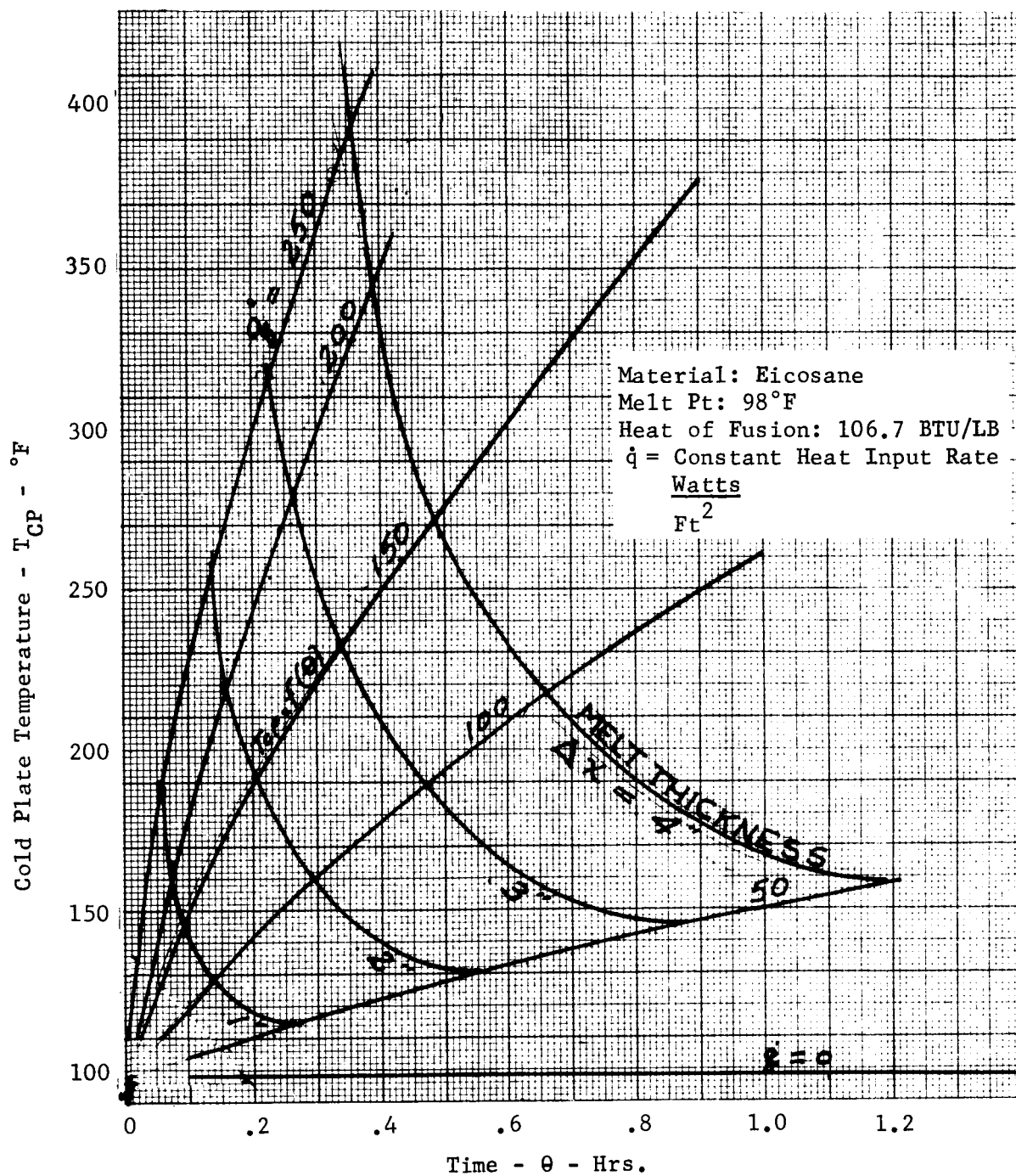


FIGURE 33 - FUSIBLE MATERIAL PERFORMANCE-EICOSANE (1 HOUR)
 FOR THE ONE DIMENSIONAL ADIABATIC MODEL

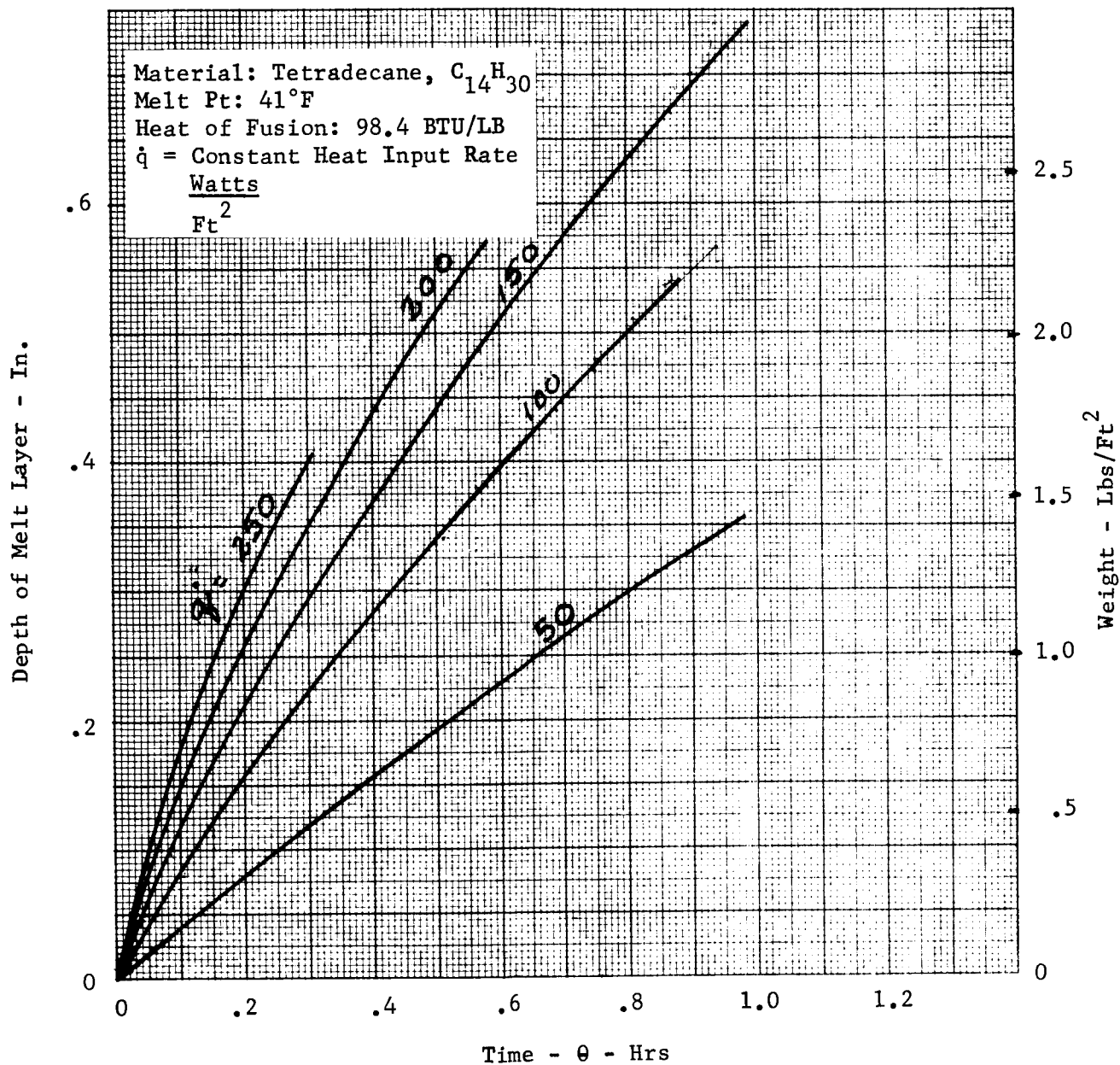


FIGURE 34 - MELT LAYER DEPTH AND WEIGHT-TETRADECANE
FOR THE ONE DIMENSIONAL ADIABATIC MODEL

Material: Hexadecane, $C_{16}H_{34}$
Melt Pt: $61^{\circ}F$
Heat of Fusion: 101.3 BTU/LB
 \dot{q} = Constant Heat Input Rate
 $\frac{\text{Watts}}{Ft^2}$

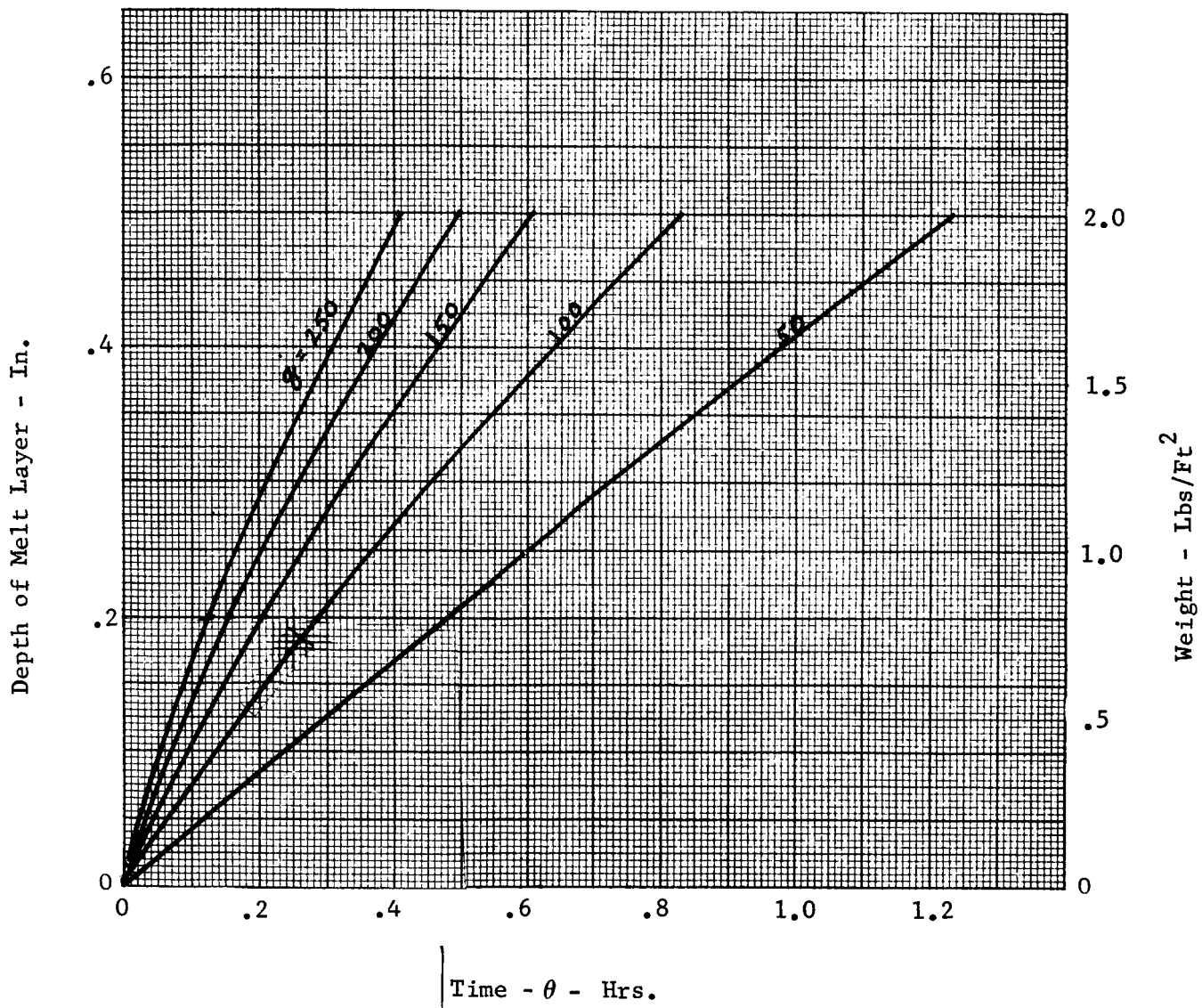


FIGURE 35 - MELT LAYER DEPTH AND WEIGHT-HEXADECANE
FOR THE ONE DIMENSIONAL ADIABATIC MODEL

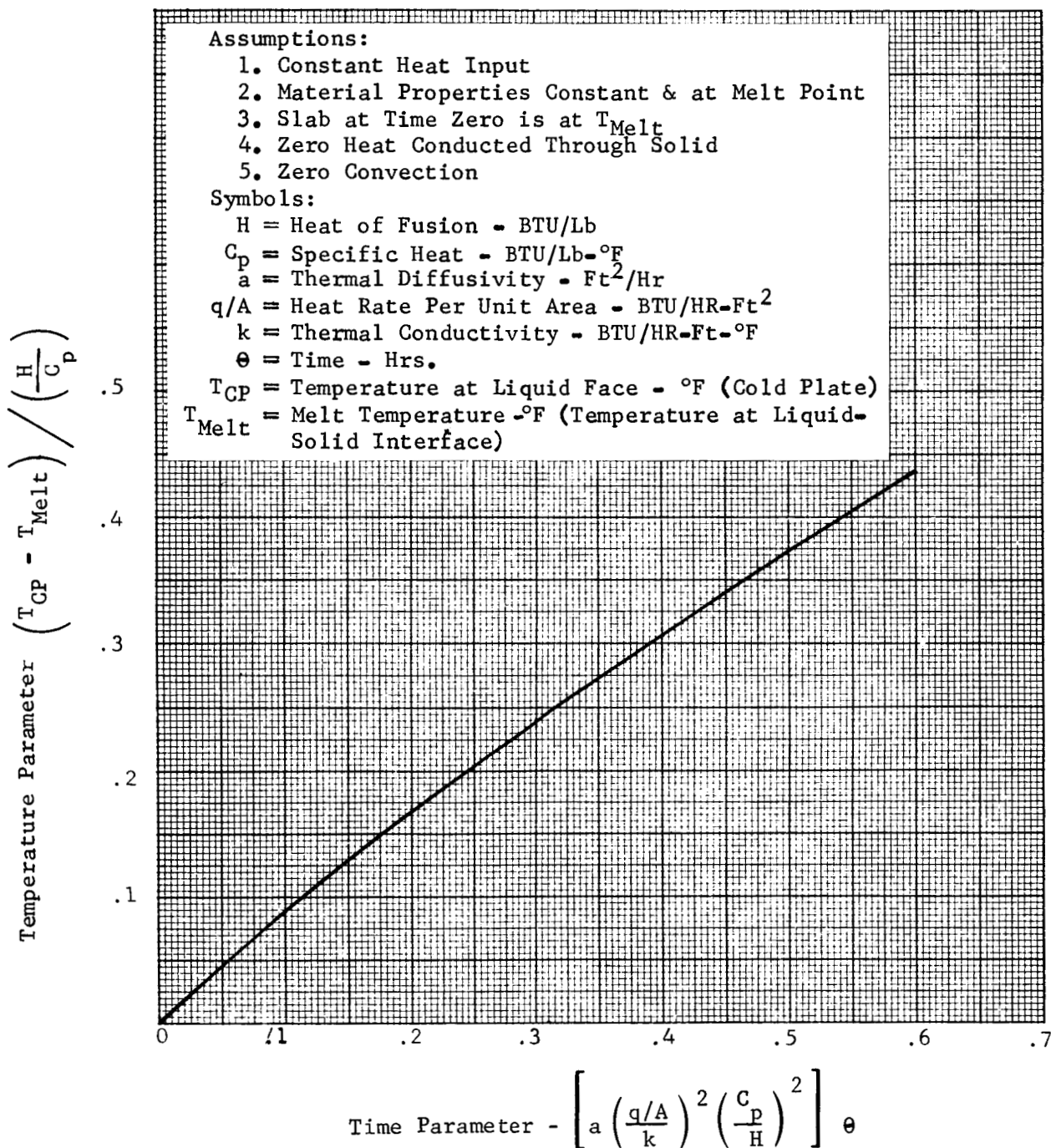


FIGURE 38 - TEMPERATURE PARAMETER VERSUS TIME PARAMETER FOR MELTING OF SEMI-INFINITE SLABS

Assumptions:

1. Constant Heat Input
2. Material Properties Constant & at Melt Point
3. Slab at Time Zero is at T_{Melt}
4. Zero Heat Conducted Through Solid
5. Zero Convection

Symbols:

- H = Heat of Fusion - BTU/Lb
 C_p = Specific Heat - BTU/Lb-°F
 a = Thermal Diffusivity - Ft²/Hr
 q/A = Heat Rate Per Unit Area - BTU/Hr-Ft²
 k = Thermal Conductivity - BTU/Hr-Ft-°F
 θ = Time - Hrs.
 Δx = Melt Thickness - Ft.

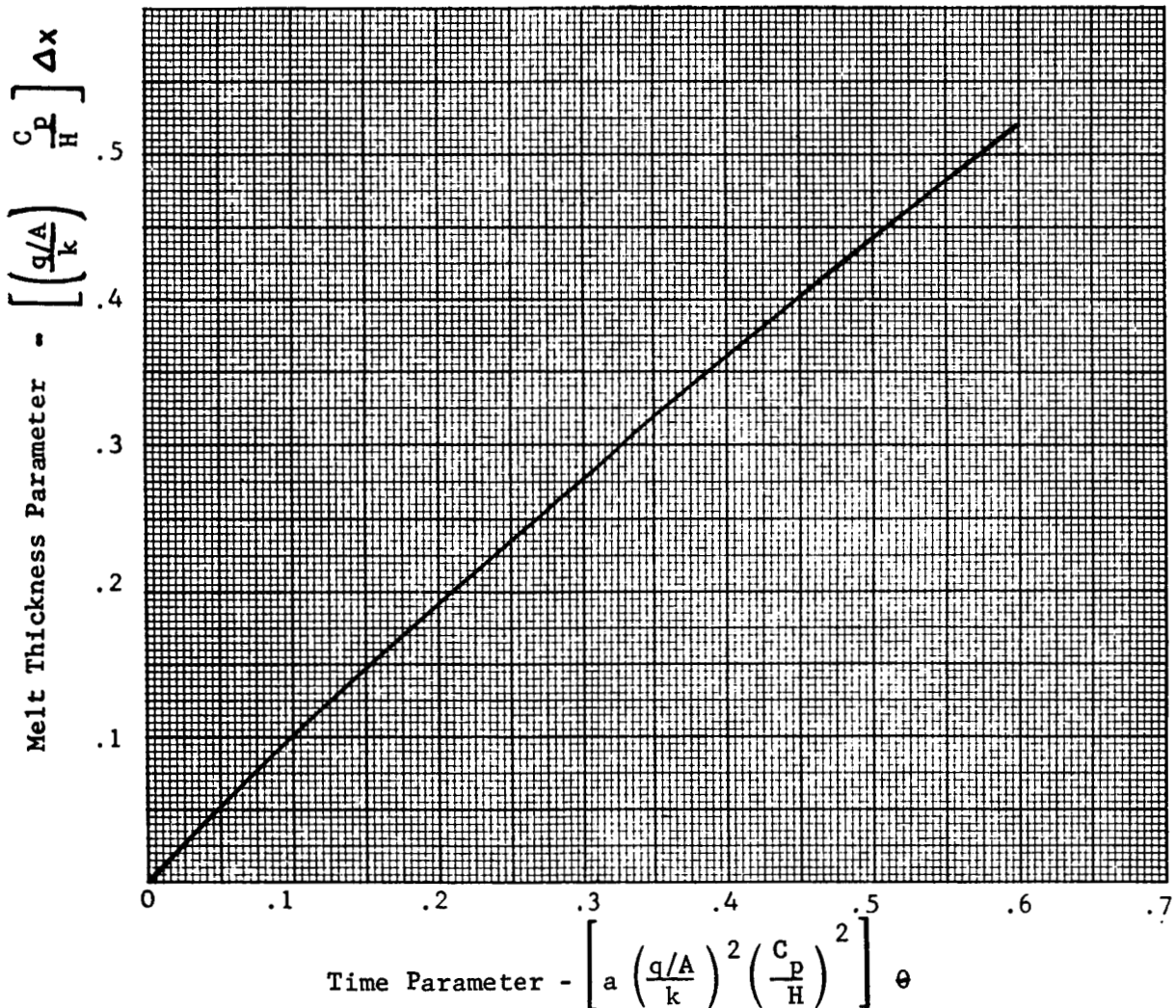


FIGURE 39 - MELT THICKNESS PARAMETER VERSUS TIME PARAMETER FOR MELTING OF SEMI-INFINITE SLABS

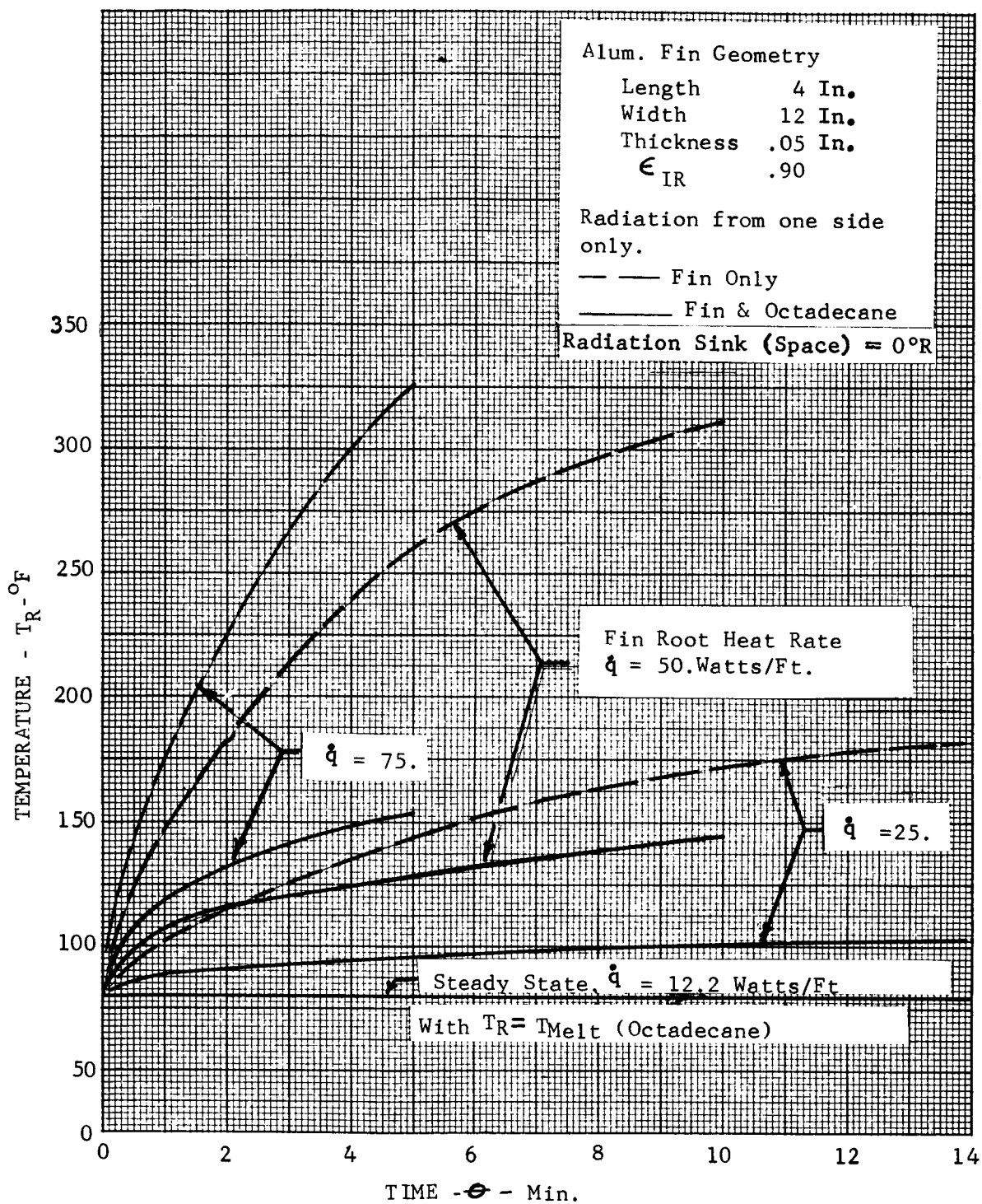


FIGURE 40 - ROOT TEMPERATURE HISTORY OF A RADIATING FIN WITH AND WITHOUT ATTACHED FUSIBLE MATERIAL

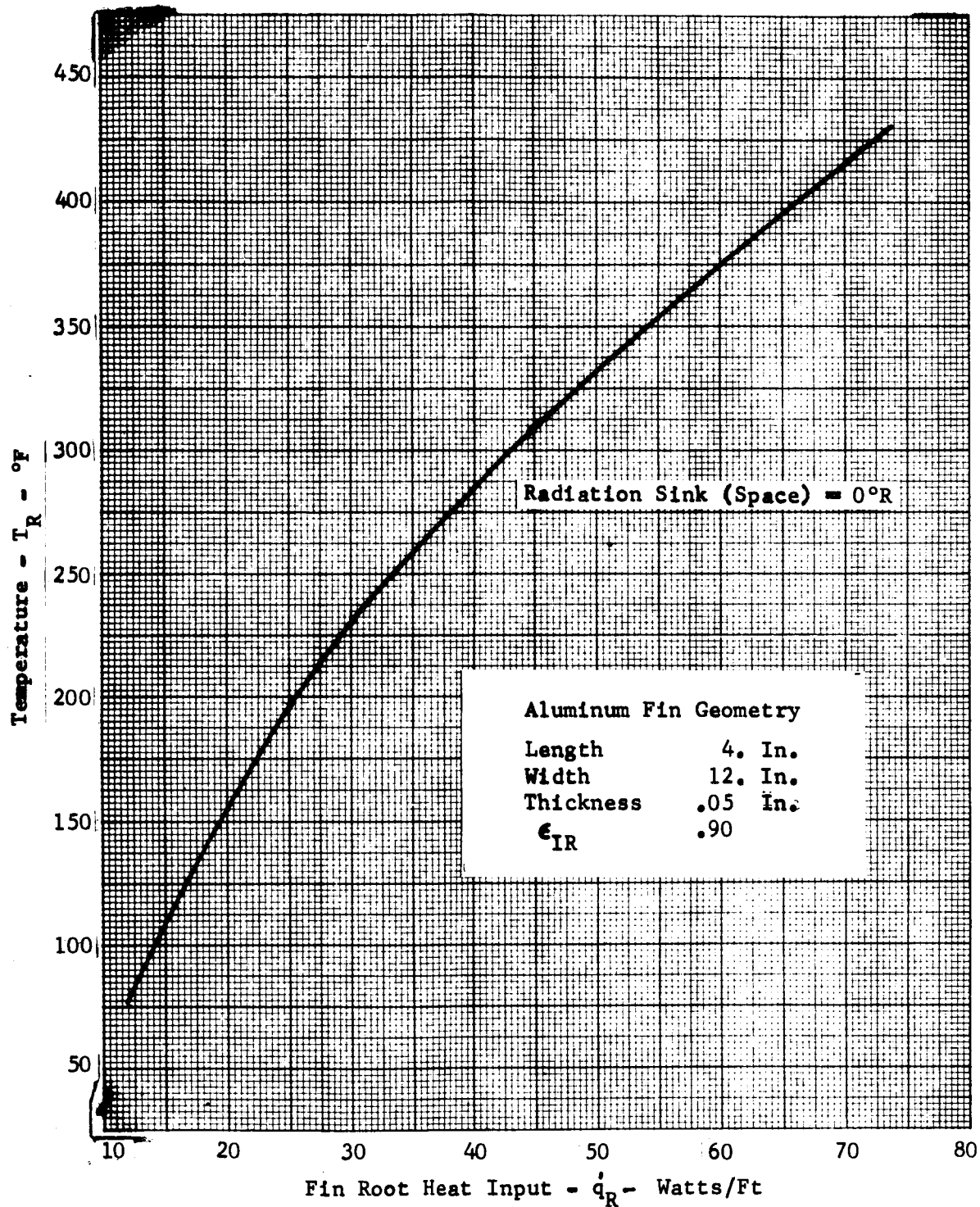


FIGURE 41 - STEADY-STATE ROOT TEMPERATURE OF A FIN RADIATING TO SPACE FROM ONE SIDE ONLY

Weight of Melted and Solidified Fusible Material - Lbs.

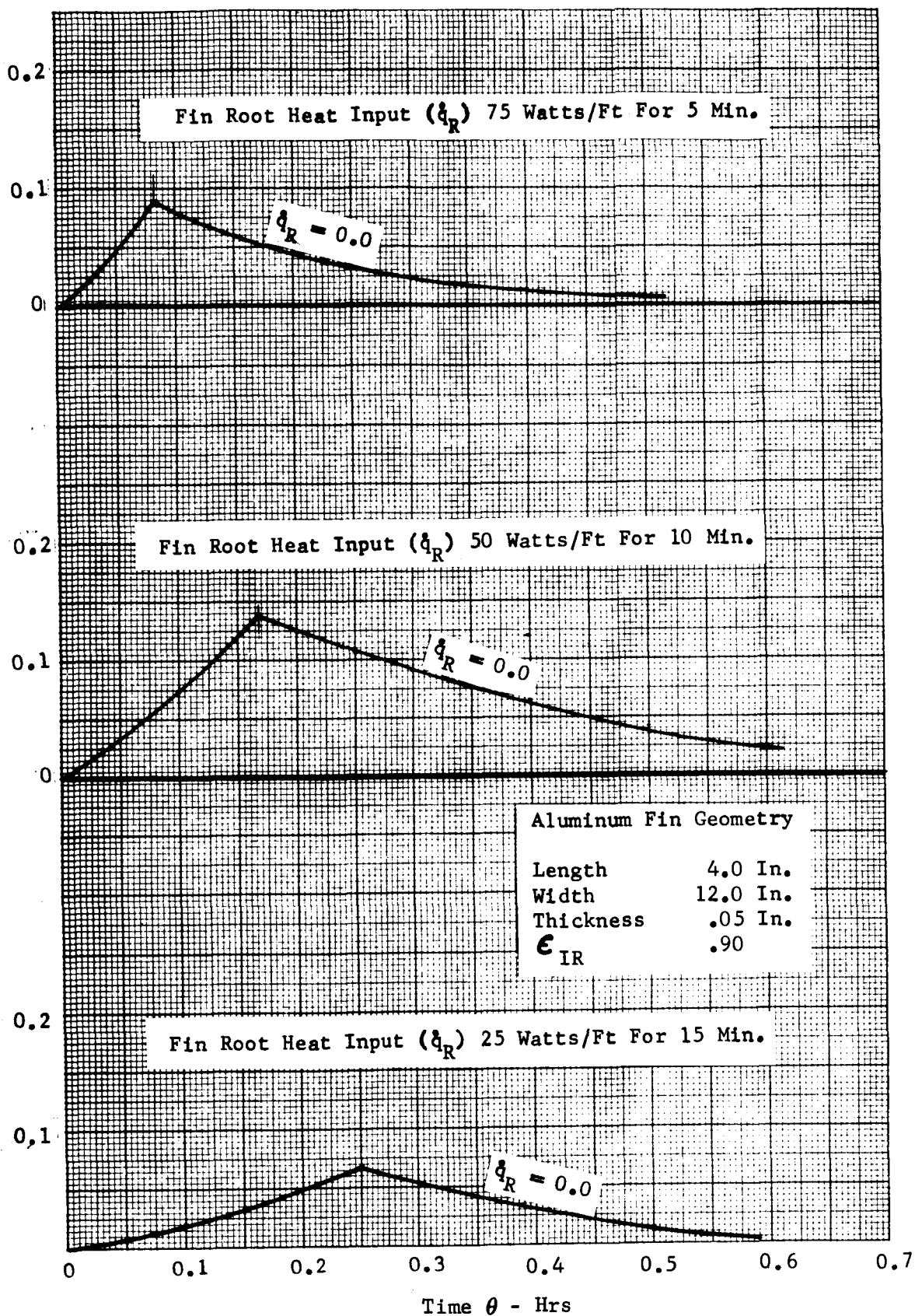


FIGURE 42 - FUSIBLE MATERIAL MELT AND SOLIDIFICATION RATE WHEN ATTACHED TO RADIATING FIN

NSL 65-16

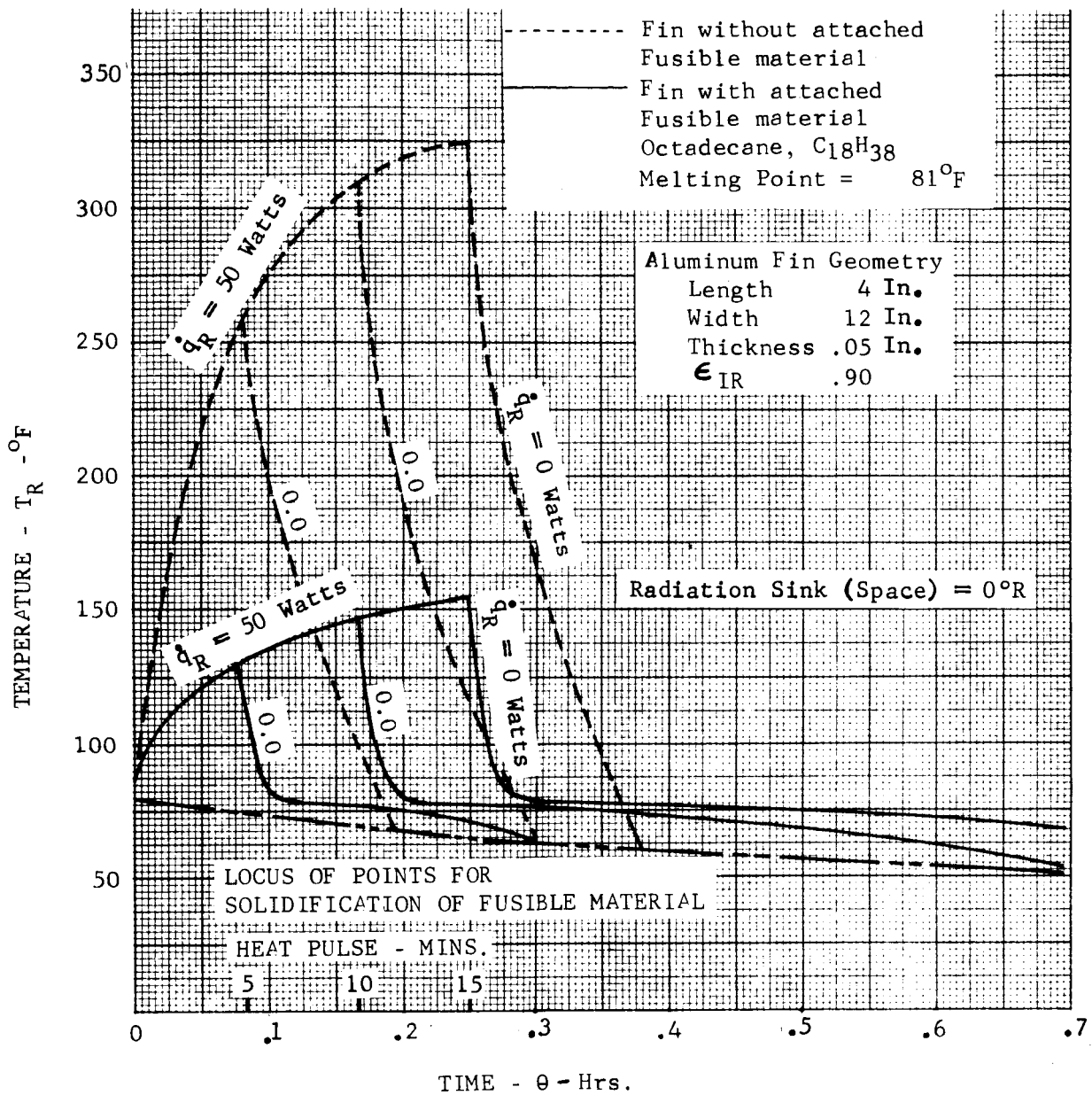


FIGURE 43 - ROOT TEMPERATURE HISTORY OF A RADIATING FIN WITH AND WITHOUT ATTACHED FUSIBLE MATERIAL AT 50 WATTS/FT.

Fusible Material - Octadecane $C_{18}H_{38}$,
 Melting Temperature = $81^{\circ}F$

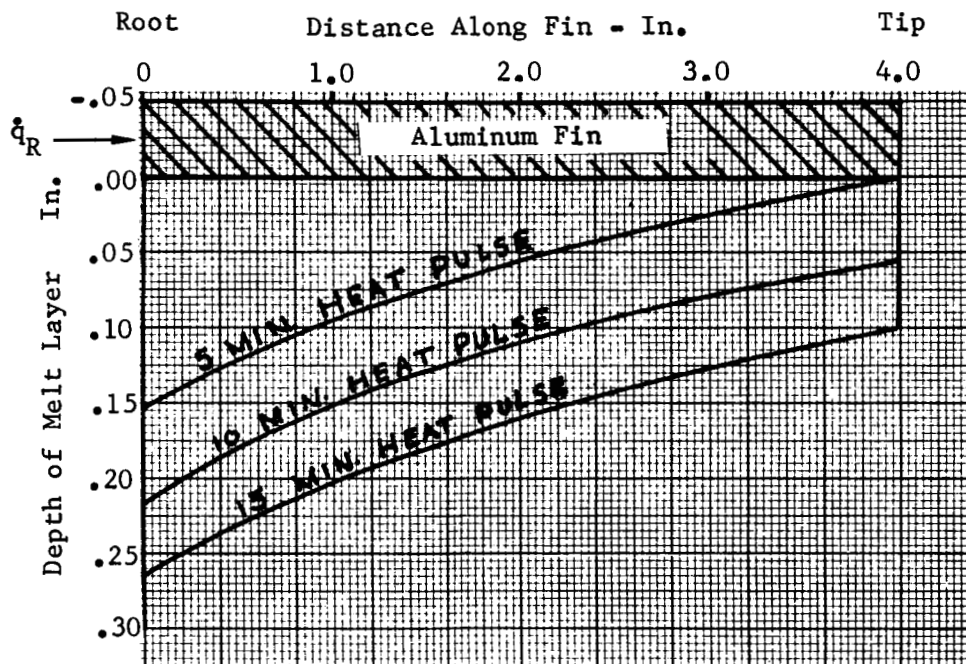


FIGURE 44 - MELT LAYER HISTORY OF FUSIBLE MATERIAL ATTACHED TO A RADIATING FIN AT 50 WATTS/FT.

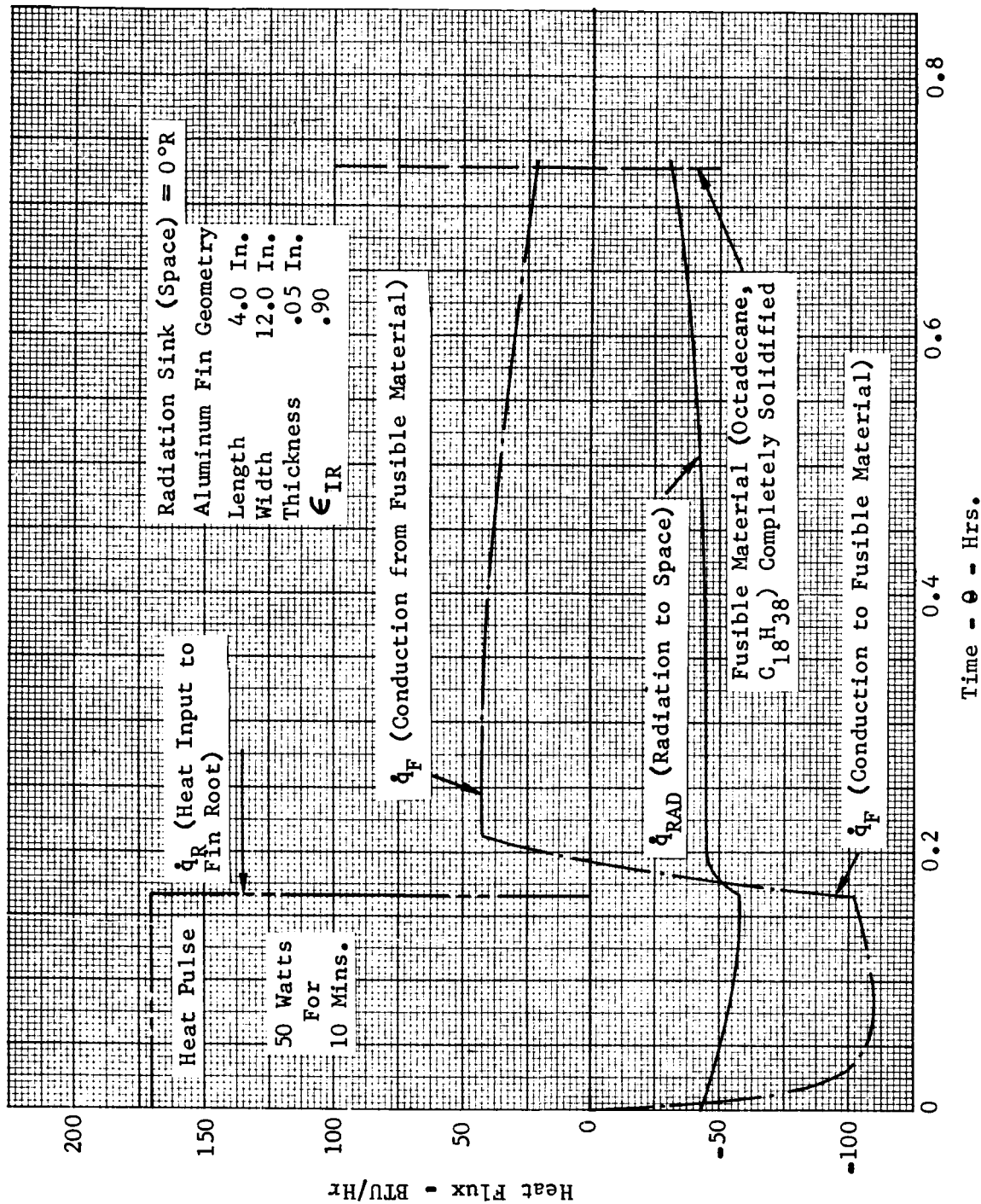


FIGURE 45 - HEAT FLUX HISTORY OF A RADIATING FIN WITH ATTACHED FUSIBLE MATERIAL AT 50 WATTS/FT.

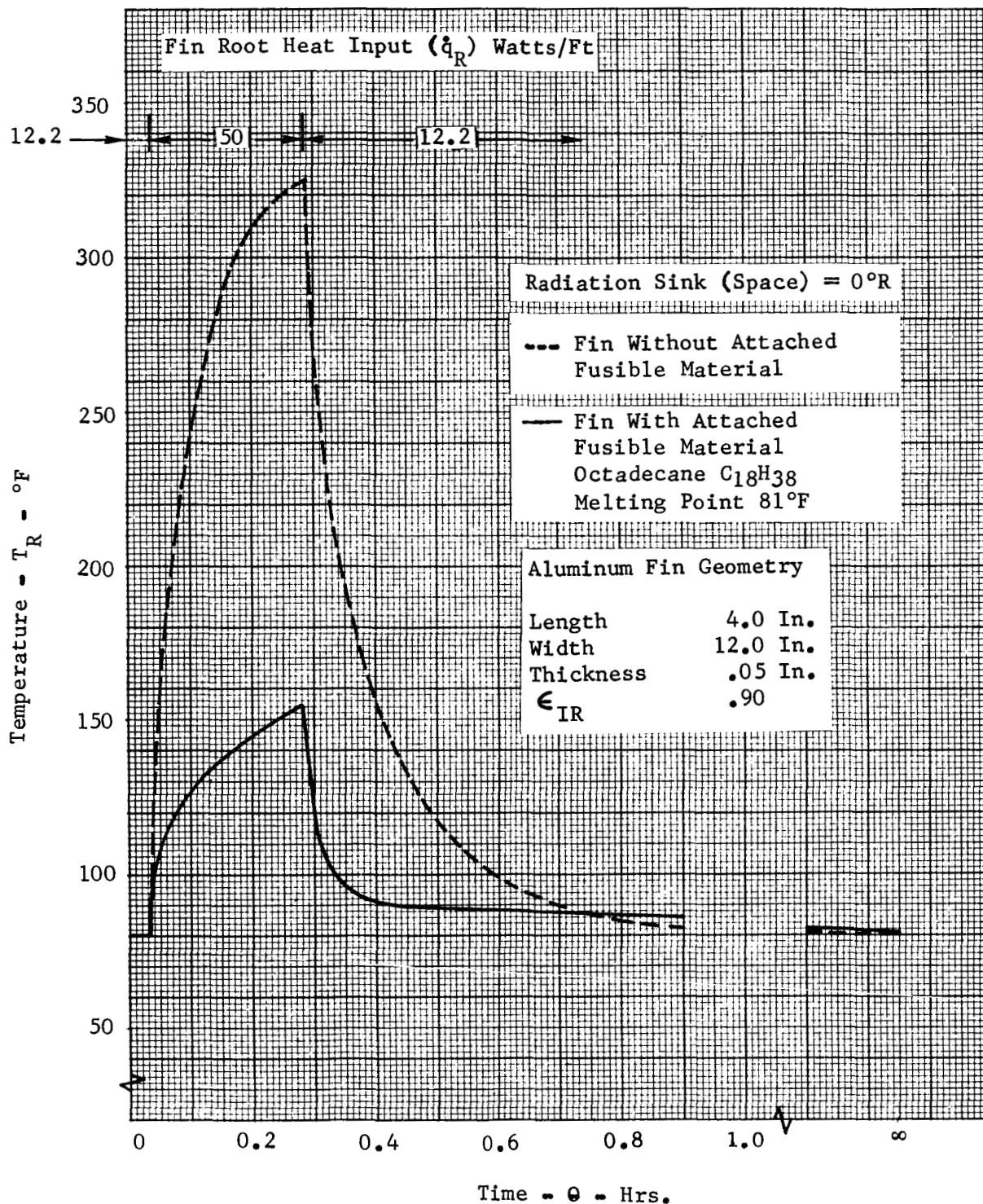


FIGURE 46 - ROOT TEMPERATURE HISTORY OF A RADIATING FIN WITH AND WITHOUT ATTACHED FUSIBLE MATERIAL WITH THE MAXIMUM HEAT RATE FOR MAINTAINING SOLID FUSIBLE MATERIAL BEFORE AND AFTER A 15 MINUTE 50 WATT/FT HEAT PULSE

NORTHROP SPACE LABORATORIES

SECTION VI

THERMAL CONTROL SYSTEM PACKAGE DESIGN AND VERIFICATION EXPERIMENTS

The verification experiments require experimental thermal control system packages which physically simulate the analytical models of the two temperature control systems analyzed. The experimental package design, construction, and operation during performance evaluation experiments will provide design data for the flight hardware design. The verification experiments have not been completed at this time due to initial failures of the fusible material containers under pressurization.

The two analytical models of the temperature control systems analyzed and requiring experimental verification are:

- a. The one dimensional adiabatic system. This system is applicable to temperature control of a device where waste heat is absorbed by the fusible material with no significant heat transfer to the external environment.
- b. The two dimensional system of a radiating fin with attached fusible material. In this system the thermal inertia of a space radiator is increased by the use of the attached fusible material.

The fusible material selected for the verification experiment was octadecane, $C_{18}H_{38}$, with a melt point of $81^{\circ}F$ and a heat of fusion of 104.9 BTU/lb.

The fusible material should be contained, for both systems, so that it is kept in contact with the heat source, i.e. the electronic package heat rejection surface or the radiating fin. The container should maintain the fusible material at approximately one atmosphere gage pressure. The maximum volume of the octadecane during testing will be approximately 7% above its liquid volume at the melt point. The total volume change from solid at $50^{\circ}F$ below melt temperature to liquid at $150^{\circ}F$ above the melt temperature is 19%.

Testing of both systems was to be performed in an evacuated bell jar with cold walls for system (b) and walls at room temperature for system (a).

The vacuum environment was required for the adiabatic system (a) test so that an adiabatic condition can be simulated by low thermal mass reflective insulation during the transient test. The vacuum environment and cold walls are required to simulate the thermal environment of the radiating fin-fusible material system (b).

The experimental package for the adiabatic one dimensional system (a) is shown on Figure 47. An electrically heated aluminum plate is used to simulate an item of heat emitting equipment.

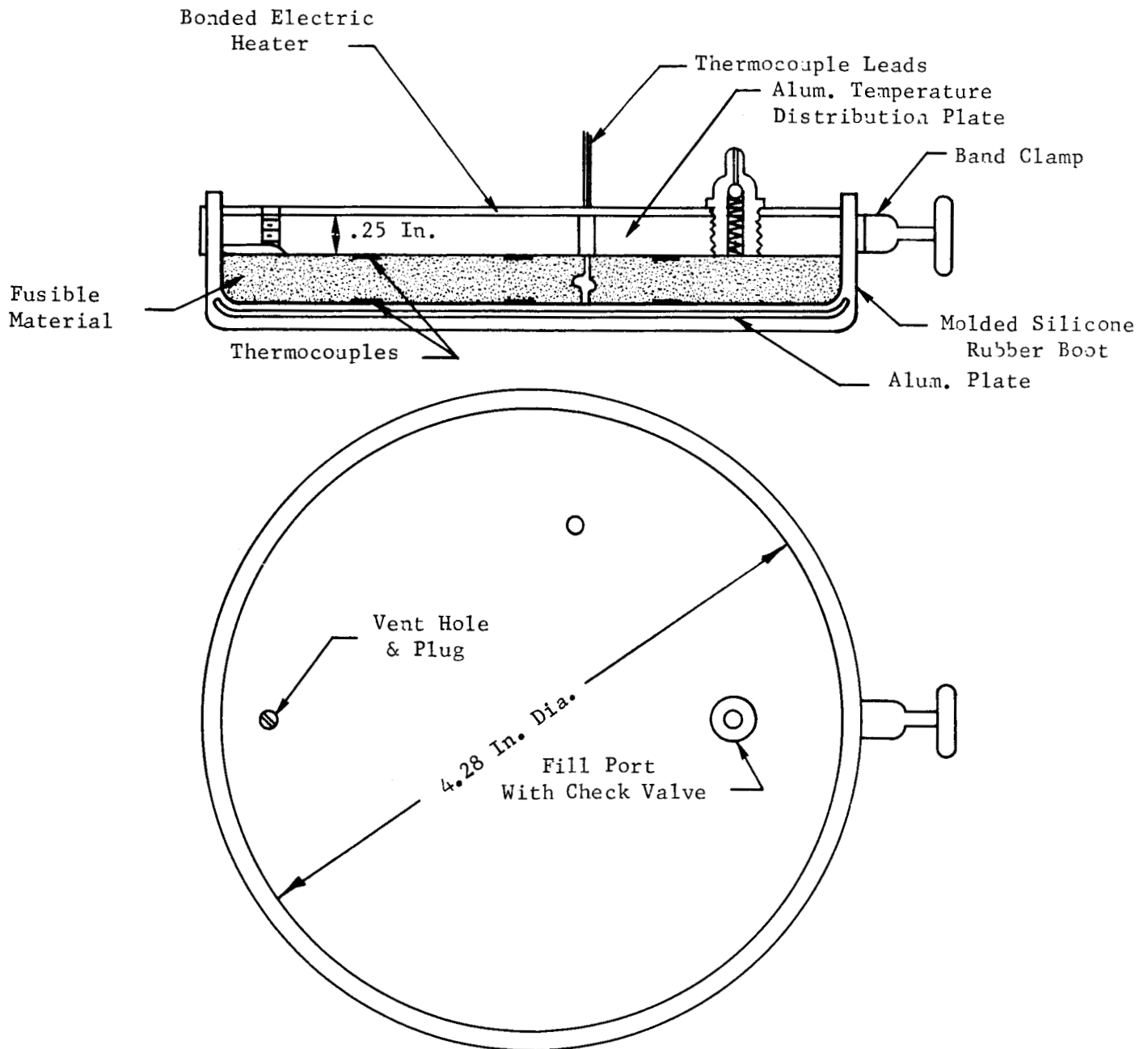
Silicone rubber G.E. RTV 11 or RTV 60 was selected as material for the fusible material container. Elastomers have many desirable properties for use as container material. They have inherent capability to provide pressurization, adapt to volume changes and maintain the fusible material in contact with the heat source. Silicone rubbers have good elasticity, are stable over a wide temperature range at one atmosphere or in a vacuum and can be molded at room temperature. An aluminum mold was manufactured in which containers of each of the silicone rubbers were molded.

Problems were encountered with the structural integrity of the containers made from silicone rubbers G.E. RTV 11 and RTV 60. Four containers were ruptured during experiments with pressurization and filling of the apparatus. The RTV 11 appeared superior to RTV 60 in tear strength and only one container was made from the latter material.

One RTV 11 container expanded successfully to 150% of its original volume at 7 psig air pressure. However, the containers ruptured near the band clamp on pressurization for leak testing on filling with Octadecane. A modified clamping installation was tried. The last container ruptured after modification of the clamping installation, while pressurizing the apparatus with liquid Octadecane for the first test run.

The extremely poor tear strength of these silicone rubbers after slight surface damage makes them undesirable for this application. Other elastomers (including other silicone rubbers) may be more suitable for this application and will be investigated and tried.

A mechanical pressurizing arrangement such as a bellows system could be used. But the simplicity of the use of an inherently elastomeric material makes it the most promising container material and justifies a continuation of effort to find a stronger and more suitable elastomer.



NOTE: Heating Area = $.10 \text{ Ft}^2$

FIGURE 47 TEST APPARATUS FOR: THE ONE DIMENSIONAL
ADIABATIC MODEL THERMAL CONTROL
BY USE OF FUSIBLE MATERIAL

NORTHROP SPACE LABORATORIES

SECTION VII

POTENTIAL IMPROVEMENTS OF THERMAL CONTROL PACKAGE

DESIGN

The major factors limiting the applicability of fusible materials for temperature control are the fusible materials weight relative to heat absorbed and the build up of the low thermal conductivity melt layer. Since melting is essentially a constant temperature process, heat of fusion temperature control could theoretically provide a constant temperature control technique, if the thermal conductivity of the liquid could be increased to infinity or the liquid melt layer removed.

Several methods of improving the performance of thermal control packages using fusible materials have been considered and evaluated as to their potential for future studies.

Improvement of effective thermal conductance by the use of finned heat dissipation surfaces, by the mixing of metallic powders or flakes into the fusion material or by choice of higher conductance fusion materials are being considered. In place of fins on the heat dissipation surface, randomly oriented aluminum or copper fibers (similar to "steel wool,") soldered to the heat dissipating surface could provide multiple highly conductive heat paths into the fusible material and increase effective thermal conductance of the melt layer.

All these methods will reduce the fusible material content per unit system weight and volume. The penalties resulting from the displacement of some of the fusible material by the metallic fillers or by the fins must be considered in evaluating the usefulness of these methods. This displacement substitutes the product of specific heat and temperature rise of the metal for the much larger heat fusion of the paraffins. Depending on application, these methods will reduce the rate of temperature increase with time (and total dissipated heat) but increase the system weight for a given total heat dissipation.

Materials other than the four paraffins presently studied should be considered. Liquid alkali metals do not look promising because of low heat of fusion, though the thermal conductivity is superior. Phase change on decrepitation of hydrated salts, for example the endothermic change from $\text{Na}_2\text{SO}_4 \cdot 10 \text{H}_2\text{O}$ to $\text{Na}_2\text{SO}_4 + 10 \text{H}_2\text{O}$ will provide heat absorption of 108 BTU per pound. Thermal conductivity of the $\text{Na}_2\text{SO}_4 + 10 \text{H}_2\text{O}$ solution may be about three times that of the liquid paraffins. Potential problems include difficulties in recrystallization and thermal contact of the crystalline form with the heat source. However, for the adiabatic system recrystallization may not be required and thermal contact could be improved, if necessary, by fins or the "metal wool" approach described above.

A concept of removing the molten liquid layer for the adiabatic system is presented on Figure 48. This system would use pressure of a vapor to force the solid fusible material against the heat dissipation surface. The liquid fusible material would be forced by the solid material into an annular ullage space provided. The system arrangement shown in Figure 48 will initially retain a cylindrical slab of solid fusible material in a metal cylinder, shown shaded in the Figure. Pressure will act on the solid fusible material slab through the "Pressure Diaphragm". The vapor pressure would be generated by a bulb, filled with a high vapor pressure fluid (e.g. Freon), which would be in thermal contact with the heat dissipation surface. Sliding of the fusible material slab will be facilitated by thermal contact of the metal cylinder with the heat dissipating surface and by the inherently slippery characteristics of paraffins close to or above their melting points. As the solid fusible material melts, the liquid melt is forced through slots into the annular ullage space, displacing the "Refill Bladder". The top illustration of Figure 48 shows an approximately half-way point in melting of the solid material, with part of fusible material molten and in the ullage space. The center illustration shows the end of the cooling period with all of the fusible material in the ullage space. Regeneration of the system, for example after a preflight checkout, requires a heat soak of the device which will liquify the fusible material in the ullage space and application of air

pressure to the refill bladder. This will return the fusible material to the center for another cooling cycle.

The advantage of this arrangement would be that an essentially constant temperature of the heat rejection surface, at the melting temperature of the fusible material, can be maintained by elimination of the temperature gradient across the melt layer.

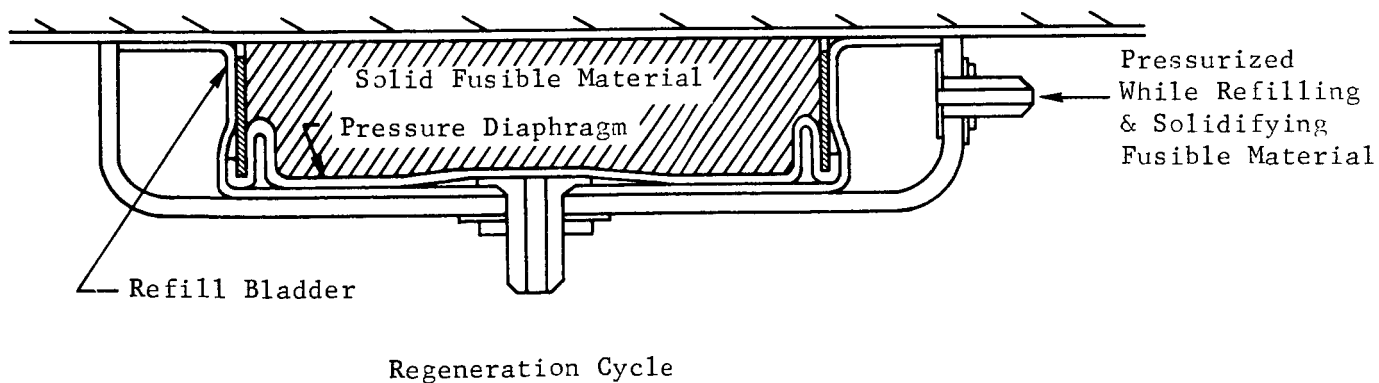
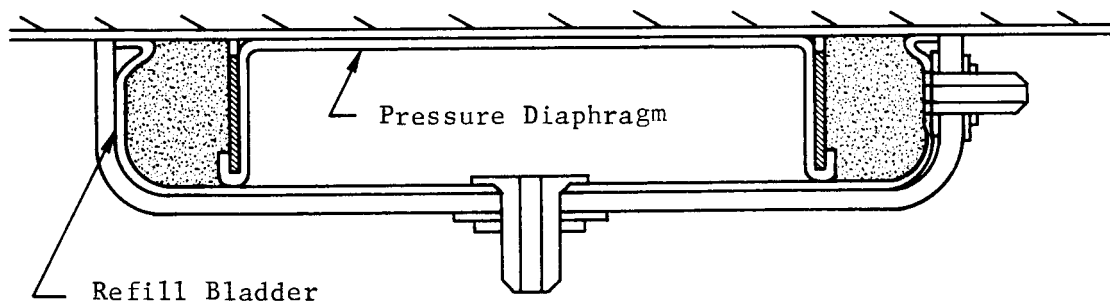
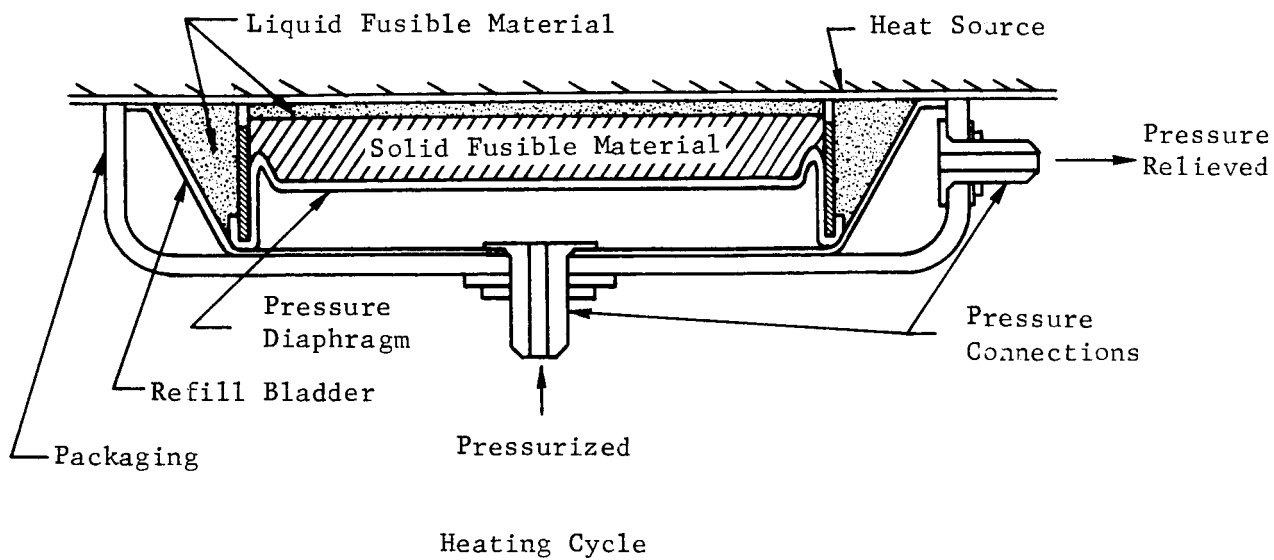


FIGURE 48 FUSIBLE MATERIAL - CONSTANT TEMPERATURE HEAT SINK APPARATUS

NORTHROP SPACE LABORATORIES

SECTION VIII

CONCLUSIONS

Endothermic melting and exothermic solidification of materials with suitable thermophysical properties is a practical means of temperature control of spacecraft components and subsystems.

The concept can be applied to a heat sink system, where the waste heat generated by an equipment item is absorbed in the melting process of a fusible material in an essentially adiabatic system. This arrangement is limited in total time integrated heat which can be absorbed by the weight of the fusible material required. This weight penalty amounts to approximately one pound per 100 BTU (29.3 watt-hours) of dissipated heat. However, where time integrated heat dissipation is small, an extremely simple and entirely passive temperature control system can be designed. Such a system can be integrated with a spacecraft component to form a self-contained unit, which can be mounted any place in the craft without reliance on heat transfer to the environment for temperature control. For a given fusible material, parametric design data and curves can be developed (as included for four materials in this report) which permit ready estimating of thermal performance and quantity of fusible material required.

The concept can also be applied to supplement other means of thermal control of spacecraft components. In combination with radiation to space, addition of fusible material to radiating surfaces can increase the thermal inertia of the system. This will permit smaller radiator areas where the waste heat histogram includes short duration power peaks. The performance of such systems can be predicted by digital computer analysis. However, the large number of variables of such system does not permit presentation of design data on generalized design curves.

Thermal control package design for fusible material applications requires containment of the fusible material in a package which will permit volume change with temperature and liquid-solid phase change and maintain the package full at all

times, thus providing contact of the fusible material with the component surface to be thermally controlled. Fabrication of this package from an elastomeric material appears at present as the most desirable way to satisfy the requirements, though other possibilities are also being considered.

NORTHROP SPACE LABORATORIES

SECTION IX

RECOMMENDATIONS

Based on the observations and conclusion of the work performed up to this time, the following recommendations for further research are made:

- (1) The work on design and development of "Fusible Material Thermal Control Packages" should be continued. It should include both, the adiabatic and the fusible-material-plus-radiating-fin systems. Thermal Control Package development should be directed towards development of space weight hardware.
- (2) Experimental verification of analytically determined performance data should be performed. This experimentation will make use of the "Fusible Material Thermal Control Packages" developed, and test performance under simulated space conditions.
- (3) Feasibility of materials other than those presently considered shall be evaluated. Phase changes on decrepitation of hydrated salts, such as the endothermic change from $\text{Na}_2\text{SO}_4 \cdot 10 \text{H}_2\text{O}$ to $\text{Na}_2\text{SO}_4 + 10 \text{H}_2\text{O}$, provide heat absorption of 108 BTU/pound and probably better thermal conductivity than liquid paraffins. Exothermic recrystallization does not take place as predictably and reliably as the resolidification of a molten paraffin. Application could be limited to the adiabatic system. But further study into applicability of this and other potential materials is recommended.
- (4) Continuation of investigation in the area of improvement of effective thermal conductance of the liquid melt layer, as outlined under "Potential Improvements of Thermal Control Package Design", is recommended. Experimental techniques should be used where required for development and verification.

REFERENCES

1. International Critical Tables of Numerical Data, Physics and Technology, McGraw-Hill Book Co., Inc., New York, 1933
2. Selected Values of Physical and Thermodynamic Properties of Hydrocarbons and Related Compounds, American Petroleum Institute Research Project 44, Carnegie Press, Pittsburgh, Pennsylvania, 1953
3. Hodgman, C.D., ed., Handbook of Chemistry and Physics, Forty Second ed., The Chemical Rubber Publishing Co., Cleveland, Ohio, 1960-61.
4. Broadhurst, M.G., Jr., "An Analysis of the Solid Phase Behavior of the Normal Paraffins." J. of Research of the NBS, Vol. 66A, No.3, May-June, 1962.
5. Kaye, J., Fand, R.M., Nance, W.G. and Nickerson, R.J., "Final Report on Heat Storage Cooling of Electronic Equipment," WADC TR 56-473, Mass. Ins. of Tech., February, 1957.
6. Schaerer, A.A., Basso, C.J., Smith, A.E. and Skinner, L.B., "Properties of Pure Normal Alkanes in the C₁₇ to C₃₆ Range," Chemical Society 77, 1955.
7. "Development of High Capacity Heat Storage Materials," Report No. 380, MIT , Instrument Lab/Cryo. Therm., Inc.
8. Sakiadis, B.C. and Coates, J., "Studies of Thermal Conductivity of Liquids," Pt. III, A.I. Ch. E. J., Vol. 3, 1957.
9. Lange, N.A., ed., Handbook of Chemistry, Eighth Ed., Handbook Publishers, Inc., Sandusky, Ohio, 1952.
10. Schiessler, R.W. and Whitmore, F.C., "Properties of High Molecular Weight Hydrocarbons," Industrial and Engineering Chem.Vol.47,No.8,1955

11. Sakiadis, B.C. and Coates, J., "Prediction of Specific Heat of Organic Liquids," A. I. Ch. E. J., March 1956.
12. Watson, K.M., "Correlation of the Physical Properties of Petroleum," The Science of Petroleum, Vol. 2, Oxford University Press, London, 1938.
13. Stone, J.P., Ewing, C.T. and Miller, R.R., "Heat Transfer Studies on Semi-Stable Organic Fluids in a Forced Convection Loop," Journal of Chemistry and Engineering Data, Vol. 7, No. 4, October 1962.
14. Powell, R.W. and Challar, A.R., "Thermal Conductivity of n-Octadecane," Ind. Eng. Chem., 53, 581, 1961.
15. Sutherland, R.D., Davis, R.S. and Seyer, W.F., "Heat-Transfer Effects Molecular Orientation of Octadecane," Ind. Eng. Chem., 51, 585, 1959.
16. Zeibland, H. and Patient, J.E., "Thermal Conductivity of Octadecane," Journal of Chemical Engineering, Data 7, Pt. 1, 530-1, 1962.
17. Watson, K.M. and Nelson, E.F., "Improved Methods of Approximating Critical and Thermal Properties of Petroleum Fractions," 85th Meeting of the American Chemical Society, Washington, D.C., March 26-31, 1933.
18. Cecil, A.B., and Munch, R.H. "Thermal Conductivity of Some Organic Liquids," Ind. Eng. Chem., Vol. 48, No.3, March 1956.
19. Frick, J.L., Share Program, "MLFTHAN-LMSC Thermal Network Analyzer," 7090 Fortran, Lockheed Missiles and Space Company, 1962.
20. Mackay, D.P. and Bacha, C.P., "Space Radiator Analysis and Design," ASD TR 61-30, Part 1, October, 1961.
21. Tatom, J.W., "Steady-State Behavior of External Surfaces in Space," ARS Journal, January 1960.